

Institut für Theoretische Physik
Universität Karlsruhe (TH)

Maximally Helicity Violating
amplitudes for
Higgs production processes

Maximal Helizitätsverletzende Amplituden
für Higgsproduktionsprozesse

Diplomarbeit

Jan Germer

November 2007

Referent: Prof. Dr. Zeppenfeld

Korreferent: Prof. Dr. Kühn

Ich versichere, dass ich diese Arbeit selbstständig verfasst und keine anderen als die angegebenen Hilfsmittel benutzt habe.

Jan Germer
Karlsruhe, den 7. November 2007

Als Diplomarbeit anerkannt.

Prof. Dr. Dieter Zeppenfeld
Karlsruhe, den 7. November 2007

Contents

1	Introduction	1
2	Gauge theories and Higgs mechanism	3
2.1	QCD	3
2.2	Color decomposition	8
2.3	Higgs couplings to fermions	10
3	MHV amplitudes	13
3.1	MHV vertices in QCD – The CSW approach	14
3.2	MHV amplitudes with a scalar	16
3.3	MHV- ϕ amplitudes in a parton level Monte Carlo simulation	19
3.4	Helicity contributions to $d\sigma/d\Delta\Phi_{jj}$	26
4	Effective theory	31
4.1	CP-even Higgs	33
4.2	CP-odd Higgs	36
4.3	Checks	38
4.3.1	Ward-Takahashi identity	38
4.3.2	Five point function for the $Hg g g g$ coupling	39
5	Effective theories vs. full calculation	41
5.1	Proton proton \rightarrow Higgs plus two jets	42
5.1.1	$qQ \rightarrow qQH$	42
5.1.2	$qg \rightarrow qgH$	43
5.1.3	$gg \rightarrow ggH$	43
5.2	Checks	43
5.2.1	Gauge invariance	43
5.2.2	Lorentz boost	44
5.3	Total cross section for different Higgs masses	44
5.4	Differential cross section: p_T distribution	48
5.5	Discussion	56
6	MHV amplitudes for the dimension 7 operators	59
7	Conclusions	63

A Feynman Rules and conventions	65
B Calculation of effective vertices	67
B.1 Effective Hgg vertex	67
B.2 Effective $Hggg$ vertex	69
B.3 Effective Agg vertex	71
B.4 Effective $Aggg$ vertex	72
C Identities between effective Lagrangians	75
D Spinor calculus	77
Bibliography	83
Zusammenfassung	85
Danksagung	89

Chapter 1

Introduction

The Standard Model (SM) of particle physics describes in a beautiful way all known fundamental particles and the interaction among them by means of a quantum field theory of an exact local $SU(3)$ gauge theory and a spontaneously broken local $SU(2)_L \times U(1)_Y$ gauge theory. The SM is consistent with the various high precision tests that have been performed under greatest efforts. Nevertheless, to be completely determined, one last parameter is missing: the mass of the so called Higgs particle. To confirm or rule out the existence of this particle and therewith the verification or falsification of the electroweak symmetry breaking mechanism, is one of the major reasons, that lead to the construction of the Large Hadron Collider (LHC). The LHC is a proton proton accelerator with a center of mass energy of 14TeV and a very high luminosity, which is about a factor hundred higher than the luminosity attained by the Tevatron experiment at Fermilab.

The unbroken $SU(3)$ symmetry in the SM is the theory of strong interactions, the so called Quantum Chromodynamics or short QCD. The non-Abelian nature of QCD allows for self interacting gauge bosons, called gluons. This and the fact, that the strong coupling constant becomes very strong at large distances, makes predictions, based on perturbative calculations very difficult to handle. Since protons are made out of strongly interacting particles (quarks and gluons), scattering processes at the LHC are dominated by QCD induced events. Great efforts have been done to make QCD calculations feasible. In recent years a new promising approach came up, making use of so called *maximally helicity violating* (MHV) amplitudes. This method was first developed for gluon amplitudes only, but has soon be extended to amplitudes containing quark antiquark pairs, massive vector bosons or scalar particles like e.g. the Higgs particle.

One of the most promising discovery channels for a SM Higgs boson at the LHC, is Higgs production via weak boson fusion. This process is actually known at next-to leading order (NLO) in the strong coupling constant α_s . The related process $pp \rightarrow Hjj$ via gluon fusion gives an irreducible background, and therefore has to be simulated with high accuracy. This process is up to now – without falling back on approximations – only known at leading order (LO). The calculation contains a top loop allowing for the Higgs gluon coupling. The NLO calculation is available in the so called *large top mass approximation* in which the Higgs couples directly to gluons. One ingredient for this

NLO calculation are the above mentioned MHV amplitudes, speeding up the calculation tremendously.

The aim of this thesis is to examine the impact of MHV amplitudes for phenomenological purposes, especially for the process $pp \rightarrow Hjj$. Since MHV plus Higgs amplitudes are only available in the $m_{top} \rightarrow \infty$ limit, the effects of this approximation are investigated and it is examined whether this approximation can be improved by considering a correction term. The thesis is organized in the following way:

Chapter 2 deals with the theory of QCD and the Higgs mechanism. Especially it is shown, that QCD tree amplitudes can be decomposed in so called *color ordered partial amplitudes*. For specific helicity configurations of the external quarks and gluons these partial amplitudes have astonishingly short analytic expressions – the MHV amplitudes. Chapter 3 explains how MHV amplitudes can be used to calculate non-MHV amplitudes, as well in the pure QCD case as in the case containing a Higgs. As an application, these amplitudes were implemented into the parton level Monte Carlo VBFNLO and tested for speed-up. Furthermore a detailed study, in respect of different helicity amplitudes contributing to the differential cross section $d\sigma/d\Delta\Phi_{jj}$, is given.

MHV amplitudes containing a Higgs are only available in the limit $m_{top} \rightarrow \infty$. In this limit the Higgs-gluon couplings can be described by an effective Lagrangian of dimension 5 (D5). Chapter 4 takes a close look at the effective theory. Beside the well known D5 Lagrangian also a correction term, considering the $1/m_{top}^2$ suppressed parts, will be derived, which can be described by an effective Lagrangian made out of dimension 7 (D7) operators.

In chapter 5 the D5 and D7 effective couplings were implemented into VBFNLO and the three subprocesses contributing to $pp \rightarrow Hjj$ were compared to the full loop calculation. As we will see, some phase space regions spoil the effective theories. The ambition is to reduce the error emerging from the D5 theory, by considering the D7 correction together with appropriate cuts on the phase space, in order to analyze if it would be reasonable to perform a NLO calculation including the D7 operators.

The NLO calculation exploits the compactness of the MHV amplitudes. Hence, having MHV amplitudes for the D7 operators would be a great help for implementing them into a NLO calculation. In chapter 6 a conjecture for MHV amplitudes for the D7 operators is given. The expressions are shown to agree numerically in the $gg \rightarrow ggH$ case.

Chapter 7 finally sums up the results, including a discussion.

Conventions and calculations concerning the derivation of the effective theory as well as identities between some effective dimension 7 Lagrangians can be found in the Appendix.

Chapter 2

Gauge theories and Higgs mechanism

In modern physics, particle interactions are described by gauge theories. Thereby one means, that the Lagrangian is locally invariant under a given group G , which means that the group transformation can be different for every space time point. The Standard Model of particle physics contains three gauge groups: $SU(3) \times SU(2)_L \times U(1)_Y$. Additionally one introduces a scalar self interacting field with tachyonic mass, the so-called Higgs field, to break the $SU(2)_L \times U(1)_Y$ invariance to $U(1)_{em}$ – describing the electroweak interactions. The $SU(3)$ symmetry remains as an exact symmetry and describes the strong interaction, the so-called Quantum Chromodynamics (QCD).

2.1 QCD

For a long time it has been dubious that a theory of exchanged vector bosons could correctly describe the strong interaction. Strongly interacting particles, like protons or neutrons, seem to be made out of constituents, called partons. There are two observations that did not seem to match up:

- The strong interaction has to be extremely strong in some circumstances, since it holds the partons together and free partons were never observed.
- In deep inelastic scattering processes – like in electron proton collisions with momentum transfer $Q^2 \geq 1\text{GeV}$ – the partons behave like free particles.

These properties are also known as confinement and asymptotic freedom. The way out of these seemingly contradictory properties is the description of interactions by non-Abelian gauge theories, also known as Yang-Mills theories.

The construction of a non-Abelian gauge theory can be motivated by studying the geometry of local gauge invariance; first in the Abelian case like the $U(1)$ symmetry leading to the quantum electrodynamic (QED), and then generalizing to an arbitrary symmetry group.

Local gauge invariance in QED

Consider the free Dirac equation

$$(i\cancel{\partial} - m) \Psi(x) = 0 \quad (2.1)$$

which is one of the Euler-Lagrange equations of

$$\mathcal{L} = \bar{\Psi}(x) (i\cancel{\partial} - m) \Psi(x) \quad (2.2)$$

Both equations are invariant under global U(1) gauge transformations

$$\Psi \rightarrow \Psi'(x) = e^{-i\lambda_q\theta} \Psi(x) \quad (2.3)$$

$$\bar{\Psi} \rightarrow \bar{\Psi}'(x) = \bar{\Psi}(x) e^{i\lambda_q\theta} \quad (2.4)$$

but are not invariant under local gauge transformations where θ depends on x , $\theta = \theta(x)$, since one is left with terms $\propto \partial_\mu\theta(x)$

$$(i\cancel{\partial} - m) \Psi'(x) = e^{-i\lambda_q\theta} (i\cancel{\partial} - m + \lambda_q\cancel{\partial}\theta(x)) \Psi(x) \quad (2.5)$$

Now one can ask for local gauge invariance. To achieve this, introduce a so-called gauge field $A_\mu(x)$ which transforms in such a way, that the bothersome term $\propto \partial_\mu\theta(x)$ gets canceled. This is done by replacing the partial derivative ∂_μ with the covariant derivative D_μ

$$D_\mu = \partial_\mu + i\lambda_q A_\mu(x) \quad (2.6)$$

It is now easy to check, that the resulting Dirac equation becomes invariant under local gauge transformations, if the gauge field transforms as

$$A'_\mu(x) = A_\mu(x) + \partial_\mu\theta(x) \quad (2.7)$$

An important property of the covariant derivative is that $D'_\mu = e^{-i\lambda_q\theta} D_\mu e^{i\lambda_q\theta}$
The electromagnetic field strength tensor, defined by

$$F_{\mu\nu}(x) = \partial_\mu A_\nu - \partial_\nu A_\mu \quad (2.8)$$

is gauge invariant. To get the Lagrangian of QED one has to add a Lorentz and gauge invariant gauge field to the Dirac Lagrangian, so that the field itself becomes a dynamical quantity. The QED Lagrangian reads

$$\mathcal{L}_{\text{QED}} = \bar{\Psi}(x) (i\cancel{D} - m) \Psi(x) - \frac{1}{4} F_{\mu\nu}(x) F^{\mu\nu}(x) \quad (2.9)$$

Generalizing to non Abelian gauge symmetries

Consider a multiplet of Dirac fields

$$\Psi(\mathbf{x}) = \begin{pmatrix} \Psi_1(x) \\ \Psi_2(x) \\ \vdots \\ \Psi_n(x) \end{pmatrix} \quad (2.10)$$

which transforms according to a representation \mathcal{D}_g of a compact symmetry group G . The infinitesimal generators T^a , $a = 1, \dots, \dim(G)$ are represented by $n \times n$ matrices. The local gauge transformation of the fields are now given by

$$\Psi(\mathbf{x}) \rightarrow \Psi'(x) = \mathcal{D}_g \Psi(x), \quad \mathcal{D}_g = \mathcal{D}_g(x) \quad (2.11)$$

Let us now construct a covariant derivative which leaves the Lagrangian invariant under local gauge transformations. Consider therefore an infinitesimal parallel transport $U(x+dx, x)$ of the field $\Psi(\mathbf{x})$, which is generated by an affine connection, or in physics called gauge field, $\mathcal{A}^\mu(x)$, an element of the Lie algebra of G

$$\Psi_{\parallel}(x+dx) = U(x+dx, x)\Psi(x) \quad (2.12)$$

$$U(x+dx, x) = \mathbb{1} + i\mathcal{A}_\mu(x)dx^\mu \quad (2.13)$$

Gauge transformations and parallel transport have to be compatible. That means that first performing a gauge transformation on the field and second parallel transporting it, has to give the same as performing the operations vice versa.

$$\Psi'_{\parallel}(x+dx) = U'(x+dx, x)\Psi'(x) = U'(x+dx, x)\mathcal{D}_g(x)\Psi(x) \quad (2.14)$$

$$\stackrel{!}{=} \mathcal{D}_g(x+dx)U(x+dx, x)\Psi(x) \quad (2.15)$$

Here one can read of the transformation law for the parallel transport operator:

$$U'(x+dx, x) = \mathcal{D}_g(x+dx)U(x+dx, x)\mathcal{D}_g^{-1}(x) \quad (2.16)$$

Inserting (2.13) and expanding to first order in dx one obtains the transformation law for the connection

$$i\mathcal{A}'_\mu(x) = \mathcal{D}_g(x)(i\mathcal{A}_\mu(x) - \partial_\mu)\mathcal{D}_g^{-1}(x) \quad (2.17)$$

The covariant derivative defined by $D_\mu = \partial_\mu - i\mathcal{A}_\mu(x)$ behaves under gauge transformations as (using (2.17))

$$\mathcal{D}_g(x)D_\mu\mathcal{D}_g^{-1}(x) = \partial_\mu - i\mathcal{A}'_\mu(x) = D'_\mu \quad (2.18)$$

As a consequence, the Dirac Lagrangian with covariant derivative

$$\mathcal{L} = \bar{\Psi}(x)(i\mathcal{D} - m)\Psi(x) \quad (2.19)$$

is invariant under local gauge transformations.

Next consider the parallel transport along a closed path (fig.2.1). The effect to the field up to $\mathcal{O}(dxdy)$ is given by the difference of the two paths $x \rightarrow x+dx \rightarrow x+dx+dy$ and $x \rightarrow x+dy \rightarrow x+dy+dx$

$$U(x+dx+dy, x+dx)U(x+dx, x) - U(x+dy+dx, x+dy)U(x+dy, x) \quad (2.20)$$

$$\begin{aligned} &= (\mathbb{1} + i\mathcal{A}_\mu(x+dx)dy^\mu)(\mathbb{1} + i\mathcal{A}_\nu(x)dx^\nu) - (\mathbb{1} + i\mathcal{A}_\mu(x+dy)dx^\mu)(\mathbb{1} + i\mathcal{A}_\nu(x)dy^\nu) \\ &= i(\partial_\mu\mathcal{A}_\nu(x) - \partial_\nu\mathcal{A}_\mu(x) - i[\mathcal{A}_\mu(x), \mathcal{A}_\nu(x)])dx^\mu dy^\nu \\ &\equiv i\mathcal{F}_{\mu\nu}(x)dx^\mu dy^\nu \end{aligned} \quad (2.21)$$

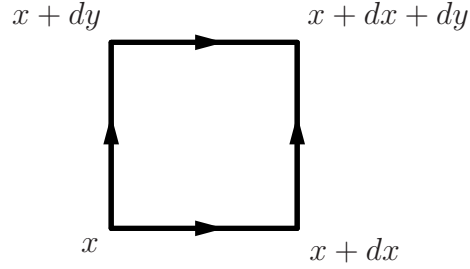


Figure 2.1: Parallel transporting a field from x to $x + dx + dy$ on to different ways. The difference between this two paths defines the field strength tensor for general gauge groups

This defines the field strength tensor for gauge fields of the Lie algebra of an arbitrary group G . One should notice that it reduces correctly to the electromagnetic field strength tensor for $G=U(1)$, since in the Abelian case the commutator vanishes. It is possible to express the field strength tensor $\mathcal{F}_{\mu\nu}(x)$ as commutator of covariant derivatives, as one can be convinced by a short calculation

$$\mathcal{F}_{\mu\nu}(x) = i [D_\mu, D_\nu] \quad (2.22)$$

Yang-Mills Lagrangian

To construct a self contained physical theory, the external gauge field \mathcal{A}_μ must itself be a dynamical quantity. To achieve this, one has to add a gauge and Lorentz invariant term to the Lagrangian, depending only on the gauge field. However, the combination

$$\mathcal{F}_{\mu\nu}(x)\mathcal{F}^{\mu\nu}(x) \quad (2.23)$$

is not gauge invariant as one can easily check by the use of (2.18) and (2.22). Fortunately one can easily construct a gauge invariant quantity out of (2.23) by taking the trace over the group space

$$\begin{aligned} \mathcal{L}_{\text{gauge}} &= -\frac{1}{2g^2} \text{Tr} (\mathcal{F}_{\mu\nu}(x)\mathcal{F}^{\mu\nu}(x)) \\ &\rightarrow -\frac{1}{2g^2} \text{Tr} (\mathcal{D}_g \mathcal{F}_{\mu\nu}(x) \mathcal{D}_g^{-1} \mathcal{D}_g \mathcal{F}^{\mu\nu}(x) \mathcal{D}_g^{-1}) \\ &= -\frac{1}{2g^2} \text{Tr} (\mathcal{F}_{\mu\nu}(x)\mathcal{F}^{\mu\nu}(x) \mathcal{D}_g^{-1} \mathcal{D}_g) \\ &= -\frac{1}{4} F_{\mu\nu}^a(x) F^{a\mu\nu}(x) \end{aligned} \quad (2.24)$$

where in the third line was made use of cyclic invariance of the trace and in the last line the trace was performed and the components of the field are written explicitly¹. The

¹ \mathcal{A}_μ can be expanded in terms of the representation matrices T_{ij}^a : $\mathcal{A}_\mu(x) = gA_\mu^a(x)T_{ij}^a$, with a proportionality constant g

representation matrices are normalized according to $\text{Tr}(T^a T^b) = \frac{1}{2} \delta^{ab}$ (corresponding to the fundamental representation). Altogether, the sum of (2.19) and (2.24) finally gives the Yang-Mills Lagrangian for gauge invariant interactions of fermions with non-Abelian gauge bosons

$$\mathcal{L}_{\text{Yang-Mills}} = \bar{\Psi}(x) (i\not{D} - m) \Psi(x) - \frac{1}{4} F_{\mu\nu}^a(x) F^{a\mu\nu}(x) \quad (2.25)$$

QCD - the Yang-Mills theory of the strong interaction

When people started to study hadron spectroscopy, they realized that one can describe the hadron spectra by introducing a new quantum number, color. Han and Nambu, Greenberg, and Gell-Mann assigned quarks to the fundamental representation of a new, internal global SU(3) symmetry. Quarks and antiquarks form a SU(3) triplet, where quarks transform under the 3-representation (i.e. fundamental representation) and the antiquarks under the $\bar{3}$ -representation. Additionally they postulated that all hadron wavefunctions must be invariant under SU(3) transformation, so that physical hadrons are singlets under color. Thus, the only allowed combinations are

$$\bar{q}_i q_i, \quad \epsilon_{ijk} q_i q_j q_k, \quad \epsilon_{ijk} \bar{q}_i \bar{q}_j \bar{q}_k \quad (2.26)$$

This not only gave the right quark multiplet observed, it also gave a way out to the Δ^{++} resonance problem, which is the excitation of three u -quarks with parallel spin and zero orbital angular momentum

$$\Delta^{++} = |u^\uparrow, u^\uparrow, u^\uparrow\rangle \quad (2.27)$$

Without the new degree of freedom, this state would violate the spin statistic theorem, since the wavefunction is totally symmetric under quark spin and flavor exchange.

But there was still the problem in formulating a theory which solves the issues mentioned in the beginning of this chapter. The answer to this seeming contradiction became apparent, when in the 70s Gross, Wilczek and Politzer observed, that non Abelian gauge theories are asymptotically free [1, 2].² The main task is now to identify the right gauge group with the strong interaction. But since the Lagrangian already contains a global color SU(3) it suggests itself to identify the color symmetry with the gauge group of the strong interaction.

The QCD Lagrangian, describing the strong interactions therefore is the Yang-Mills theory of SU(3). It contains six quark fields – also called quark flavors – which are given as three families of quark doublets

$$\begin{pmatrix} u \\ d \end{pmatrix} \quad \begin{pmatrix} s \\ c \end{pmatrix} \quad \begin{pmatrix} t \\ b \end{pmatrix} \quad (2.28)$$

where the upper quark carries electric charge $+\frac{2}{3}$ and the lower $-\frac{1}{3}$. The quarks are called (u)p, (d)own, (s)trange, (c)harm, (t)op and (b)ottom. Altogether one gets

$$\mathcal{L}_{\text{QCD}} = \sum_{q,c,\bar{c}} \bar{\Psi}_{q,\bar{c}}(x) (i\not{D}_{\bar{c}c} - m_q \delta_{\bar{c}c}) \Psi_{q,c} - \frac{1}{4} \sum_a F_{\mu\nu}^a(x) F^{a\mu\nu}(x) \quad (2.29)$$

²For their discovery, Gross, Wilczek and Politzer were awarded the Nobel Prize in Physics in 2004

where $\Psi_{q,c}$ denote the quark field with flavor q , mass m_q and color c .

Finally, Wilson discovered by using an approximation scheme in which the continuum gauge theory is replaced by a discrete statistical mechanical system on a four dimensional Euclidian lattice, that for sufficiently strong coupling, QCD exhibits confinement of color: the only finite energy asymptotic states of the theory are those that are singlets of color SU(3)[3]. Therefore QCD implicitly contains the ad hoc postulate that hadrons are color singlets and explains that no free quarks are observed.

The running coupling constant is described by the Callan-Symanzik equation and is given in second order perturbation theory by [4]

$$\alpha_s(Q^2) = \frac{\alpha_s(M^2)}{1 + \frac{\alpha_s(M^2)}{4\pi} \beta_0 \log \frac{Q^2}{M^2}} \quad (2.30)$$

which shows explicitly that for high momenta or short distances the coupling constant becomes small. For small enough value one can expand the calculation in a perturbation series.

The quantization of the theory is best done with the help of the Feynman path integral formalism. The quark propagator and the vertices are derived in a straight-forward fashion. But there is a subtlety in deriving the gluon propagator due to gauge invariance. The problem can be solved using the method of Faddeev-Popov by introducing a gauge fixing term [5]. The Feynman rules used in this thesis can be found in Appendix A.

2.2 Color decomposition

If one is interested in calculating scattering amplitudes in QCD it is often a good idea to treat the color structure of the amplitude in a specific manner.³ Consider a gauge group SU(N_c), a generalization of the QCD gauge group SU(3) (by generalizing to arbitrary N_c the gauge theory structure becomes more apparent). The generators of the SU(N_c) are traceless, hermitian $N_c \times N_c$ matrices, denoted by $(T^a)_i^{\bar{j}}$. Quarks and antiquarks carry fundamental color index $i, \bar{i} = 1, 2, \dots, N_c$, while gluons carry adjoint color index $a = 1, 2, \dots, N_c^2 - 1$. They are normalized according to

$$\text{Tr}(T^a T^b) = C(r) \delta^{ab} \quad (2.31)$$

where $C(r)$ is a constant, depending of the representation r chosen. In the following I take $C(r) = \frac{1}{2}$, but one has to be careful because often $C(r)$ is taken to be 1 whereupon partial amplitudes may vary by factors of $\sqrt{2}$. Now first of all consider a pure gluonic scattering amplitude. In a generic Feynman diagram one has a group theory structure constant f^{abc} defined by

$$[T^a, T^b] = i f^{abc} T^c \quad (2.32)$$

for each three-gluon vertex and contracted pairs $f^{abe} f^{cde}$ for each four gluon vertex. Since gluon propagators contain a factor of δ^{ab} they contract many of the indices. The number of the indices that stay uncontracted is equal to the number of external gluons.

³The argumentation follows the one of [9]

To expose the general color structure of an amplitude, express the structure constant f^{abc} in favor of the T^a 's, by multiplying (2.32) with T^c and taking the trace:

$$f^{abc} = -2i (\text{Tr} (T^a T^b T^c) - \text{Tr} (T^b T^a T^c)) \quad (2.33)$$

That means that the color structure of our amplitude is made out of products of the form

$$\text{Tr}(\dots T^a \dots) \text{Tr}(\dots T^a \dots) \dots \quad (2.34)$$

One can reduce the number of traces by ‘‘Fierz rearranging’’ the contracted T^a 's

$$(T^a)_{i_1}^{\bar{j}_1} (T^a)_{i_2}^{\bar{j}_2} = \frac{1}{2} \left(\delta_{i_1}^{\bar{j}_2} \delta_{i_2}^{\bar{j}_1} - \frac{1}{N_c} \delta_{i_1}^{\bar{j}_1} \delta_{i_2}^{\bar{j}_2} \right) \quad (2.35)$$

Consider e.g. a product of the form

$$\begin{aligned} & 2 (\text{Tr} (T^a T^b T^e) - \text{Tr} (T^b T^a T^e)) \cdot (\text{Tr} (T^c T^d T^e)) \quad (2.36) \\ &= 2 \left((T^a)_{i_1}^{i_2} (T^b)_{i_2}^{i_3} (T^e)_{i_3}^{i_1} - (T^b)_{i_1}^{i_2} (T^a)_{i_2}^{i_3} (T^e)_{i_3}^{i_1} \right) (T^c)_{j_1}^{j_2} (T^d)_{j_2}^{j_3} (T^e)_{j_3}^{j_1} \\ &= 2 \left((T^a)_{i_1}^{i_2} (T^b)_{i_2}^{i_3} (T^c)_{j_1}^{j_2} (T^d)_{j_2}^{j_3} - (T^b)_{i_1}^{i_2} (T^a)_{i_2}^{i_3} (T^c)_{j_1}^{j_2} (T^d)_{j_2}^{j_3} \right) \\ & \quad \times \frac{1}{2} \left(\delta_{i_3}^{j_1} \delta_{j_3}^{i_1} - \frac{1}{N_c} \delta_{i_3}^{i_1} \delta_{j_3}^{j_1} \right) \\ &= \text{Tr} (T^a T^b T^c T^d) - \text{Tr} (T^b T^a T^c T^d) \quad (2.37) \end{aligned}$$

since the terms containing a factor $1/N_c$ cancel. In the same way one can anticipate that any tree diagram for n -gluon scattering can be reduced to a sum of terms with the color information borne by a single trace of color matrices. Berends and Giele proved by induction, that this is in fact possible [8]:

$$\mathcal{A}_n^{tree}(\{k_i, \lambda_i, a_i\}) = g^{n-2} \sum_{\sigma \in S_n/Z_n} \text{Tr} (T^{a_{\sigma(1)}} \dots T^{a_{\sigma(n)}}) A_n^{tree}(\sigma(1^{\lambda_1}), \dots, \sigma(n^{\lambda_n})) \quad (2.38)$$

where g is the strong coupling, k_i and λ_i are the gluon momenta and helicities. The A_n^{tree} are the so-called partial (or color stripped) amplitudes which contain all the kinematic information. The sum goes over all permutations but cyclic ones.

The partial amplitudes have the following properties [8]

- $A_n^{tree}(1, \dots, n)$ is invariant under cyclic permutations
- reflection property: $A_n^{tree}(1, \dots, n) = (-1)^n A_n^{tree}(n, \dots, 1)$
- the sub-cyclic sum equals zero: $\sum_{C(1, \dots, n-1)} A_n^{tree}(1, \dots, n) = 0$
- A_n^{tree} is gauge invariant

In a similar fashion, it is also possible to represent an n -point amplitude \mathcal{A}_n with m $q\bar{q}$ pairs as a sum of products of color factors \mathcal{T}_n and partial amplitudes A_n , but now the color decomposition is a little bit more involved. Since for each quark-gluon

vertex one gets an additional color factor $T_i^{\bar{j}}$, now the total color factor splits up to a product of m strings of color matrices T^a . For just one $q\bar{q}$ pair the tree amplitudes can be reduced to

$$\mathcal{A}_n^{tree}(\{k_i, \lambda_i, a_i\}) = g^{n-2} \sum_{\sigma \in S_{n-2}} (T^{a_{\sigma(3)}} \dots T^{a_{\sigma(n)}})_{i_2}^{\bar{j}_1} A_n^{tree}(1_{\bar{q}}^{\lambda_1}, 2_q^{\lambda_2}, \sigma(3^{\lambda_3}), \dots, \sigma(n^{\lambda_n})) \quad (2.39)$$

where $1_{\bar{q}}$ and 2_q denote the antiquark and the quark, respectively. The general decomposition with an arbitrary number of $q\bar{q}$ pairs can be found in [10].

2.3 Higgs couplings to fermions

The standard model is, as already mentioned, a gauge theory of local

$$\text{SU}(3) \times \text{SU}(2)_L \times \text{U}(1)_Y \quad (2.40)$$

gauge invariance. The $\text{SU}(3)$ is responsible for the strong interaction, while $\text{SU}(2)_L \times \text{U}(1)_Y$ generate the electroweak sector. The corresponding Lagrangian can be split into three individual parts

$$\mathcal{L}_{\text{classic}} = \mathcal{L}_{\text{fermion}} + \mathcal{L}_{\text{gauge}} + \mathcal{L}_{\text{Higgs}} \quad (2.41)$$

The Higgs field is needed to break $\text{SU}(2)_L \times \text{U}(1)_Y \rightarrow \text{U}(1)_{em}$, by which the weak gauge bosons obtain their masses. In the following I will restrict to quark fields and consider the creation of their masses in a gauge invariant way. The mechanism of electroweak symmetry breaking will not be discussed. The interested reader is referred to [4, 6]. The SM is a chiral theory: left-handed fields $\Psi'_L(x) = \frac{1}{2}(1 - \gamma_5)\Psi'(x)$ are associated with the fundamental representation of $\text{SU}(2)_L$ and arranged in isospin doublets, while the right-handed fields $\Psi'_R(x) = \frac{1}{2}(1 + \gamma_5)\Psi'(x)$ are put into a one-dimensional trivial representation of $\text{SU}(2)_L$ (the prime denotes that the fields are eigenstates of the electroweak interaction). The fermion fields in 2.41 are massless, since an add-hoc introduction of a mass term would give

$$-m_q \bar{q}q = -m_q \bar{q} \left(\frac{1}{2}(1 - \gamma_5) + \frac{1}{2}(1 + \gamma_5) \right) q = -m_q (\bar{q}_R q_L + \bar{q}_L q_R) \quad (2.42)$$

which is manifestly non-invariant under $\text{SU}(2)_L$ transformations, since q_L and q_R live in different representations (q_L is part of the doublet while q_R is of the singlet). The same Higgs field used to break electroweak symmetry can be used to generate masses of the fermions in a gauge invariant way. The Higgs part of the Lagrangian in (2.41) (without leptons) is

$$\begin{aligned} \mathcal{L}_{\text{Higgs}} = & (D_\mu \Phi)^\dagger (D^\mu \Phi) - V(\Phi) \\ & - \sum_{i,j} \left(\begin{pmatrix} \bar{u}'_{iL} \\ \bar{d}'_{iL} \end{pmatrix} Y_{ij}^u \Phi^c u_j'^R + \begin{pmatrix} \bar{u}'_{iL} \\ \bar{d}'_{iL} \end{pmatrix} Y_{ij}^d \Phi d_j'^R + h.c. \right) \end{aligned} \quad (2.43)$$

where Y^f denote Yukawa coupling matrices. After expanding the Higgs field around its vacuum expectation value, short VEV, the fermions gain masses due to the Yukawa

coupling to the VEV, and as a “by-product” of the Higgs mechanism the fermions also couple to the remaining physical degree of freedom of the Higgs field – the Higgs boson. The coupling strength of the Higgs boson is proportional to the fermion mass divided by the VEV v of the Higgs field. The Feynman rules for the Higgs fermion vertex can be found in Appendix A.

Chapter 3

MHV amplitudes

In the late 1980's S. J. Parke and T. R. Taylor conjectured, that the amplitudes for scattering an arbitrary number of gluons to lowest order in the coupling constant, are given by very compact analytic expressions for specific helicity configurations of the gluons [7]. The scattering amplitudes of n ingoing gluons where all or all but one have the same helicity vanish at tree level (for $n > 3$). The first non vanishing amplitudes, called *maximally helicity violating amplitudes* or short MHV-amplitudes, give the scattering amplitudes of n incoming gluons where all but two gluons have the same helicity. Written in terms of spinor inner products, the color-ordered (or partial) amplitudes are given by

$$A_n^{tree}(1^+, \dots, j^-, \dots, k^-, \dots, n^+) = i \left(\sqrt{2} \right)^n \frac{\langle jk \rangle^4}{\langle 12 \rangle \langle 23 \rangle \cdots \langle n-1, n \rangle \langle n1 \rangle} \quad (3.1)$$

$$A_n^{tree}(1^-, \dots, j^+, \dots, k^+, \dots, n^-) = i \left(\sqrt{2} \right)^n \frac{[jk]^4}{[12][23] \cdots [n-1, 1][n1]} \quad (3.2)$$

where j and k denote the gluons with negative or positive helicity respectively¹. The validity of this expression was rigorously proven to be correct by Berends and Giele using their recursion relation for off shell currents [8]. The definition of the spinors $\langle i|$ and $|j\rangle$ are given in Appendix D and follows the notation of [9]. One can obtain the amplitude for n_1 incoming gluons and n_2 outgoing gluons (with $n_1 + n_2 = n$) by crossing symmetry, that is replace $p^\mu \rightarrow -p^\mu$ and reverse the helicity of the crossed gluon.

As a comment to this amplitude, notice that it is possible to extend the MHV amplitudes to amplitudes containing one or two massless quark anti-quark pairs. Since the color information has been stripped off, massless fermions in the theory might as well be gluinos. Therefore one can use supersymmetric Ward identities, to construct MHV amplitudes with quark anti-quark pairs out of (3.1). For details the interested reader is referred to [9].

¹For $n = 3$ the amplitude vanishes if all helicities are the same. For any other helicity configuration, the amplitude is also given by (3.1) and (3.2), respectively

3.1 MHV vertices in QCD – The CSW approach

Witten observed that perturbative scattering amplitudes in Yang-Mills theory have unexpected properties, such as holomorphy of the maximally helicity violating amplitudes [11]. This allows to transform these amplitudes from momentum space to twistor space.

Inspired by the twistor transformation of MHV amplitudes, Cachazo, Svrcek and Witten found a novel diagrammatic expression for calculating scattering amplitudes in Yang-Mills theory, which can be used as an alternative to the usual Feynman diagrammatic approach [12]. They show, that it is possible to continue the MHV amplitudes off-shell and use them as vertices in tree diagrams to generate non MHV amplitudes. For the definition of the MHV vertices a different representation for the spinors than the one given in the appendix is useful:

First recall that the Lie algebra of the complexified Lorentz group in four dimensions is isomorphic to $SU(2) \times SU(2)$. Therefore one can classify the representations as (p,q) with p,q integers or half integers. Define now

- λ_a , $a = 1, 2$ as a left handed spinor transforming as $(\frac{1}{2}, 0)$
- $\tilde{\lambda}_{\dot{a}}$, $\dot{a} = 1, 2$ as a right handed spinor transforming as $(0, \frac{1}{2})$

The vector representation of the $SO(1,3)$ is the $(\frac{1}{2}, \frac{1}{2})$ representation. Therefore every four vector p_μ can be represented as a “bi-spinor” $p_{a\dot{a}}$. The mapping can be made explicit with help of the generalized Pauli matrices $\sigma^\mu = (\mathbb{1}, \vec{\sigma})$:

$$p_\mu \rightarrow p_{a\dot{a}} = \sigma_{a\dot{a}}^\mu p_\mu \quad (3.3)$$

$$p_{a\dot{a}} = \lambda_a \tilde{\lambda}_{\dot{a}} + \mu_a \tilde{\mu}_{\dot{a}} \quad (3.4)$$

where in the last line it was made use of the fact that any 2×2 matrix has at most rank two and hence can be written with the help of some spinors λ, μ and $\tilde{\lambda}, \tilde{\mu}$. If p_μ is a null vector ($p_\mu p^\mu = 0$) we can write

$$p_{a\dot{a}} = \lambda_a \tilde{\lambda}_{\dot{a}} \quad (3.5)$$

since $p_\mu p^\mu = \det(p_{a\dot{a}})$ and hence the rank of the matrix is less than two. With this definition of the spinors, one can define the Lorentz invariant quantities

$$\langle \lambda_1, \lambda_2 \rangle \equiv \epsilon_{ab} \lambda_1^a \lambda_2^b \quad (3.6)$$

$$[\tilde{\lambda}_1, \tilde{\lambda}_2] \equiv \epsilon_{\dot{a}\dot{b}} \tilde{\lambda}_1^{\dot{a}} \tilde{\lambda}_2^{\dot{b}} \quad (3.7)$$

The amplitude (3.1) is made out of left handed spinor product, where each gluon is on-shell and hence $p_{a\dot{a}} = \lambda_a \tilde{\lambda}_{\dot{a}}$. But since one wants to continue the amplitudes off-shell a suitable definition for the spinor λ_a – where p_μ is not on-shell – is needed. This can be constructed by the following way: As long as $p_{a\dot{a}}$ is lightlike, we can pick up an arbitrary negative helicity spinor $\eta^{\dot{a}}$ to get the left handed part of $p_{a\dot{a}}$ by contracting it with $\eta^{\dot{a}}$: $\lambda_a = p_{a\dot{a}} \eta^{\dot{a}} / [\tilde{\lambda}, \eta]$. The factor $1/[\tilde{\lambda}, \eta]$ is not relevant, since the tree amplitudes that will be computed are invariant under rescaling of the λ 's for all the off-shell, internal lines. Inspired by this property, one can now define the off-shell continuation. Just pick an

arbitrary right handed spinor $\eta^{\dot{a}}$ and define λ_a for an internal line carrying momentum $p_{a\dot{a}}$ by

$$\lambda_a = p_{a\dot{a}}\eta^{\dot{a}} \quad (3.8)$$

It is important to use the same η for all the off-shell lines in all diagrams contributing to a given amplitude! The propagator of the off-shell gluon which carries momentum q is chosen to be $1/q^2$.

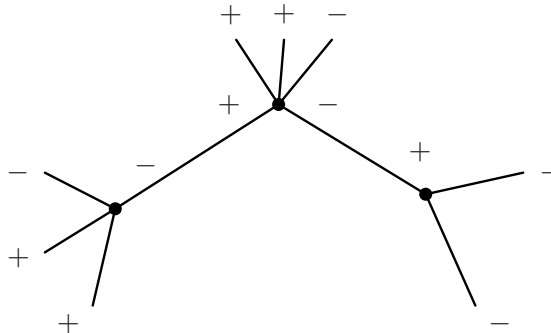


Figure 3.1: Example for an amplitude made out of MHV vertices. 3 MHV vertices are connected by 2 propagators

Figure 3.1 shows an example for a tree amplitude made out of MHV vertices. Remember that the MHV amplitude is defined for n incoming gluons, and each gluon has a definite helicity. This is for both, on-shell and off-shell gluons. If a gluon is considered to be outgoing it's helicity has to be reversed. Therefore the two ends of a propagator must have opposite helicity, since if for example one end of a propagator has incoming momenta q and positive helicity, the other end has incoming momenta $-q$ and negative helicity.

One can count the number v of vertices needed to get a non MHV amplitude: Consider an amplitude with a total of n gluons where m gluons have negative helicity. The total number of negative helicity gluons emerging from the vertices is $2v$, the number of propagators is $v - 1$. Each propagator connects exactly one negative helicity end with a positive one. Therefore the number of external negative helicity gluons m equals $2v - (v - 1)$. Hence one gets $v = m - 1$. The rules for constructing a non MHV amplitude with n gluons whereof m have negative helicity are:

- sum over all topologically different diagrams with $v = m - 1$ vertices and n outgoing gluons
- label the outer gluons e.g clockwise and sum over cyclic permutation of the gluons
- imply momentum conservation at each vertex
- choose one reference spinor for all vertices to get the off-shell spinors as defined above
- the analytic expression for each diagram is given by the product of the MHV vertices times the scalar propagators $1/q^2$

An explicit example for calculating a non MHV amplitude out of MHV-vertices will be given in section 3.3. Since pure gluonic MHV amplitudes can be extended by the use of supersymmetric Ward identities to MHV amplitudes containing one or two quark-antiquark pairs, it would not be surprising if there also exists a formalism, which extends the CSW formalism to amplitudes containing massless quarks. Indeed Georgiou and Khoze extended the number of MHV vertices by ones containing one or two $q\bar{q}$ pairs [14]. They showed that with this set of MHV vertices it is possible to calculate partial amplitudes in the same way as described above.

3.2 MHV amplitudes with a scalar

It is now of great phenomenological interest to extend this method to processes involving a massive Higgs boson. Dixon, Glover, and Khoze found a way how to generate MHV vertices containing a Higgs [13]. In the following the basic features will be summarized. Since in the Standard Model the gluon-Higgs coupling is dominated via a top loop, it seems to be a promising approach to integrate out the heavy top quark and consider the effective gluon-Higgs coupling via the dimension-5 operator proportional to $H\text{Tr}G_{\mu\nu}G^{\mu\nu}$.² For this effective coupling one gets for the Higgs plus n gluon (color-ordered) amplitudes, where all gluons have positive helicity:

$$A_n(H, 1^+, 2^+, \dots, n^+) \propto \frac{m_H^4}{\langle 12 \rangle \langle 23 \rangle \cdots \langle n-1, n \rangle \langle n1 \rangle} \quad (3.9)$$

where m_H is the mass of the Higgs boson.³ Now the first attempt would be to generate the Higgs plus three gluon amplitude $A_3(H, 1^-, 2^+, 3^+)$ from an off shell continuation of the Higgs plus two gluon amplitude above combined with the pure QCD MHV vertex $A_3(-, -, +)$. This attempt failed, the resulting amplitude is not independent of the reference momenta used to define the off-shell gluon. But this is not really surprising since the numerator of (3.9) can be written as a sum of the gluon momenta $(\sum_{1 \leq i < j \leq n} q_i)^2 = (\sum_{1 \leq i < j \leq n} \langle ij \rangle [ji])^2$, and hence (3.9) contains also anti-holomorphic spinor products $[ji]$.

This problem can be solved in the following way. The MHV twistor-space structure of the Higgs plus gluon amplitudes is best apparent by splitting the Higgs coupling to gluons into two terms, containing purely selfdual (SD) and purely antiselfdual (ASD) gluon field strength,

$$G_{SD}^{\mu\nu} = \frac{1}{2}(G^{\mu\nu} + *G^{\mu\nu}), \quad G_{ASD}^{\mu\nu} = \frac{1}{2}(G^{\mu\nu} - *G^{\mu\nu}), \quad *G^{\mu\nu} \equiv \frac{i}{2}\epsilon^{\mu\nu\rho\sigma}G_{\rho\sigma} \quad (3.10)$$

By considering the Higgs field H as the real part of a complex field $\phi = \frac{1}{2}(H + iA)$ one can make this division explicit:

$$\mathcal{L}_{H,A}^{int} = \frac{C}{2} \left[H\text{Tr}G_{\mu\nu}G^{\mu\nu} + iA\text{Tr}G_{\mu\nu}*G^{\mu\nu} \right] \quad (3.11)$$

$$= C \left[\phi\text{Tr}G_{SD\mu\nu}G_{SD}^{\mu\nu} + \phi^\dagger\text{Tr}G_{ASD\mu\nu}G_{ASD}^{\mu\nu} \right] \quad (3.12)$$

²Details to the effective Higgs gluon coupling are postponed to Chapter 4.

³Proven in [13], Appendix B.

with the normalization constant $C = \alpha_s/6\pi v$. The tree level Higgs-gluon amplitudes can be decomposed into color-ordered partial amplitudes, similar to the QCD case:

$$\mathcal{A}(H, \{k_i, \lambda_i, a_i\}) = iCg^{n-2}(\sqrt{2})^n \sum_{\sigma \in S_n/Z_n} \text{Tr}(T^{a_{\sigma(1)}} \dots T^{a_{\sigma(n)}}) A_n(H, \sigma(1^{\lambda_1} \dots n^{\lambda_n})) \quad (3.13)$$

with $\text{Tr}(T^a T^b) = \frac{1}{2}\delta^{ab}$. The basic idea is now, that due to selfduality the amplitudes for ϕ and ϕ^\dagger in each case have a simpler structure. And since $H = \phi + \phi^\dagger$ the Higgs amplitude can be recovered as the sum of the ϕ and ϕ^\dagger amplitudes. As a by-product one also obtains the amplitude for a pseudoscalar Higgs A as the difference of the ϕ and ϕ^\dagger amplitudes: $A = \frac{1}{i}(\phi - \phi^\dagger)$, since the effective coupling in the $m_{top} \rightarrow \infty$ limit of a pseudoscalar Higgs to gluons is proportional to $A \text{Tr} G_{\mu\nu}^* G^{\mu\nu}$. Using Berends-Giele recursion relations and off-shell currents, one can prove that, as in the QCD case, the helicity amplitudes for ϕ and n gluons of positive helicity vanish, as do the amplitudes where $n - 1$ gluons have positive helicity:

$$A_n(\phi, 1^\pm, 2^+, \dots, n^+) = 0 \quad (3.14)$$

The first non vanishing ϕ amplitudes, which are the ϕ -MHV amplitudes, are those with exactly two negative helicity gluons and an arbitrary number of positive helicity gluons. The first known ϕ -MHV amplitudes have the same structure as the QCD amplitudes, the only difference is that now the sum of the gluon momenta equals the momenta of the Higgs boson, whereas in pure QCD the sum equals zero. The color stripped amplitudes are:

$$A_2(\phi, 1^-, 2^-) = \frac{\langle 12 \rangle^4}{\langle 12 \rangle \langle 21 \rangle} = -\langle 12 \rangle^2 \quad (3.15)$$

$$A_3(\phi, 1^-, 2^-, 3^+) = \frac{\langle 12 \rangle^4}{\langle 12 \rangle \langle 23 \rangle \langle 31 \rangle} = \frac{\langle 12 \rangle^3}{\langle 23 \rangle \langle 31 \rangle} \quad (3.16)$$

$$A_4(\phi, 1^-, 2^-, 3^+, 4^+) = \frac{\langle 12 \rangle^4}{\langle 12 \rangle \langle 23 \rangle \langle 34 \rangle \langle 41 \rangle} \quad (3.17)$$

This leads to the assertion for all ϕ -MHV amplitudes:

$$A_n(\phi, 1^+, \dots, j^-, \dots, k^-, \dots, n^+) = \frac{\langle jk \rangle^4}{\langle 12 \rangle \langle 23 \rangle \dots \langle n-1, n \rangle \langle n1 \rangle} \quad (3.18)$$

Comparing the structure of (3.18) with the pure QCD amplitude (3.1) one observes that the amplitudes have identical form. Therefore one proposes that the off-shell continuation of the ϕ -MHV amplitudes is identical to the pure gluonic case: everywhere an off-shell leg i with momentum k_i appears, one constructs the corresponding holomorphic spinor by $\lambda_{i,a} = (k_i)_{a\dot{a}} \xi^{\dot{a}}$. Again $\xi^{\dot{a}}$ is an arbitrary reference spinor, chosen to be the same for all MHV diagrams contributing to a given amplitude. By combining now the ϕ -MHV amplitudes with pure QCD MHV amplitudes one can construct non-MHV amplitudes in the same way as in the CSW approach.

For the ϕ^\dagger field one has similar expressions. Here the amplitudes with n or $n - 1$ gluons of negative helicity vanish:

$$A_n(\phi^\dagger, 1^\mp, 2^-, \dots, n^-) = 0 \quad (3.19)$$

The ϕ^\dagger -anti-MHV amplitudes are:

$$A_2(\phi^\dagger, 1^+, 2^+) = \frac{[12]^4}{[12][21]} = -[12]^2 \quad (3.20)$$

$$A_3(\phi^\dagger, 1^+, 2^+, 3^-) = \frac{[12]^4}{[12][23][31]} = \frac{[12]^3}{[23][31]} \quad (3.21)$$

$$A_n(\phi^\dagger, 1^-, \dots, i^+, \dots, j^+, \dots, n^-) = \frac{[ij]^4}{[12][23] \cdots [n-1, n][n1]} \quad (3.22)$$

They are called “anti-MHV” amplitudes, since the amplitude is made of anti-holomorphic spinor products $[ij]$. One has to combine them with pure QCD anti-MHV amplitudes to get non-MHV ϕ^\dagger amplitudes. One can also obtain these amplitudes by applying parity to the ϕ amplitudes, that is computing with ϕ , reversing the helicity of every gluon and exchanging $\langle ij \rangle \leftrightarrow [ij]$.

Of special interest here and in the following is the $gg \rightarrow ggH$ scattering amplitude. The ϕ and ϕ^\dagger amplitudes contributing are depicted in table 3.1. The simplest helicity configuration for this process is the $--++$ case, since one only needs to add the MHV amplitudes for ϕ and ϕ^\dagger whose analytic expressions are given by (3.18) and (3.22) for $n = 4$. The other helicity configurations have only a contribution of either the ϕ or the ϕ^\dagger amplitude. However, calculating them requires more effort, since for the next to MHV amplitude (the ϕ amplitude with three negative helicity gluons or the ϕ^\dagger amplitude with three positive helicity gluons respectively, short NMHV amplitude) one has two topological distinct diagrams contributing to the amplitude shown in figure 3.2. These amplitudes are made out of one ϕ -MHV vertex and one QCD MHV-vertex. Further one has to sum over the 4 cyclic permutations of the gluons giving a total of 7 terms (the 2. diagram in figure 3.2 with the tree negative helicity gluons on the left hand vertex does not contribute, since this is not a MHV vertex).

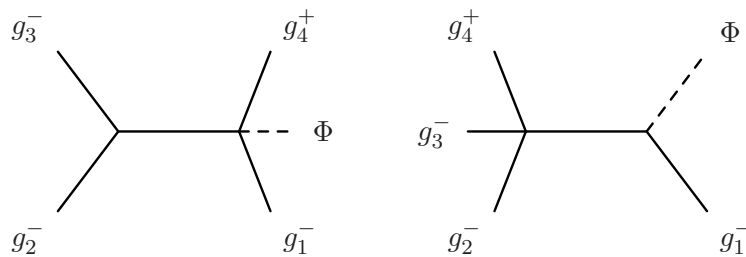


Figure 3.2: The two topological distinct diagrams contributing to the ϕ -NMHV amplitude. The g_i 's are the gluons carrying negative and positive helicities respectively. To obtain the full amplitude one has to sum over the cyclic permutations of the gluons.

It becomes worse for the NNMHV amplitude (next-to-next-to MHV), since there are 3 topological different diagrams made out of 3 MHV vertices, one ϕ -MHV vertex and two QCD MHV-vertices, leading to 10 contributions to be summed over (see figure 3.3). However, the most involved ϕ and ϕ^\dagger amplitudes can also be expressed by analytic expressions, as one can see from (3.9), where all gluons carry positive helicity. Since for this helicity configuration, the ϕ amplitude vanishes, it is equivalent to the ϕ^\dagger amplitude! Similarly the “all minus” ϕ amplitude is given by the same expression but right handed

helicities	++++	+++-	++--	+---	----
ϕ	-	-	MHV	NMHV	NNMHV
ϕ^\dagger	NNMHV	NMHV	MHV	-	-

Table 3.1: helicity amplitudes contributing to the $ggggH \rightarrow 0$ process. The $gg \rightarrow ggH$ process can be obtained by crossing

spinors exchanged by left handed ones. Remember that since this amplitude is not holomorphic in λ_a nor in $\lambda_{\dot{a}}$ it is not feasible to use them as MHV-vertices.

Again it is possible to extend the MHV rules to MHV rules containing one or two $q\bar{q}$ pairs by embedding the theory into a supersymmetric theory [15]. As in the pure gluonic case, one can construct ϕ -MHV vertices containing $q\bar{q}$ pairs. By combining them with QCD MHV vertices – the ones with and without quarks – one can now compute non ϕ -MHV amplitudes containing quarks by the same scalar graph approach.

One can now anticipate, that the method for constructing MHV amplitudes for effective theories generalizes to other effective theories in QCD. Consider an interaction that can be described by higher dimensional operators in the effective action. The idea for constructing MHV rules for this effective action, is to split the field strength into a selfdual and an antiselfdual part. The interaction amplitude should then be given by purely holomorphic expressions and purely antiholomorphic ones respectively. There is another example for an effective theory, this time described by the dimension-6 operator $\text{Tr}(G_\mu^\nu G_\nu^\rho G_\rho^\mu)$ [13]. The authors sketch that MHV vertices for this theory can be constructed in the same way as it was explained above. In Chapter 6 this method will be used to construct MHV amplitudes for certain dimension-7 operators. These new amplitudes will be used as MHV-vertices as well.

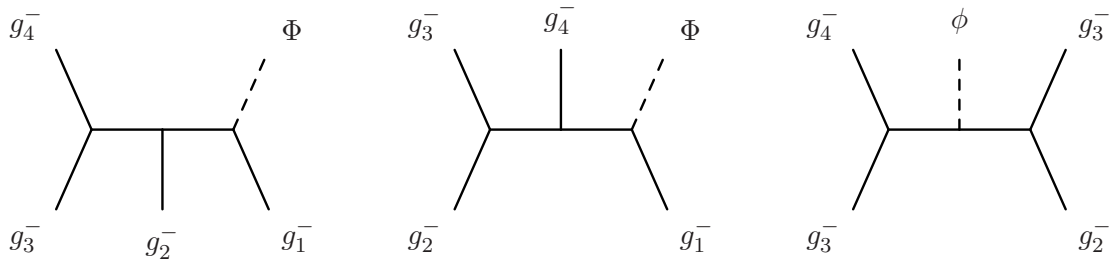


Figure 3.3: The tree topological distinct diagrams contributing to the ϕ NNMHV amplitude. To obtain the full amplitude one has to sum over the cyclic permutations of the gluons.

3.3 MHV- ϕ amplitudes in a parton level Monte Carlo simulation

Let's now turn to the process $pp \rightarrow Hjj$. If one wants to calculate differential cross sections one has to consider the tree subprocesses $qq \rightarrow qqH$, $qg \rightarrow qgH$ and $gg \rightarrow ggH$. This process is included to leading order in the parton level Monte Carlo program VBFNLO [16]. In the SM the dominant production mode for this process is the one

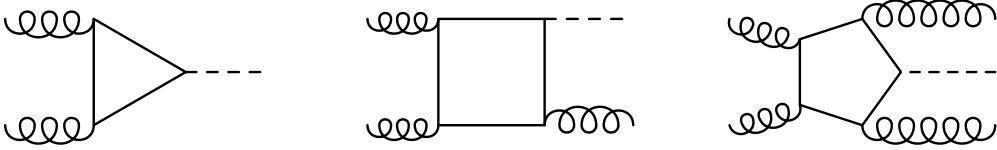


Figure 3.4: Diagrams relevant for Higgs production via gluon fusion

where the Higgs boson couples to gluons via a top loop. Therefore the LO calculation already includes one loop diagrams, containing three, four and five point functions depicted in figure 3.4.

In the large top mass approximation, however, the calculation simplifies enormously, since each loop can be replaced by an effective Higgs gluon coupling. This has two advantages: first, one does not have to deal with numerical instabilities arising from vanishing Gram determinants and second, the calculation is far faster than the full loop calculation. But even then, the calculation of (differential) cross sections in the large top mass limit can take a long time, since if one wants small theoretical errors, one has to calculate the amplitude for many phase space points ($\propto 10^7 - 10^8 PSP$). For this reason, the time spent in calculating an amplitude is an important issue of a Monte Carlo program. And since for the large top mass approximation there is the scalar graph approach described above for calculating scattering amplitudes, it is interesting to compare the time needed for calculating the cross section for $pp \rightarrow Hjj$ – once calculated by using Feynman diagrams and once by using MHV techniques.

To make a real comparison of the time needed for calculating the amplitudes, in both cases the Monte Carlo program VBFNLO was used with an additional switch, allowing one to choose in which way the amplitudes should be calculated.

Implementing the ϕ -MHV amplitudes into VBFNLO

First of all study the process $gg \rightarrow ggH$. For this process five different helicity configurations appear, as shown in in table 3.1. The amplitudes are calculated in the subroutine **HiggsGG**, the code is embedded into the file **gf_higgsME.f**. The simplest helicity configuration is the one with two positive and two negative helicity gluons, since then both, the ϕ and the ϕ^\dagger amplitudes are MHV amplitudes, given by (3.18) and (3.22) for $n = 4$. The analytic expression for the left handed spinor λ_a and right handed spinor $\tilde{\lambda}_{\dot{a}}$ corresponding to the gluon with momentum p can be obtained in the following way:

$$\begin{aligned}
 (\sigma^\mu)_{a\dot{a}} p_\mu &= \lambda_a \tilde{\lambda}_{\dot{a}} \\
 - \begin{pmatrix} p_0 + p_3 & p_1 - ip_2 \\ p_1 + ip_2 & p_0 - p_3 \end{pmatrix}_{a\dot{a}} &= \lambda_a \tilde{\lambda}_{\dot{a}} \\
 \Rightarrow \lambda_a &= \begin{cases} \begin{pmatrix} \sqrt{p_0 + p_3} \\ \frac{p_1 + ip_2}{\sqrt{p_0 + p_3}} \end{pmatrix} & \text{for } p_0 \neq -p_3 \\ \begin{pmatrix} 0 \\ \sqrt{2p_0} \end{pmatrix} & \text{for } p_0 = -p_3 \end{cases} & (3.23)
 \end{aligned}$$

$$\tilde{\lambda}_{\dot{a}} = -\lambda_a^\dagger \quad (3.24)$$

with $(\sigma^\mu)_{a\dot{a}} = (-\mathbb{1}, \vec{\sigma})$. The last minus sign can be dropped, since calculating scattering amplitudes involve always an even number of spinors. If the considered gluon is outgoing the helicity has to be reversed and $p_i \rightarrow -p_i$. The calculation of the next-to-maximally helicity violating amplitudes, that is the ϕ amplitude with three negative and one positive helicity (ingoing) gluons and the ϕ^\dagger amplitude with three positive helicity and one negative helicity gluons respectively, is more involved, since now one has to connect two MHV amplitudes with a scalar propagator. For the ϕ amplitude one has to sum over a total of seven diagrams, which are essentially made out of two types of diagrams and the cyclic permutations of their external gluon legs. The two types of diagrams and the corresponding analytic expressions are:

$$\begin{array}{c}
 \Phi \\
 \diagdown \\
 4^- \text{---} \xi^+ \text{---} \xi^- \\
 \diagup \\
 3^- \\
 \phi \\
 \diagdown \\
 4^-
 \end{array}
 \begin{array}{c}
 1^+ \\
 \diagdown \\
 2^- \\
 \diagup \\
 1^+ \\
 2^- \\
 \diagdown \\
 3^-
 \end{array}
 = \frac{\langle 34 \rangle^4}{\langle 34 \rangle \langle 4\xi \rangle \langle \xi 3 \rangle} \frac{1}{q_{12}^2} \frac{\langle 2\xi \rangle^4}{\langle 12 \rangle \langle 2\xi \rangle \langle \xi 1 \rangle} \quad (3.25)$$

$$\begin{array}{c}
 3^- \\
 \phi \\
 \diagdown \\
 4^-
 \end{array}
 \begin{array}{c}
 \xi^- \text{---} \xi^+ \\
 \diagup \\
 2^- \\
 \diagdown \\
 3^-
 \end{array}
 \begin{array}{c}
 1^+ \\
 \diagdown \\
 2^- \\
 \diagup \\
 1^+ \\
 2^- \\
 \diagdown \\
 3^-
 \end{array}
 = \frac{\langle 4\xi \rangle^4}{\langle 4\xi \rangle \langle \xi 4 \rangle} \frac{1}{q_{13}^2} \frac{\langle 23 \rangle^4}{\langle 12 \rangle \langle 23 \rangle \langle 3\xi \rangle \langle \xi 1 \rangle} \quad (3.26)$$

where $q_{ij} = (q_i + q_{i+1} + \dots + q_j)$ and ξ is given by

$$\begin{aligned}
 \xi_a &\equiv (\sigma^\mu)_{a\dot{a}} q_\mu \tilde{\eta}^{\dot{a}} \\
 &= - \begin{pmatrix} q_0 + q_3 & q_1 - iq_2 \\ q_1 + iq_2 & q_0 - q_3 \end{pmatrix}_{a\dot{a}} \tilde{\eta}^{\dot{a}} \\
 &= \begin{pmatrix} q_0 + q_3 + q_1 - iq_2 \\ q_1 + iq_2 + q_0 - q_3 \end{pmatrix}_a
 \end{aligned} \quad (3.27)$$

in the last line, for simplicity, the arbitrary spinor $\tilde{\eta}$ was chosen to be $\tilde{\eta}^{\dot{a}} = (-1, -1)^T$. The right handed off-shell spinor is

$$\xi_{\dot{a}} \equiv \eta^a (\sigma^\mu)_{a\dot{a}} q_\mu \quad (3.28)$$

where η can be chosen such that $\xi_{\dot{a}} = \xi_{\dot{a}}^\dagger$. Remember that the diagram (3.26) with all negative helicity gluons on the right hand side is absent, since the corresponding vertex is not a MHV vertex. The full expression for the partial amplitude with gluons

of helicity $+- --$ is then given by (with ξ carrying momenta q_{ij})

$$\begin{aligned}
A_4(\phi, g_1^+, g_2^-, g_3^-, g_4^-) &= \frac{\langle 34 \rangle^4}{\langle 34 \rangle \langle 4\xi \rangle \langle \xi 3 \rangle} \frac{1}{q_{12}^2} \frac{\langle 2\xi \rangle^4}{\langle 12 \rangle \langle 2\xi \rangle \langle \xi 1 \rangle} + \frac{\langle 23 \rangle^4}{\langle 23 \rangle \langle 3\xi \rangle \langle \xi 2 \rangle} \frac{1}{q_{41}^2} \frac{\langle 4\xi \rangle^4}{\langle 41 \rangle \langle 1\xi \rangle \langle \xi 4 \rangle} \\
&+ \frac{\langle 4\xi \rangle^4}{\langle 41 \rangle \langle 1\xi \rangle \langle \xi 4 \rangle} \frac{1}{q_{23}^2} \frac{\langle 23 \rangle^4}{\langle 23 \rangle \langle 3\xi \rangle \langle \xi 2 \rangle} + \frac{\langle 2\xi \rangle^4}{\langle 12 \rangle \langle 2\xi \rangle \langle \xi 1 \rangle} \frac{1}{q_{34}^2} \frac{\langle 34 \rangle^4}{\langle 34 \rangle \langle 4\xi \rangle \langle \xi 3 \rangle} \\
&+ \frac{\langle 4\xi \rangle^4}{\langle 4\xi \rangle \langle \xi 4 \rangle} \frac{1}{q_{13}^2} \frac{\langle 23 \rangle^4}{\langle 12 \rangle \langle 23 \rangle \langle 3\xi \rangle \langle \xi 1 \rangle} + \frac{\langle 3\xi \rangle^4}{\langle 3\xi \rangle \langle \xi 3 \rangle} \frac{1}{q_{42}^2} \frac{\langle 42 \rangle^4}{\langle 41 \rangle \langle 12 \rangle \langle 2\xi \rangle \langle \xi 4 \rangle} \\
&+ \frac{\langle 2\xi \rangle^4}{\langle 2\xi \rangle \langle \xi 2 \rangle} \frac{1}{q_{31}^2} \frac{\langle 34 \rangle^4}{\langle 34 \rangle \langle 41 \rangle \langle 1\xi \rangle \langle \xi 3 \rangle}
\end{aligned}$$

This expression can for sure be simplified, what should be done before implementing it into a program. This lengthy form is intentional, so that the several parts can be reconstructed.

To get the NMHV- ϕ^\dagger amplitude one either calculates the amplitudes in the same manner as for ϕ , just switching the helicities and replacing $\langle \cdot, \cdot \rangle \leftrightarrow [\cdot, \cdot]$, or simpler, one just takes the complex conjugate of the ϕ -MHV amplitude with reversed helicities. This is possible, since one can always choose $\tilde{\lambda}_a$ to be the complex conjugate of λ_a as mentioned above.

Now, the only missing helicity configurations are the ones with all gluons carrying either positive or negative helicities. Calculating them by connecting MHV vertices would require 10 independent diagrams containing two propagators. Fortunately for this helicity configuration one can use the compact expression given in (3.9):

$$A_4(\phi, g_1^-, g_2^-, g_3^-, g_4^-) = \frac{m_H^4}{[12][23][34][41]}$$

Finally, since all partial amplitudes for ϕ and ϕ^\dagger are available, one can reconstruct the partial amplitudes for the Higgs H and the pseudoscalar Higgs A . Because $H = \phi + \phi^\dagger$ the Higgs amplitude can be recovered as the sum of the ϕ and ϕ^\dagger amplitudes. The amplitude for the pseudoscalar Higgs is i times the difference of the ϕ and ϕ^\dagger amplitudes $A = i(\phi - \phi^\dagger)$.⁴ To obtain the full amplitude one has to multiply the partial amplitudes with the corresponding color factor and sum over all non-cyclic permutations as shown in (3.13). The color factors are the same as the ones for the amplitudes calculated in VBFNLO. Define

$$\begin{aligned}
c_1 &\equiv \text{Tr}(T^{a_1} T^{a_2} T^{a_3} T^{a_4}) + \text{Tr}(T^{a_4} T^{a_3} T^{a_2} T^{a_1}) \\
c_2 &\equiv \text{Tr}(T^{a_1} T^{a_3} T^{a_4} T^{a_2}) + \text{Tr}(T^{a_2} T^{a_4} T^{a_3} T^{a_1}) \\
c_3 &\equiv \text{Tr}(T^{a_1} T^{a_4} T^{a_2} T^{a_3}) + \text{Tr}(T^{a_3} T^{a_2} T^{a_4} T^{a_1})
\end{aligned} \tag{3.29}$$

⁴one has to consider an additional minus sign, since $iA\text{Tr}G_{\mu\nu}^*G^{\mu\nu} = -\frac{1}{2}A\epsilon_{\mu\nu\rho\sigma}G^{\mu\nu}G^{\rho\sigma}$.

With this definition, the full amplitude and the color summed amplitude square are given by

$$\begin{aligned} \mathcal{A} &= \underbrace{ig^2(\sqrt{2})^4}_{\frac{i2\alpha_s^2}{rv}} \sum_{i=1}^3 c_i A_4^i \\ \Rightarrow \sum_{\text{col}} |\mathcal{A}|^2 &= \frac{4\alpha_s^4}{r^2 v^2} \left(C_1 \sum_{i=1}^3 |A_4^i|^2 + C_2 \sum_{i,j=1;i \neq j}^3 A_4^i A_4^{j*} \right) \end{aligned}$$

with $r = 3$ for a CP-even, $r = 2$ for a CP-odd Higgs and

$$\begin{aligned} C_1 &\equiv \sum_{\text{col}} c_i c_i = \frac{(N^2 - 1)(N^4 - 2N^2 + 6)}{8N^2} = \frac{23}{3} \quad (\text{no summation over } i) \\ C_2 &\equiv \sum_{\text{col}} c_i c_j = -\frac{(N^2 - 1)(N^2 - 3)}{4N^2} = -\frac{4}{3} \quad i \neq j \end{aligned}$$

If one wants to implement MHV amplitudes for the subprocesses $qg \rightarrow qgH$ or $qq \rightarrow qqH$ one needs additional MHV vertices containing one or two quark-antiquark pairs. The expressions for the MHV amplitudes with $q\bar{q}$ pairs is strongly related to purely gluonic MHV amplitudes by supersymmetric Ward identities. The analytic expression for the MHV amplitudes and how to use them as vertices to obtain non-MHV amplitudes with $q\bar{q}$ pairs is described in detail in [14, 15]. Going into detail would not bring further insight. One should just notice, that since all particles are ingoing, the helicity of the quark is opposite to the antiquark. Therefore the $qg \rightarrow qgH$ amplitude only contains MHV and NMHV amplitudes, and more pleasant, for the $qQ \rightarrow qQH$ scattering only MHV amplitudes appear, making the calculation extremely simple. When implementing the amplitudes into a program, one again has to be very careful with the conventions chosen. In this case, when implementing them into an existing program like VBFNLO one can just attach the amplitudes loosely, fixing missing constants and phases by comparing with the already existing amplitudes calculated by the program using Feynman diagrams.

Having both types of amplitudes in the same Monte Carlo program, one can now test the speed-up. To get the real amount of time spent, the program was compiled using **gprof** which is a GNU profiler. This allows one to see where the program spent its' time and which functions called which other functions while it was executing. The program was run on a "Intel(R) Pentium(R) 4 CPU 3.00GHz" machine with 1GB RAM and SUSE 10.0 as operating system. In all three cases a set of minimal cuts was applied:

$$p_{T,min} \geq 20, \quad \eta_{max} \leq 5, \quad R_{jj} \geq 0.6 \quad (3.30)$$

In the following the time spent for the three different subprocesses $gg \rightarrow ggH$, $gq \rightarrow gqH$ and $qq \rightarrow qqH$ will be compared. Additionally it is distinguished whether the Higgs is CP-even, CP-odd or a linear combination of both.

gg \rightarrow ggH – MHV amplitudes vs. Feynman diagrams:

The tables are organized in the following way: First of all, they give the total cross section, which is a kind of check that indeed both ways of calculating the amplitudes give the same result and are programmed without errors. Second it lists the total amount of time spent for running the program. The next number gives the time spent in the subroutine which is responsible for calculating the matrix elements, followed by the number of times this subroutine was called. The last line finally gives the average amount of time needed to calculate the matrix element for one single call. The calculation was performed for 2^{24} phase space points.

CP-even Higgs	Feynman diagrams	MHV
σ_{tot}	2075.97 ± 1.43 fb	2075.97 ± 1.43 fb
total time	1590.99 sec	1053.5 sec
time spent in HiggsGG	809.35 sec	290.39 sec
# of HiggsGG calls	12966121	12966121
HiggsGG $\frac{\text{time}}{\text{calls}}$	$6.24 \cdot 10^{-5} \frac{\text{sec}}{\text{calls}}$	$2.24 \cdot 10^{-5} \frac{\text{sec}}{\text{calls}}$

One can see that the calculation of the amplitudes for a CP-even Higgs with MHV techniques is 2.79 times faster than the calculation with Feynman diagrams.

CP-odd Higgs	Feynman diagrams	MHV
σ_{tot}	4618.11 ± 3.16 fb	4618.11 ± 3.16 fb
total time	1528.92 sec	1068.5 sec
time spent in HiggsGG	749.95 sec	304.08 sec
# of HiggsGG calls	12973963	12973963
HiggsGG $\frac{\text{time}}{\text{calls}}$	$5.78 \cdot 10^{-5} \frac{\text{sec}}{\text{calls}}$	$2.34 \cdot 10^{-5} \frac{\text{sec}}{\text{calls}}$

For the CP-odd Higgs the calculation with MHV diagrams is 2.47 times faster. The time needed for the MHV approach is almost like in the CP-even case, but calculating with Feynman diagrams is faster in the CP-odd case, because of the simpler tensor structure of the vertices.

CP-even + CP-odd Higgs	Feynman diagrams	MHV
σ_{tot}	6694.77 ± 4.62 fb	6694.77 ± 4.62 fb
total time	2820.47 sec	1123.36 sec
time spent in HiggsGG	2019.92 sec	327.35 sec
# of HiggsGG calls	12981120	12981120
HiggsGG $\frac{\text{time}}{\text{calls}}$	$15.56 \cdot 10^{-5} \frac{\text{sec}}{\text{calls}}$	$2.52 \cdot 10^{-5} \frac{\text{sec}}{\text{calls}}$

The calculation for the Higgs with CP-even and CP-odd coupling with MHV amplitudes is 6.17 times faster than calculating using Feynman diagrams. The main reason for this is that when calculating the amplitude for a given helicity configuration with MHV techniques, one always has to calculate the ϕ and ϕ^\dagger amplitudes which are just linear combinations of the H and A amplitudes. Therefore in this case one has to perform only one calculation, compared to calculating using Feynman diagrams, where one has to compute the CP-even and CP-odd case separately.

$qg \rightarrow qgH$ – MHV amplitudes vs. Feynman diagrams:

For this subprocess the calculation was performed for 2^{22} phase space points. The calculation with MHV techniques is hardly faster than VBFNLO. Only for a Higgs which has CP-even and CP-odd coupling, the MHV approach is considerably faster (almost a factor 2) for the same reasons as for the ggH case. The following list shows the average time needed to calculate the matrix element for one single call:

process	Feynman diagrams	MHV
CP-even Higgs	$3.82 \cdot 10^{-5} \frac{\text{sec}}{\text{calls}}$	$3.45 \cdot 10^{-5} \frac{\text{sec}}{\text{calls}}$
CP-odd Higgs	$3.75 \cdot 10^{-5} \frac{\text{sec}}{\text{calls}}$	$3.28 \cdot 10^{-5} \frac{\text{sec}}{\text{calls}}$
CP-even + CP-odd Higgs	$5.65 \cdot 10^{-5} \frac{\text{sec}}{\text{calls}}$	$3.30 \cdot 10^{-5} \frac{\text{sec}}{\text{calls}}$

$qq \rightarrow qqH$ – MHV amplitudes vs. Feynman diagrams:

The results for this subprocess are comparable to the ones for the qgH scattering. Again only for a Higgs with CP-even and CP-odd character the calculation with MHV amplitudes is really faster:

process	Feynman diagrams	MHV
CP-even Higgs	$5.90 \cdot 10^{-6} \frac{\text{sec}}{\text{calls}}$	$4.74 \cdot 10^{-6} \frac{\text{sec}}{\text{calls}}$
CP-odd Higgs	$5.81 \cdot 10^{-6} \frac{\text{sec}}{\text{calls}}$	$4.74 \cdot 10^{-6} \frac{\text{sec}}{\text{calls}}$
CP-even + CP-odd Higgs	$7.60 \cdot 10^{-6} \frac{\text{sec}}{\text{calls}}$	$5.38 \cdot 10^{-6} \frac{\text{sec}}{\text{calls}}$

Altogether one can say, that only for the $gg \rightarrow ggH$ scattering the calculation with MHV vertices is considerably faster than calculating with Feynman diagrams. The main reason for this is, that for the process involving only gluons, there are many more Feynman diagrams to be considered compared to the processes containing quarks, which makes the calculation longer. From the MHV point of view, naively this process is easiest to calculate, since one has only two types of MHV vertices to combine: one with gluons and a ϕ field and one containing only gluons, whereas as soon as quarks appear, there are four different MHV vertices which have to be taken into account: the two vertices above and the ones containing a quark antiquark pair. On the other hand, the quark anti-quark pair puts additional constraints on the helicity configuration that may appear ($\text{helicity}(q) = -\text{helicity}(\bar{q})$), whereby the helicity configurations that are most complicated to calculate are absent (e.g. for the qqH scattering only MHV amplitudes are present). One may now wonder why the ggH process is faster then

the qgH process. The answer is due to the fact that first of all, the usual complicated NNMHV ggH amplitudes are calculated by using the compact expression (3.9) and second, the qgH scattering consists of four subprocesses one has to sum over, depending on the initial and final state partons.

The benefit of using MHV vertices may become even more apparent when more partons are present, such as $gg \rightarrow gggH$ appearing e.g. in the next-to leading order calculation for the process examined here.

3.4 Helicity contributions to $d\sigma/d\Delta\Phi_{jj}$

It is possible to distinguish the tensor structure of the effective Hgg coupling experimentally. This is best done by looking at the distribution $d\sigma/d\Delta\Phi_{jj}$, since $\Delta\Phi_{jj}$ is a parity odd variable [18]. $\Delta\Phi_{jj}$ is defined as the azimuthal angle of the away jet minus the azimuthal angle of the towards jet – when looking into one particular beam direction. The value of $\Delta\Phi_{jj}$ does not change when looking into the opposite beam direction. For the following discussion, an additional cut on the minimal pseudorapidity between the two jets, $\eta_{jj} = |\eta_{j1} - \eta_{j2}|$, was performed, since then the difference between CP-even and CP-odd coupling becomes more apparent:

$$p_{T,min} \geq 20, \quad \eta_{max} \leq 5, \quad R_{jj} \geq 0.6, \quad \eta_{jj} > 3 \quad (3.31)$$

In figure 3.5 one can see the differential cross section for $\Delta\Phi_{jj}$ for a CP-even and a CP-

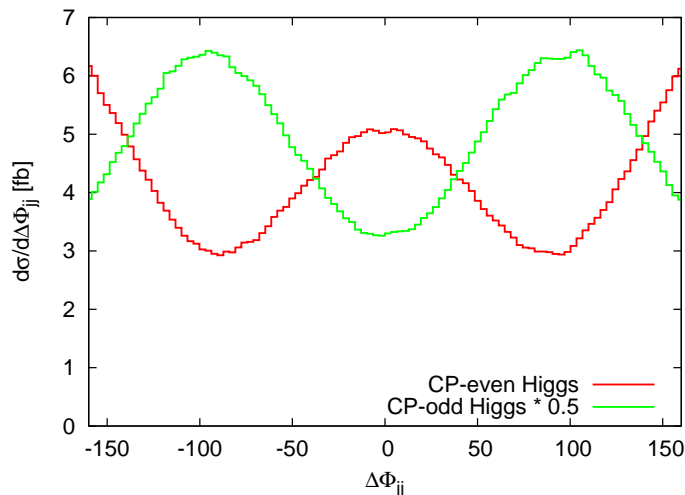


Figure 3.5: Differential cross section of $\Delta\Phi_{jj}$ for $gg \rightarrow ggH/A$. Red curve: CP-even Higgs. Green curve: CP-odd Higgs. The differential cross section of the CP-odd Higgs was scaled by a factor 0.5

odd Higgs. It takes just the subprocess $gg \rightarrow ggH$ into account. The CP-even Higgs distribution has its maxima at $\Delta\Phi_{jj} = 0$, while the CP-odd Higgs takes its minima. The distribution for a Higgs which is a linear combination of both would also give such a characteristic oscillation, with the minima and maxima respectively shifted away from zero. One may wonder if some specific helicity configurations are responsible for the oscillation while other perform the offset. For this process there are 16 possible helicity configurations, which can be divided into five classes, with each helicity configuration of a class giving exactly the same contribution to the total cross section:

-
- (1) All helicities (initial and final state) are the same, e.g. $-- \rightarrow --$ ($2\times$)
 $\approx 57\%$ of σ_{tot}
- (2) Initial and final state helicities respectively are different, e.g. $-+ \rightarrow +-$ ($4\times$)
 $\approx 32\%$ of σ_{tot}
- (3) Initial state helicities are the same, final state differ, e.g. $-- \rightarrow -+$ ($4\times$)
 $\approx 6\%$ of σ_{tot}
- (4) Initial state helicities differ, final state are the same, e.g. $+ - \rightarrow --$ ($4\times$)
 $\approx 5\%$ of σ_{tot}
- (5) The two initial and final state helicities are the same, but the sign of initial and final state differs, e.g. $-- \rightarrow ++$ ($2\times$)
 $\approx 0\%$ of σ_{tot}

The helicity configurations that belong to (1) and (2) are those that lead to the MHV amplitudes for ϕ and ϕ^\dagger (remember that MHV amplitudes are defined for all particles incoming). They are responsible for the main part of the total cross section, together they contribute about 90%. (3) – (5) yield zero in pure QCD but are present here because of the scalar, see (3.1) and (3.18). (3) and (4) are the NMHV amplitudes for ϕ and ϕ^\dagger while (5) is the NNMHV amplitude. One may suspect that the large invariant mass \sqrt{s} of the incoming partons is responsible for the suppression of the NMHV and NNMHV amplitudes. This can be motivated by comparing the analytic expression for the partial amplitudes of (1) and (5):

$$\frac{\langle ij \rangle^4}{\langle 12 \rangle \langle 23 \rangle \langle 34 \rangle \langle 41 \rangle} \leftrightarrow \frac{m_H^4}{[12][23][34][41]} \quad (3.32)$$

Having a look at (3.23) one can see, that the spinor products are of the magnitude of the energy of the partons $\langle ij \rangle \propto TeV$ while $m_H \propto 0.1TeV$, thus (5) gets suppressed by a factor $\propto 10^{-4}$.

Figure 3.6 shows the contributions to $d\sigma/\Delta\Phi_{jj}$ of the different helicity configurations

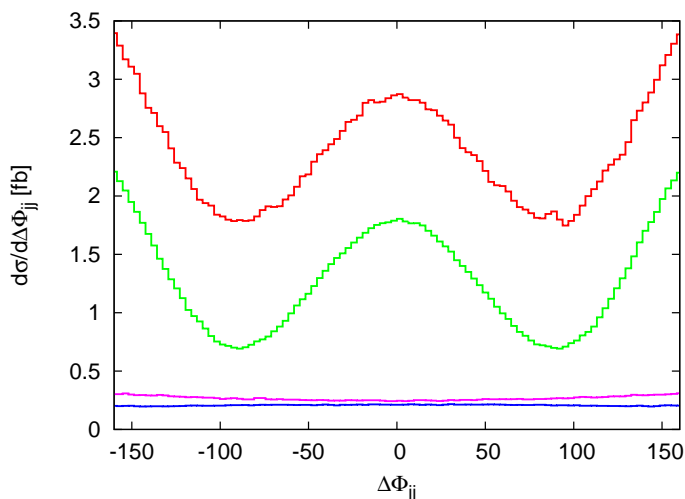


Figure 3.6: Differential cross section of $\Delta\Phi_{jj}$ for $gg \rightarrow ggH$. The different helicity configurations are shown separately:
Red: Type (1) : $-- \rightarrow --$.
Green: Type (2) : $-+ \rightarrow +-$.
Purple: Type (3) : $-- \rightarrow -+$.
Blue: Type (4) : $+ - \rightarrow --$.

(1) to (5). Only the helicity configurations (1) and (2) have the oscillating behavior, while (3), (4), and (5) do not oscillate (since the cross section of (5) is so small it's not shown, but it would not show an oscillating behavior at all). The amplitudes of (3), (4) and (5) for H are equivalent to the amplitudes for ϕ and ϕ^\dagger respectively, while the amplitudes for (1) and (2) are given by the sum and difference of ϕ and ϕ^\dagger . One should notice that the complex combinations of H and A that form ϕ and ϕ^\dagger show no oscillation – for any helicity configuration (see figure 3.7). Thus the result that one has

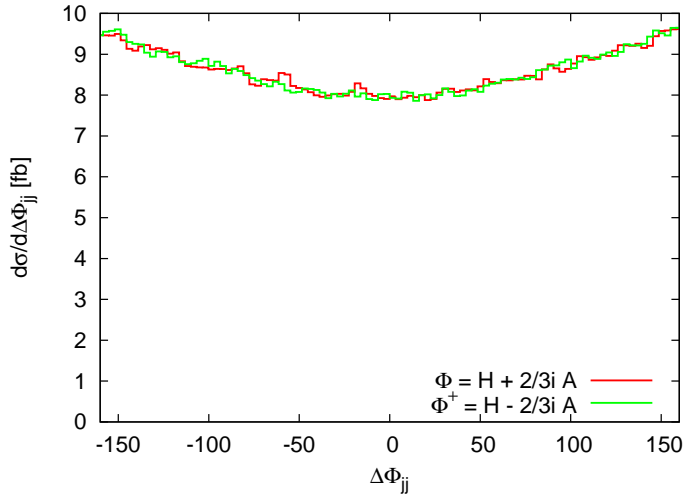


Figure 3.7: Differential cross section for ϕ and ϕ^\dagger of $\Delta\Phi_{jj}$ for $gg \rightarrow ggH$. No oscillation occurs.

obtained for a CP-even Higgs also holds for a CP-odd Higgs or a linear combination of both (with real coefficients): The only amplitudes that oscillate in $\Delta\Phi_{jj}$ are the ones that are given by a linear combination of ϕ and ϕ^\dagger – and are therefore (at least in the four gluon case) the MHV amplitudes.

A similar behavior occurs in case of the quark gluon scattering, see figure 3.8. Here

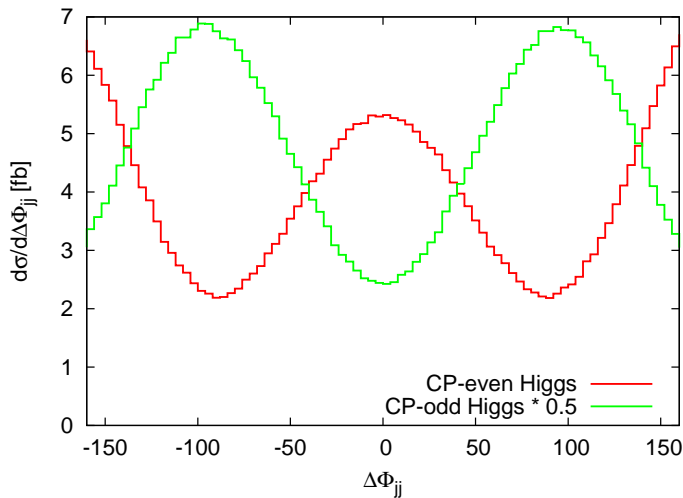
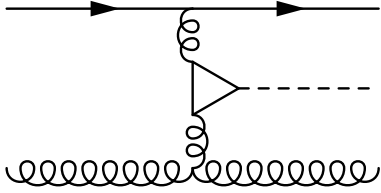


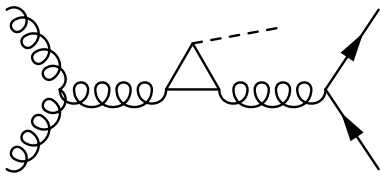
Figure 3.8: Differential cross section of $\Delta\Phi_{jj}$ for $qq \rightarrow qqH/A$. Red curve: CP-even Higgs. Green curve: CP-odd Higgs. The differential cross section of the CP-odd Higgs was scaled by a factor 0.5

it is reasonable to distinguish whether one or two quarks are in the initial or final state. The total cross section for qqH scattering with CP-even Higgs and the cuts (3.31) is about $1.5pb$. The following processes contribute to the total cross section:



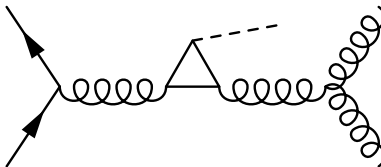
$qq \rightarrow qqH$: This process contains one quark and one gluon in the initial and final state, respectively. The Higgs is produced via t-channel exchange of a gluon, as shown on the left-hand side. It is the main process of the qqH scattering, representing 99,0% of σ_{tot} . Having

a look at the contributions for $\Delta\Phi_{jj}$ for different helicity configurations, one finds an analog behavior as for the ggH case: The corresponding MHV amplitudes are the only ones that oscillate, whilst the NMHV amplitudes show no oscillation at all, see figure 3.9. (The NNMHV amplitudes are not present in this process due to the quark pair). The $\Delta\Phi_{jj}$ distribution of the complex combination of the CP-even and CP-odd amplitude, $\phi^{(\dagger)} = H \pm 2/3iA$, behave exactly like in the ggH case, figure 3.7, viz. it does not oscillate. The only amplitudes that oscillate with $\Delta\Phi_{jj}$ are thus the ones which are given by a linear combination of the ϕ and ϕ^\dagger amplitudes – just as for the ggH scattering.



$gg \rightarrow q\bar{q}H$: This process, in which two gluons annihilate in the initial state and a quark antiquark pair is produced in the final state, is strongly suppressed since it is a s-channel process, constituting only 0.9% to the total cross section. It is interesting to notice, that in this case one has no oscillation in the differential $\Delta\Phi_{jj}$ contribution of the cross section, figure 3.10 (left), nei-

ther for helicity configuration that lead to MHV amplitudes nor helicity configurations leading to NMHV amplitudes.



$q\bar{q} \rightarrow ggH$: This process is similar to the one above, but now there is a quark antiquark pair annihilating in the initial state and a gluon pair in the final state. Since it is also a s-channel process it is strongly suppressed. The importance of this process reduces further, when the parton distribution function is taken into account, since it is unlikely to find a quark antiquark pair of the

same flavor in the two protons. One is left with a contribution to the total cross section of less than 0.1%. The $\Delta\Phi_{jj}$ distribution is shown in figure 3.10 (right), which is like the case above – with no oscillation for any helicity configuration.

The $qq \rightarrow qqH$ subprocess behaves in terms of the $\Delta\Phi_{jj}$ distribution as one would expect from the qqH and ggH subprocess. Since in this case one only has helicity configurations that belong to MHV amplitudes (due to the two quark pairs), one finds the characteristic oscillation for any helicity configuration. The oscillation for a CP-even and CP-odd Higgs respectively is identical (up to scaling) to the qqH and ggH case. Further the ϕ and ϕ^\dagger distribution is not oscillating, just as for the other subprocesses. Three different channels contribute to the total cross section for qqH scattering. One channel alone does not represent a physical amplitude due to interference terms, nevertheless it might be worth looking at them separately. The total cross section corresponding to this process is $\sigma_{tot} = 232.6 \pm 0.1fb$. The contribution due to t-channel gluon exchange constitutes 88.3% of σ_{tot} , whilst the u-channel constitutes 11.8%. The s-channel is strongly suppressed and makes only 0.3% of σ_{tot} . Since the sum of all three

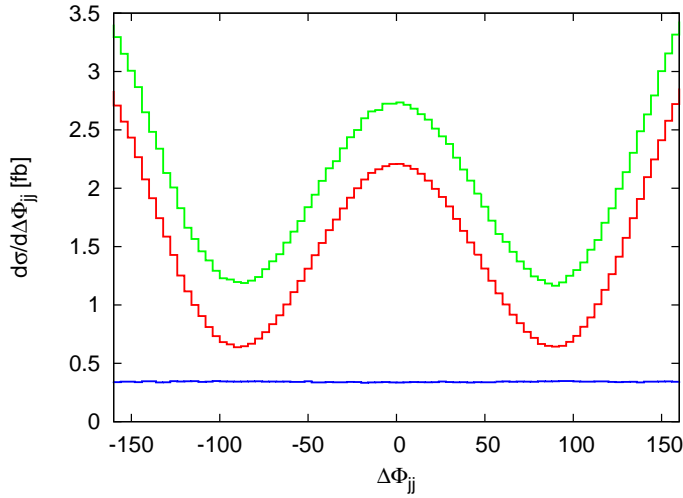


Figure 3.9: Differential cross section of $\Delta\Phi_{jj}$ for $qq \rightarrow qqH$. Different helicity configurations are shown separately:
 Green: Type (1) : $-- \rightarrow --$.
 Red: Type (2) : $-+ \rightarrow +-$.
 Blue: Remaining helicities.

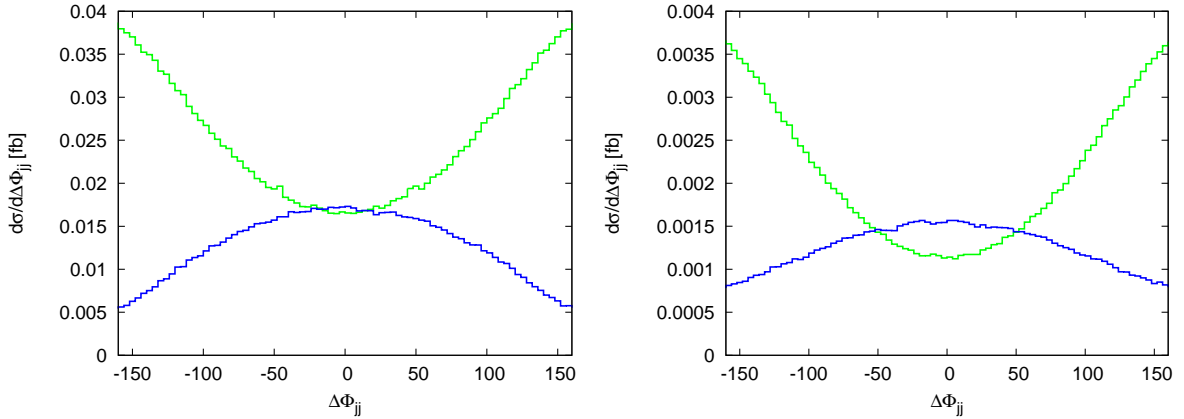


Figure 3.10: $\Delta\Phi_{jj}$ distribution for $gg \rightarrow q\bar{q}H$ (left) and $q\bar{q} \rightarrow ggH$ (right). The green curve takes helicity configurations into account that lead to MHV amplitudes, while the blue curve contains helicities leading to NMHV amplitudes.

channels leads to a cross section which is 100.3% of σ_{tot} , contributions due to interference effects have to be very small. Although not shown explicitly here, the $\Delta\Phi_{jj}$ distribution of the t-channel and the u-channel show the familiar oscillation, while the distribution given by the s-channel is not oscillating at all. This is consistent with the result for qqH scattering, since there as well one finds no oscillation for the s-channel induced MHV amplitudes.

Chapter 4

Effective theory

The production of a Standard Model-like Higgs boson at the LHC is dominated by gluon fusion. This process is actually known up to NNLO accuracy, and it is known that the NLO as well the NNLO calculation give large corrections ($K^{NNLO} \equiv \sigma^{NNLO}/\sigma^{LO} \approx 2$), and are needed to decrease the renormalization and factorization scale dependencies [19, 20]. Also of phenomenological interest are scattering amplitudes like $gg \rightarrow ggH$ or $gg \rightarrow gggH$. The first appears at leading order as a background to production of a Higgs boson via weak boson fusion, and therefore the latter is needed at next-to-leading order. While the WBF process is currently known at next-to-leading order in α_s , the full NLO calculation for Higgs plus two jets in gluon fusion is not available. However, the NLO correction to this process was performed by Campbell, Ellis and Zanderighi [21] in the large top mass approximation. In the following two sections the effective theory will be examined, and checked on what terms it is valid. Furthermore we will have a look at the corrections to the $m_{top} \rightarrow \infty$ limit, described by an effective Lagrangian which is $\propto \mathcal{O}(1/m_{top}^2)$ and contains operators of dimension 7.

To see that the large top mass limit is a good approximation, first look at the $H \rightarrow gg$ decay, given by [24]

$$\Gamma(H \rightarrow gg) = \frac{\alpha_s^2 g^2 m_H^3}{128\pi^3 m_W^2} \left| \sum_i \tau_i [1 + (1 - \tau_i)f(\tau_i)] \right|^2 \quad (4.1)$$

with

$$f(\tau) = \begin{cases} \left[\sin^{-1} \left(\sqrt{\frac{1}{\tau}} \right) \right]^2, & \text{if } \tau \geq 1 \\ -\frac{1}{4} \left[\ln \left(\frac{\eta_+}{\eta_-} \right) - i\pi \right]^2, & \text{if } \tau < 1 \end{cases} \quad (4.2)$$

where

$$\tau = 4 \frac{m_i^2}{m_H^2}, \quad \eta_{\pm} \equiv (1 \pm \sqrt{1 - \tau}) \quad (4.3)$$

and the sum over i goes over all quark flavors. The production cross section of a Higgs boson at a hadron collider at leading order is proportional to the decay width [24, 25]. $F(\tau) \equiv \tau [1 + (1 - \tau)f(\tau)]$ approaches $2/3$ when $\tau \rightarrow \infty$. The evolution of $F(\tau)$ is

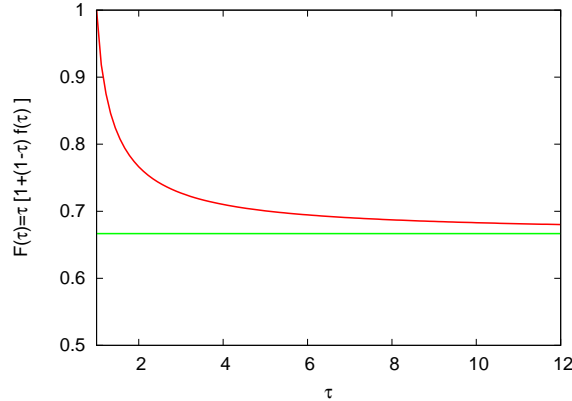


Figure 4.1: The red curve shows the value of $F(\tau)$ which fastly approximates the value $2/3$, displayed by the green curve.

shown in figure 4.1. One can see, that if the Higgs mass m_H is smaller than the quark mass m_i one can approximate $F(\tau)$ with $2/3$ making only a small error. If e.g. one has a Higgs with $m_H = 120\text{GeV}$ and taking $m_{top} = 175\text{GeV}$ one gets $F(4m_{top}/m_H) = 0.69$ making an error of less than 3%. One may wonder, if the approximation is still valid for the gluons being off-shell, like in the process $qQ \rightarrow qQH$ via gluon fusion. Later, it will be shown, that in this case one has to perform additional cuts on the phase space if one wants to keep the approximation valid.

The strategy to find the effective theory describing the (effective) Higgs gluon coupling is the following: First of all, one has to calculate the amplitude of the process involving a massive quark loop, in the limit that $m_{Higgs} \ll m_{quark}$. The only standard model particle that may satisfy this condition – consistent with the LEP precision data – is the top quark. Therefore set $m_{quark} = m_{top}$.¹ Second, one writes down all possible operators with the dimension needed, that is, dimension five for the leading term in the $1/m_t$ expansion, and dimension seven for term proportional to $(1/m_t)^2$. Finally one has to find a linear combination of these operators which leads to exactly the amplitude calculated. This combination may not be unique, but different representations of the effective Lagrangian are related by partial integration of the action. The effective Lagrangian will be decomposed as

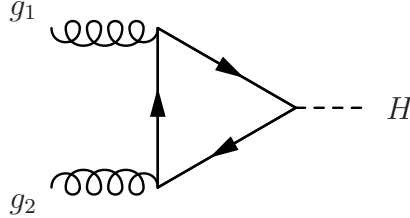
$$\mathcal{L}_{eff} = \mathcal{L}_{D5} + \mathcal{L}_{D7} \cdot \left(\frac{1}{m_t^2}\right) + \mathcal{L}_{D9} \cdot \left(\frac{1}{m_t^2}\right)^2 + \dots \quad (4.4)$$

where \mathcal{L}_{D5} and \mathcal{L}_{D7} are field combinations of dimension five and dimension seven, respectively. In the following the analytic expressions for \mathcal{L}_{D5} and \mathcal{L}_{D7} will be derived, for a SM like CP-even Higgs as well as for a CP-odd Higgs appearing e.g. in supersymmetric extensions of the SM or in two Higgs doublet models (2HDM) [22, 23]. The Feynman rules for a given effective Lagrangian were calculated with help of MATHEMATICA [27] using the package ‘‘FeynCalc’’ [28].

¹For all other SM quarks one has $m_{quark} \ll m_{Higgs}$. Since $F(\tau) \rightarrow 0$ for $\tau \rightarrow 0$ these contributions are strongly suppressed and can be neglected.

4.1 CP-even Higgs

The Higgs couples to two gluons via a triangle loop:



The calculation of the three point function can be found in Appendix B.1. If one expands the Amplitude as

$$T^{\mu_1\mu_2} = T_{D5}^{\mu_1\mu_2} + T_{D7}^{\mu_1\mu_2} \cdot \left(\frac{1}{m_t^2}\right) + T_{D9}^{\mu_1\mu_2} \cdot \left(\frac{1}{m_t^2}\right)^2 + \dots \quad (4.5)$$

one gets

$$T_{D5}^{\mu_1\mu_2} = -\frac{i\alpha_s}{3\pi v} \delta^{a_1 a_2} (g^{\mu_1\mu_2} q_1 \cdot q_2 - q_1^{\mu_2} q_2^{\mu_1}) \quad (4.6)$$

$$T_{D7}^{\mu_1\mu_2} = \frac{i\alpha_s}{180\pi v} \delta^{a_1 a_2} [(g^{\mu_1\mu_2} q_1 \cdot q_2 - q_1^{\mu_2} q_2^{\mu_1})(-7q_1 \cdot q_2 - 9q_1^2 - 9q_2^2) + g^{\mu_1\mu_2} q_1^2 q_2^2 - q_1^2 q_2^{\mu_1} q_2^{\mu_2} - q_2^2 q_1^{\mu_1} q_1^{\mu_2} + (q_1 \cdot q_2) q_1^{\mu_1} q_2^{\mu_2}] \quad (4.7)$$

As we will see, one also needs the analytic expression of the four point function to define (4.4). It is derived in Appendix B.2. The result expanded in powers of $1/m_t^2$ is given by

$$B^{\mu_1\mu_2\mu_3} = B_{D5}^{\mu_1\mu_2\mu_3} + B_{D7}^{\mu_1\mu_2\mu_3} \cdot \left(\frac{1}{m_t^2}\right) + B_{D9}^{\mu_1\mu_2\mu_3} \cdot \left(\frac{1}{m_t^2}\right)^2 + \dots \quad (4.8)$$

with the coefficients $B_{D5}^{\mu_1\mu_2\mu_3}$ and $B_{D7}^{\mu_1\mu_2\mu_3}$ given by (B.26) and (B.27) respectively.

To find the effective Lagrangian that leads to these vertices, one has to write down all gauge- and Lorentz-invariant combinations of operators that may contribute to the effective vertices and match coefficients. The effective Lagrangian that gives the D5 vertices is simple to construct. It has to be a combination of one Higgs field (or derivatives thereof) and gluon fields, together they must form an operator of dimension 5. There is only one unique combination that is Lorentz and gauge invariant, and CP-even²:

$$\mathcal{L}_{D5} \propto H \text{Tr} (G_{\mu\nu} G^{\mu\nu}) \quad (4.9)$$

with the gluonic field strength tensor $G_{\mu\nu} = \frac{1}{g} \mathcal{F}_{\mu\nu}$ from (2.22). The Hgg vertex corresponding to (4.9) is (with the proportionality constant β):

$$\langle 0 | \text{T} \left\{ H A_{\mu_1}^{a_1} A_{\mu_2}^{a_2} \cdot i \int d^4x \mathcal{L}_{D5} \right\} | 0 \rangle \Big|_{\substack{\text{amputated} \\ \text{connected}}} \stackrel{\text{F.T.}}{=} -i\beta 2\delta^{a_1 a_2} (g^{\mu_1\mu_2} q_1 \cdot q_2 - q_1^{\mu_2} q_2^{\mu_1}) \quad (4.10)$$

²The combination containing a dual field strength tensor leads to a CP-odd coupling and will be discussed later.

On the right hand side one has the Fourier transform for convenience, and overall momentum conservation is understood. Comparing (4.6) with (4.10) one can read off the constant $\beta = \alpha_s/6\pi v$, and the leading order effective Higgs gluon interaction becomes:

$$\mathcal{L}_{\text{D5}} = \frac{\alpha_s}{6\pi v} H \text{Tr} (G_{\mu\nu} G^{\mu\nu}) = \frac{\alpha_s}{12\pi v} H G_{\mu\nu}^a G^{a\mu\nu} \quad (4.11)$$

To get the Lagrangian that leads to the D7 vertex contributions one needs additional field strength tensors. Remember the definition of the field strength tensor (2.22):

$$G_{\mu\nu}(x) = \frac{i}{g} [D_\mu, D_\nu] \quad (4.12)$$

Define in the same way

$$\begin{aligned} [D_\mu, [D_\nu, D_\rho]] &= [\partial_\mu - igA_\mu^a t^a, -igt^b(\partial_\nu A_\rho^b - \partial_\rho A_\nu^b + gf^{bcd} A_\nu^c A_\rho^d)] \\ &= -igt^a [\partial_\mu \partial_\nu A_\rho^a - \partial_\mu \partial_\rho A_\nu^a + gf^{abc}((\partial_\mu A_\nu^b) A_\rho^c + A_\nu^b \partial_\mu A_\rho^c) \\ &\quad + gf^{abc} A_\mu^b (\partial_\nu A_\rho^c - \partial_\rho A_\nu^c + gf^{cde} A_\nu^d A_\rho^e)] \\ &\equiv -igt^a G_{\mu\nu\rho}^a \end{aligned} \quad (4.13)$$

and

$$\begin{aligned} [D_\beta, [D_\mu, [D_\nu, D_\rho]]] &= -igt^a [\partial_\beta \partial_\mu \partial_\nu A_\rho^a - \partial_\beta \partial_\mu \partial_\rho A_\nu^a \\ &\quad + gf^{abc}(\partial_\beta \partial_\mu A_\nu^b A_\rho^c + \partial_\mu A_\nu^b \partial_\beta A_\rho^c + \partial_\beta A_\nu^b \partial_\mu A_\rho^c + A_\nu^b \partial_\beta \partial_\mu A_\rho^c) \\ &\quad + gf^{abc} \partial_\beta A_\mu^b (\partial_\nu A_\rho^c - \partial_\rho A_\nu^c + gf^{cde} A_\nu^d A_\rho^e) \\ &\quad + gf^{abc} A_\mu^b (\partial_\beta \partial_\nu A_\rho^c - \partial_\beta \partial_\rho A_\nu^c + gf^{cde} (\partial_\beta A_\nu^d A_\rho^e + A_\nu^d \partial_\beta A_\rho^e)) \\ &\quad + gf^{agh} A_\beta^g (\partial_\mu \partial_\nu A_\rho^h - \partial_\mu \partial_\rho A_\nu^h + gf^{hbc} (\partial_\mu A_\nu^b A_\rho^c + A_\nu^b \partial_\mu A_\rho^c) \\ &\quad + gf^{hbc} A_\mu^b (\partial_\nu A_\rho^c - \partial_\rho A_\nu^c + gf^{cde} A_\nu^d A_\rho^e))] \\ &\equiv -igt^a G_{\beta\mu\nu\rho}^a \end{aligned} \quad (4.14)$$

One should notice that the fields in (4.13) and (4.14) can also be expressed in terms of (4.12) and the covariant derivative in the adjoint representation

$$D_\mu^{ab} = \partial_\mu \delta^{ab} - gA_\mu^c f^{abc} \quad (4.15)$$

It is easily checked, that

$$G_{\mu\nu\rho}^a = D_\mu^{ab} G_{\nu\rho}^b \quad (4.16)$$

$$G_{\beta\mu\nu\rho}^a = D_\beta^{ab} G_{\mu\nu\rho}^b = D_\beta^{ab} D_\mu^{bc} G_{\nu\rho}^c \quad (4.17)$$

The D7 effective Lagrangian, which has to be of dimension seven, is made out of different gauge and Lorentz invariant combinations of $G_{\mu\nu}$, $G_{\mu\nu\rho}$, $G_{\beta\mu\nu\rho}$, $\partial_\mu H$, H , $\partial_\mu \partial^\mu H$ like e.g.:

$$\begin{aligned} \partial_\mu \partial^\mu H \text{Tr} (G_{\mu\nu} G^{\mu\nu}), & \quad H \text{Tr} (G_{\mu\nu\rho} G^{\mu\nu\rho}) \\ H \text{Tr} (G_{\mu\nu}^\mu G_{\mu\nu}^\nu), & \quad H \text{Tr} (G_{\mu\nu\rho}^\mu G^{\nu\rho}) \\ H \text{Tr} (G_{\mu\nu}^\nu G_{\nu\rho}^\rho G_{\rho\mu}^\mu) & \end{aligned}$$

These expressions are manifestly Lorentz-invariant. They are also gauge invariant due to the trace taken over the color space, as one can see following the same steps as in (2.24). The Feynman rules for the Hgg vertices corresponding to different operators are:

$$\langle 0 | T \left\{ H A_{\mu_1}^{a_1} A_{\mu_2}^{a_2} \cdot i \int d^4 x \mathcal{L}_{\text{eff}} \right\} | 0 \rangle \Big|_{\substack{\text{amputated} \\ \text{connected}}} \stackrel{\text{F.T.}}{=} \quad (4.18)$$

$$= \begin{cases} 2i q_H^2 T_T^{\mu_1 \mu_2} \delta^{a_1 a_2}, & \mathcal{L}_{\text{eff}} = \partial_\mu \partial^\mu H \text{Tr} (G_{\mu\nu} G^{\mu\nu}) \\ 2i (q_1 \cdot q_2) T_T^{\mu_1 \mu_2} \delta^{a_1 a_2}, & \mathcal{L}_{\text{eff}} = H \text{Tr} (G_{\mu\nu\rho} G^{\mu\nu\rho}) \\ iT_L^{\mu_1 \mu_2} \delta^{a_1 a_2}, & \mathcal{L}_{\text{eff}} = H \text{Tr} (G_{\mu\nu}^\mu G_{\mu\nu}^\nu) \\ i(q_1^2 + q_2^2) T_T^{\mu_1 \mu_2} \delta^{a_1 a_2}, & \mathcal{L}_{\text{eff}} = H \text{Tr} (G_{\mu\nu\rho}^\mu G^{\nu\rho}) \\ 0, & \mathcal{L}_{\text{eff}} = H \text{Tr} (G_{\mu\nu}^\nu G_{\mu\rho}^\rho G_\rho^\mu) \end{cases} \quad (4.19)$$

Again, the momentum conserving delta function on the right hand side was neglected. The two different tensor structures are given by

$$T_T^{\mu_1 \mu_2} = g^{\mu_1 \mu_2} q_1 \cdot q_2 - q_1^{\mu_2} q_2^{\mu_1} \quad (4.20)$$

$$T_L^{\mu_1 \mu_2} = g^{\mu_1 \mu_2} q_1^2 q_2^2 - q_1^2 q_2^{\mu_1} q_2^{\mu_2} - q_2^2 q_1^{\mu_1} q_1^{\mu_2} + (q_1 \cdot q_2) q_1^{\mu_1} q_2^{\mu_2} \quad (4.21)$$

By using momentum conservation, $q_H = q_1 + q_2$, one sees that the different parts are not all independent of each other. The first one in (4.19) is, at least for the Hgg vertex, a linear combination of the second and the fourth. Indeed, one can show that the operators are related. This becomes manifest by integrating them by parts, as shown in Appendix C:

$$\frac{1}{2} (\partial_\mu \partial^\mu H) G^{a\nu\rho} G_{\nu\rho}^a = H G^{a\nu\rho} G_{\mu\nu\rho}^{a\mu} + H G_{\mu\nu\rho}^a G^{a\mu\nu\rho} + \text{surface terms} \quad (4.22)$$

By comparing (4.19) with (4.7) one can write down the effective D7 Lagrangian. One choice is e.g.

$$\mathcal{L}_{\text{D7}} = \frac{\alpha_s}{360\pi v} \left[H G_{\mu\rho}^{a\mu} G_{\nu\rho}^{a\nu} - 9 H G_{\mu\nu\rho}^{a\mu} G^{a\nu\rho} - \frac{7}{2} H G_{\mu\nu\rho}^a G^{a\mu\nu\rho} \right. \\ \left. + i g C H \text{Tr} (G_{\beta\gamma}^\alpha G^\beta_\gamma G^\gamma_\alpha) \right] \quad (4.23)$$

The Lagrangian is not completely determined, since the last operator in (4.19) does not contribute to the Hgg coupling. It contains at least three vector operators and hence it appears first with the $Hggg$ coupling. Calculating the $Hggg$ vertex $V_{3,\text{D7}}$ out of (4.23) and subtracting it from $B_{\text{D7}}^{\mu_1 \mu_2 \mu_3}$ given in (B.27) one has

$$B_{\text{D7}}^{\mu_1 \mu_2 \mu_3} - V_{3,\text{D7}} = \frac{48 + C}{240} \cdot \frac{\alpha_s g}{\pi v} \left(g^{\mu_1 \mu_3} q_3^{\mu_2} q_1 \cdot q_2 + q_3^{\mu_1} (q_1^{\mu_2} q_2^{\mu_3} - g^{\mu_2 \mu_3} q_1 \cdot q_2) \right. \\ \left. - g^{\mu_1 \mu_2} q_2^{\mu_3} q_1 \cdot q_3 + q_2^{\mu_1} (g^{\mu_2 \mu_3} q_1 \cdot q_3 - q_3^{\mu_2} q_1^{\mu_3}) - g^{\mu_1 \mu_3} q_1^{\mu_2} q_2 \cdot q_3 + g^{\mu_1 \mu_2} q_1^{\mu_3} q_2 \cdot q_3 \right) f_{a_1 a_2 a_3} \quad (4.24)$$

and the missing constant is determined to $C = -48$. Having fixed all parameters one should look for a more convenient representation of (4.23). It would be desirable to have at least one part proportional to \mathcal{L}_{D5} . This is possible for an on-shell Higgs, because then one can replace $\partial_\mu \partial^\mu H$ with $-m_H^2 H$ in (4.22). One operator on the right hand side of (4.22) can be replaced in favor of $m_H^2 H \text{Tr}(G_{\mu\nu} G^{\mu\nu})$. When replacing one operator, it is best to keep the one that – at least for the Hgg vertex – is proportional to $q_1^2 + q_2^2$ instead of $q_1 \cdot q_2$, since $q_1^2 + q_2^2$ indicates the virtuality of the gluon and should be small, while it is quite impossible to make predictions on the magnitude of $q_1 \cdot q_2$. With this selection \mathcal{L}_{D7} becomes

$$\mathcal{L}_{D7} = \frac{\alpha_s}{360\pi v} \left[\frac{7}{4} m_H^2 H G_{\mu\nu}^a G^{a\mu\nu} - \frac{11}{2} H G^{a\mu}{}_{\mu\nu\rho} G^{a\nu\rho} + H G^{a\mu}{}_{\mu\rho} G^{a\nu}{}_{\nu}{}^\rho \right. \\ \left. - 48ig H \text{Tr}(G^\alpha{}_\beta G^\beta{}_\gamma G^\gamma{}_\alpha) \right] \quad (4.25)$$

One can perform the last trace

$$i \text{Tr}(G^\alpha{}_\beta G^\beta{}_\gamma G^\gamma{}_\alpha) = \frac{i}{4} (d^{abc} + if^{abc}) G^{a\alpha}{}_\beta G^{b\beta}{}_\gamma G^{c\gamma}{}_\alpha \quad (4.26)$$

$$= -\frac{1}{4} f^{abc} G^{a\alpha}{}_\beta G^{b\beta}{}_\gamma G^{c\gamma}{}_\alpha \quad (4.27)$$

where the part proportional to the totally symmetric symbol d^{abc} vanishes, since it is contracted with totally antisymmetric field strength tensors $G^{a\mu\nu}$.

$$\mathcal{L}_{D7} = \frac{\alpha_s}{360\pi v} \left[\frac{7}{4} m_H^2 H G_{\mu\nu}^a G^{a\mu\nu} - \frac{11}{2} H G^{a\mu}{}_{\mu\nu\rho} G^{a\nu\rho} + H G^{a\mu}{}_{\mu\rho} G^{a\nu}{}_{\nu}{}^\rho \right. \\ \left. + 12g H f^{abc} G^{a\alpha}{}_\beta G^{b\beta}{}_\gamma G^{c\gamma}{}_\alpha \right] \quad (4.28)$$

4.2 CP-odd Higgs

The derivation of the effective Lagrangian for a CP-odd Higgs is quite similar to the CP-even case. The coupling of a CP-odd Higgs to fermions contains an additional γ^5 leading to a totally antisymmetric tensor structure for the (effective) vertices. Hence they can be expressed with help of the totally antisymmetric Levi-Cevita tensor in four dimensions. Each part of the effective Lagrangian that describes the CP-odd Higgs-gluon coupling must therefore contain a dual field strength tensor defined by

$$*G^{\mu\nu} = \frac{i}{2} \epsilon^{\mu\nu\rho\sigma} G_{\rho\sigma} \quad (4.29)$$

where $\epsilon^{\mu\nu\rho\sigma}$ is the totally antisymmetric tensor with the convention $\epsilon^{0123} = +1$. To find the effective Lagrangian one again has to calculate the three- and four point functions containing two and three gluons respectively and a CP-odd Higgs. The calculation and corresponding expressions for $T_{D5}^{\mu_1\mu_2}$, $T_{D7}^{\mu_1\mu_2}$, $B_{D5}^{\mu_1\mu_2\mu_3}$ and $B_{D7}^{\mu_1\mu_2\mu_3}$ are given in Appendix B.3 and B.4. For the effective Lagrangian of dimension 5, \mathcal{L}_{D5} , there is again only one

possible combination of a Higgs field and field strength tensors: it has to be proportional to $A\epsilon^{\mu\nu\rho\sigma}\text{Tr}(G^{\mu\nu}G^{\rho\sigma})$. Calculating the Feynman rules for the Agg vertex and comparing with (B.33) one finds

$$\mathcal{L}_{\text{D5}} = \frac{-i\alpha_s}{4\pi v} A \text{Tr}(G_{\mu\nu} * G^{\mu\nu}) = \frac{\alpha_s}{16\pi v} A \epsilon^{\mu\nu\rho\sigma} G_{\mu\nu}^a G_{\rho\sigma}^a \quad (4.30)$$

For the construction of the D7 Lagrangian one can use the same field strength tensors defined in (4.13) and (4.14), but the contraction must contain one ϵ -tensor, like e.g.

$$\begin{aligned} \partial_\mu \partial^\mu A \epsilon^{\mu\nu\rho\sigma} \text{Tr}(G_{\mu\nu} G_{\rho\sigma}), & \quad A \epsilon^{\mu\nu\rho\sigma} \text{Tr}(G_{\mu\nu\alpha} G_{\rho\sigma}^\alpha) \\ A \epsilon^{\mu\nu\rho\sigma} \text{Tr}(G_{\alpha\mu\nu} G_{\rho\sigma}^\alpha), & \quad A \epsilon^{\mu\nu\rho\sigma} \text{Tr}(G_{\alpha\mu\nu}^\alpha G_{\rho\sigma}) \\ A \epsilon^{\mu\nu\rho\sigma} \text{Tr}(G_{\mu\nu} G_\rho^\alpha G_{\alpha\sigma}) & \end{aligned}$$

Again all dimension 7 operators given above are not independent. In appendix C it is shown that

$$\epsilon^{\mu\nu\alpha\beta} G_{\mu\nu\rho}^a G_{\alpha\beta}^{\rho} = \frac{1}{4} \epsilon^{\mu\nu\alpha\beta} G_{\rho\mu\nu}^a G_{\alpha\beta}^{\rho} \quad (4.31)$$

$$\frac{1}{2} (\partial_\mu \partial^\mu A) \epsilon^{\nu\rho\alpha\beta} G_{\alpha\beta}^a G_{\nu\rho}^a = A \epsilon^{\nu\rho\alpha\beta} G_{\mu\nu\rho}^a G_{\alpha\beta}^{\mu} + A \epsilon^{\nu\rho\alpha\beta} G_{\alpha\beta}^a G_{\mu\nu\rho}^{\mu} \quad (4.32)$$

Calculating the Feynman rules for the Agg vertex for the different Lagrangians gives:

$$\langle 0 | \text{T} \left\{ A A_{\mu_1}^{a_1} A_{\mu_2}^{a_2} \cdot i \int d^4 x \mathcal{L}_{\text{eff}} \right\} | 0 \rangle \Big|_{\substack{\text{amputated} \\ \text{connected}}} \stackrel{\text{F.T.}}{=} \quad (4.33)$$

$$= \begin{cases} -4i q_A^2 \epsilon^{\mu_1 \mu_2 q_1 q_2} \delta^{a_1 a_2}, & \mathcal{L}_{\text{eff}} = \partial_\mu \partial^\mu A \epsilon^{\mu\nu\rho\sigma} \text{Tr}(G_{\mu\nu} G_{\rho\sigma}) \\ -4i (q_1 \cdot q_2) \epsilon^{\mu_1 \mu_2 q_1 q_2} \delta^{a_1 a_2}, & \mathcal{L}_{\text{eff}} = A \epsilon^{\mu\nu\rho\sigma} \text{Tr}(G_{\alpha\mu\nu} G_{\rho\sigma}^\alpha) \\ -i (q_1 \cdot q_2) \epsilon^{\mu_1 \mu_2 q_1 q_2} \delta^{a_1 a_2}, & \mathcal{L}_{\text{eff}} = A \epsilon^{\mu\nu\rho\sigma} \text{Tr}(G_{\mu\nu\alpha} G_{\rho\sigma}^\alpha) \\ -2i (q_1^2 + q_2^2) \epsilon^{\mu_1 \mu_2 q_1 q_2} \delta^{a_1 a_2}, & \mathcal{L}_{\text{eff}} = A \epsilon^{\mu\nu\rho\sigma} \text{Tr}(G_{\alpha\mu\nu}^\alpha G_{\rho\sigma}) \\ 0, & \mathcal{L}_{\text{eff}} = A \epsilon^{\nu\rho\alpha\beta} \text{Tr}(G_{\mu\nu} G_\rho^\alpha G_{\alpha\sigma}) \end{cases} \quad (4.34)$$

Comparing this with (B.33) one can start to build \mathcal{L}_{D7} . Again there are several possible representations, one choice is

$$\begin{aligned} \mathcal{L}_{\text{D7}} = -\frac{\alpha_s}{24\pi v} & \left[\frac{1}{8} (\partial^2 A) \epsilon^{\mu\nu\rho\sigma} G_{\mu\nu}^a G_{\rho\sigma}^a + \frac{1}{4} A \epsilon^{\nu\rho\alpha\beta} G_{\mu\nu\rho}^{\mu} G_{\alpha\beta}^a \right. \\ & \left. + \text{Cig} A \text{Tr}(\epsilon^{\mu\nu\alpha\beta} G_{\mu\nu} G_{\beta\gamma} G_{\alpha}^\gamma) \right] \quad (4.35) \end{aligned}$$

where again the D7 operators are chosen in such a way, that the first operator is (for an on-shell Higgs) proportional to the D5 operator and the second operator is proportional to $q_1^2 + q_2^2$ instead of $q_1 \cdot q_2$, for the same reasons as in the CP-even case. The constant

C has to be fixed by comparing the *Aggg* effective D7 vertex (B.39) with the Feynman rules $V_{3,D7}^A$ obtained directly from \mathcal{L}_{D7}

$$\begin{aligned}
B_{D7}^{\mu_1\mu_2\mu_3} - V_{3,D7}^A = & -\frac{2-C}{24} \cdot \frac{\alpha_s g}{\pi v} (\epsilon^{\mu_3 q_1 q_2 q_3} g^{\mu_1 \mu_2} + \epsilon^{\mu_2 q_1 q_2 q_3} g^{\mu_1 \mu_3} - \epsilon^{\mu_2 \mu_3 q_1 q_3} q_2^{\mu_1} \\
& - \epsilon^{\mu_2 \mu_3 q_1 q_2} q_3^{\mu_1} + \epsilon^{\mu_1 q_1 q_2 q_3} g^{\mu_2 \mu_3} + \epsilon^{\mu_1 \mu_3 q_2 q_3} q_1^{\mu_2} - \epsilon^{\mu_1 \mu_3 q_1 q_2} q_3^{\mu_2} + \epsilon^{\mu_1 \mu_2 q_2 q_3} q_1^{\mu_3} \\
& + \epsilon^{\mu_1 \nu 2 q_1 q_3} q_2^{\mu_3} + \epsilon^{\mu_1 \mu_2 \mu_3 q_3} q_1 \cdot q_2 + \epsilon^{\mu_1 \mu_2 \mu_3 q_2} q_1 \cdot q_3 + \epsilon^{\mu_1 \mu_2 \mu_3 q_1} q_2 \cdot q_3) f^{a_1 a_2 a_3}
\end{aligned} \quad (4.36)$$

Fixing $C = 2$ and performing the trace over the color space, one obtains for an on-shell CP-odd Higgs

$$\begin{aligned}
\mathcal{L}_{D7} = & \frac{i\alpha_s}{360\pi v} \left[-\frac{15}{4} m_A^2 A G_{\mu\nu}^a * G^{a\mu\nu} + \frac{15}{2} A G^{a\mu}{}_{\mu\nu\rho} * G^{a\nu\rho} \right. \\
& \left. - 15g A f^{abc} G^{a\mu}{}_{\nu} G^{b\nu}{}_{\rho} * G^{c\rho}{}_{\mu} \right]
\end{aligned} \quad (4.37)$$

For convenience everything is expressed with help of the dual field strength tensor defined in (4.29).

If one compares (4.28) with (4.37) one finds that both effective Lagrangians look quite similar. The operators for the CP-odd Lagrangian look almost like the ones of the CP-even Lagrangian, but in each term one field strength tensor is replaced by a dual one. The CP-even case contains one more operator ($\propto H G^{a\mu}{}_{\mu\rho} G^{a\nu}{}_{\nu\rho}$) which does not appear in the CP-odd Lagrangian since there is no analog dual one.

4.3 Checks

Two kinds of checks were made to test the calculations of the three and four point functions. The first test exploits the Ward-Takahashi identity to express the color stripped four point function as a difference of color-stripped three point functions. Second, the five point function that couples the Higgs to four gluons was calculated. It was expanded into a power series in $1/m_t^2$ in the same way as the three and four point functions:

$$P^{\mu_1\mu_2\mu_3\mu_4} = P_{D5}^{\mu_1\mu_2\mu_3\mu_4} + P_{D7}^{\mu_1\mu_2\mu_3\mu_4} \cdot \left(\frac{1}{m_t^2}\right) + P_{D9}^{\mu_1\mu_2\mu_3\mu_4} \cdot \left(\frac{1}{m_t^2}\right)^2 + \dots \quad (4.38)$$

If everything goes right, the effective vertices for the *Hgggg* coupling derived from the effective Lagrangian directly, must coincide with $P_{D5}^{\mu_1\mu_2\mu_3\mu_4}$ and $P_{D7}^{\mu_1\mu_2\mu_3\mu_4}$ respectively.

4.3.1 Ward-Takahashi identity

The Ward identity in QED [29] states, that if $\mathcal{M}(k) = \epsilon_\mu(k) \mathcal{M}^\mu(k)$ is the amplitude for some QED process involving an external photon with momentum k , then this amplitude vanishes if one replaces ϵ_μ with k_μ . The generalization is the Ward-Takahashi identity [30]. It relates n point correlation functions to a difference of two $(n-1)$ point correlation functions, when an external photon is replaced with its' momentum. This identity can

also be applied to the QCD case, if one just considers the color-stripped part of an amplitude.

The three point function $T^{\mu_1\mu_2}$ is, apart from the color factor δ^{ab} , identical to the corresponding QED three point function, and hence has to vanish when it is contracted with $q_{1\mu_1}$ or $q_{2\mu_2}$.

If one expresses the three and four point functions as

$$T_1^{\mu_1\mu_2} = \text{Tr}(t^{a_1} t^{a_2}) \tilde{T}_1^{\mu_1\mu_2} \quad (4.39)$$

$$B_1^{\mu_1\mu_2\mu_3} = \text{Tr}(t^{a_1} t^{a_2} t^{a_3}) \tilde{B}_1^{\mu_1\mu_2\mu_3} \quad (4.40)$$

and contracts the $\tilde{B}_1^{\mu_1\mu_2\mu_3}$ with $q_1^{\mu_1}$ one gets (using $\not{q}_1 = (\not{k} + \not{q}_1 + m) - (\not{k} + m)$):

$$\begin{aligned} q_{1\mu_1} \cdot \tilde{B}_1^{\mu_1\mu_2\mu_3} &= C \int \frac{d^4k}{(2\pi)^4} \text{Tr} \left\{ \frac{(\not{k} + m) [(\not{k} + \not{q}_1 + m) - (\not{k} + m)] (\not{k} + \not{q}_1 + m)}{(k^2 - m^2)((k + q_1)^2 - m^2)} \right. \\ &\quad \left. \times \frac{\gamma^{\mu_2} (\not{k} + \not{q}_{12} + m) \gamma^{\mu_3} (\not{k} + \not{q}_{123} + m)}{((k + q_{12})^2 - m^2)((k + q_{123})^2 - m^2)} \right\} \\ &= g \left(\tilde{T}_1^{\mu_2\mu_3}(q_{12}, q_3) - \tilde{T}_1^{\mu_2\mu_3}(q_2, q_3) \right) \end{aligned} \quad (4.41)$$

If one replaces $q_1^{\mu_1}$ by $q_2^{\mu_2}$ or $q_3^{\mu_3}$ one obtains two more identities:

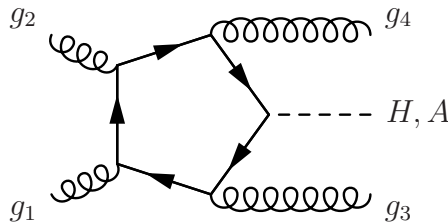
$$q_{2\mu_2} \cdot \tilde{B}_1^{\mu_1\mu_2\mu_3} = g \left(\tilde{T}_1^{\mu_1\mu_3}(q_1, q_{23}) - \tilde{T}_1^{\mu_1\mu_3}(q_{12}, q_3) \right)$$

$$q_{3\mu_3} \cdot \tilde{B}_1^{\mu_1\mu_2\mu_3} = g \left(\tilde{T}_1^{\mu_1\mu_2}(q_1, q_2) - \tilde{T}_1^{\mu_1\mu_2}(q_1, q_{23}) \right)$$

The identity takes the same form for the CP-even and CP-odd case. I checked with the help of MATHEMATICA that these three relations are indeed satisfied – for the CP-even as well as for the CP-odd Higgs.

4.3.2 Five point function for the $Hg\bar{g}\bar{g}\bar{g}$ coupling

The five point function is given by a Higgs coupling to four gluons via a top-quark pentagon loop.



The corresponding five point correlation function was calculated for a CP-even and for a CP-odd Higgs. The result was expanded into a power series in $1/m_t$ as shown in (4.38). As a cross-check, the obtained expressions were tested using the Ward-Takahashi identity. That is, the color-stripped five point correlation function were

reduced to differences of (color-stripped) four point correlation functions. This was done order by order in the $1/m_t$ expansion.

In both cases, the CP-even and CP-odd, the $\Phi gggg$ vertices³ obtained from \mathcal{L}_{D5} and \mathcal{L}_{D7} coincide with the corresponding expression of the expansion, $P_{D5}^{\mu_1\mu_2\mu_3\mu_4}$ and $P_{D7}^{\mu_1\mu_2\mu_3\mu_4}$.

³ Φ stands for a CP-even or CP-odd Higgs H and A respectively

Chapter 5

Effective theories vs. full calculation

In the following the effective theories of the last chapter will be compared with the full loop calculation for the process $pp \rightarrow H + 2j$. To make a meaningful comparison, one must not only look at total cross sections, but also compare differential distributions. The main task is to find out, in which range of the phase space for a given Higgs mass the approximation is valid, and where it starts to break down. The parton level Monte Carlo program VBFNLO has the full leading order calculation for this process, involving a heavy fermion loop. The large top mass approximation $m_t \rightarrow \infty$ is also included. The only missing parts are the D7 Lagrangian of the last section. It is useful to implement the different dimension 7 operators, which form the D7 Lagrangian, in such a way, that one can analyze them separately. Thus, the effective Lagrangian was split in the following way:

$$\mathcal{L}_{\text{eff}}^{\text{H}} = \mathcal{L}_{\text{D5}}^{\text{H}} + \frac{1}{m_t^2} (\mathcal{L}_{\text{D7-I}}^{\text{H}} + \mathcal{L}_{\text{D7-II}}^{\text{H}} + \mathcal{L}_{\text{D7-III}}^{\text{H}} + \mathcal{L}_{\text{D7-IV}}^{\text{H}}) \quad (5.1)$$

$$\mathcal{L}_{\text{eff}}^{\text{A}} = \mathcal{L}_{\text{D5}}^{\text{A}} + \frac{1}{m_t^2} (\mathcal{L}_{\text{D7-I}}^{\text{A}} + \mathcal{L}_{\text{D7-II}}^{\text{A}} + \mathcal{L}_{\text{D7-III}}^{\text{A}}) \quad (5.2)$$

with for the CP-even Higgs

and for the CP-odd Higgs

$$\begin{aligned} \mathcal{L}_{\text{D5}}^{\text{H}} &= \frac{\alpha_s}{12\pi v} H G_{\mu\nu}^a G^{a\mu\nu} & \mathcal{L}_{\text{D5}}^{\text{A}} &= \frac{-i\alpha_s}{8\pi v} A G_{\mu\nu}^a *G_{\mu\nu}^a \\ \mathcal{L}_{\text{D7-I}}^{\text{H}} &= \frac{\alpha_s}{360\pi v} \cdot \frac{7}{4} m_H^2 H G_{\mu\nu}^a G^{a\mu\nu} & \mathcal{L}_{\text{D7-I}}^{\text{A}} &= \frac{-i\alpha_s}{360\pi v} \cdot \frac{15}{4} m_A^2 A G_{\mu\nu}^a *G^{a\mu\nu} \\ \mathcal{L}_{\text{D7-II}}^{\text{H}} &= \frac{-\alpha_s}{360\pi v} \cdot \frac{11}{2} H G^{a\mu}{}_{\nu\rho} G^{a\nu\rho} & \mathcal{L}_{\text{D7-II}}^{\text{A}} &= \frac{i\alpha_s}{360\pi v} \cdot \frac{15}{2} A G^{a\mu}{}_{\nu\rho} *G^{a\nu\rho} \\ \mathcal{L}_{\text{D7-III}}^{\text{H}} &= \frac{\alpha_s g}{360\pi v} \cdot 12 H f^{abc} G^{a\mu}{}_{\nu} G^{b\nu}{}_{\rho} G^{c\rho}{}_{\mu} & \mathcal{L}_{\text{D7-III}}^{\text{A}} &= \frac{-i\alpha_s g}{360\pi v} \cdot 15 A f^{abc} G^{a\mu}{}_{\nu} G^{b\nu}{}_{\rho} *G^{c\rho}{}_{\mu} \\ \mathcal{L}_{\text{D7-IV}}^{\text{H}} &= \frac{\alpha_s}{360\pi v} \cdot H G^{a\mu}{}_{\mu\rho} G^{a\nu}{}_{\nu}{}^{\rho} \end{aligned}$$

Additional subroutines were implemented into the file **gf_higgsME.f** for each D7 Lagrangian given above, respectively. The implementation was done in such a way, that one can use the quark and gluon currents calculated by VBFNLO and contract them with the effective H/Agg , H/Aggg and H/Agggg couplings, in the same manner as it is

realized for the full calculation or the effective D5 coupling. There are some subtleties one has to consider when implementing the vertices given by the D7 Lagrangians into VBFNLO: First of all, when calculating the Feynman rules for a given vertex, all gluons have to be outgoing. Second, the Feynman rules given in Appendix A differ in the conventions to the ones used to calculate scattering amplitudes in VBFNLO, which agree with [31]. These Feynman rules have an additional minus sign for the gluon-fermion vertex. Therefore one has to consider an additional factor (-1) for the phase when implementing the three gluon-Higgs vertex, since this is the only case where an odd number of gluon-fermion vertices appears in the calculation.

There is one ambiguity when taking the D7 correction into account. One can take the scattering amplitude up to $\mathcal{O}(1/m_t^2)$ leading to a squared matrix element of $\mathcal{O}(1/m_t^4)$, or one can ask for the squared matrix element being at most of order $(1/m_t^2)$. Both should give similar results as long as the approximation is valid. In the following the latter choice was made, that is

$$|M|^2 = \left| M_{D5} + \frac{1}{m_t^2} M_{D7} \right|^2 \stackrel{\mathcal{O}(1/m_t^2)}{=} |M_{D5}|^2 + 2 \frac{1}{m_t^2} \text{Re}(M_{D5} M_{D7}^*)$$

where M_{D5} and M_{D7} refer to the matrix element one derives using the D5 or D7 Lagrangian respectively. By making this choice one may reckon that negative weights to the cross section occur. Even though negative weights are unphysical, at least they are a good indicator for the phase space region where the approximation breaks down.

5.1 Proton proton \rightarrow Higgs plus two jets

The process $pp \rightarrow Hjj$ via gluonfusion can be divided into three main subprocesses, differing in the number of external quarks. Since the possibility to find a quark or gluon with a certain kinematics inside a proton is very unequal for a center of mass energy of 14TeV, the three subprocesses should be considered separately.¹

5.1.1 $qQ \rightarrow qQH$

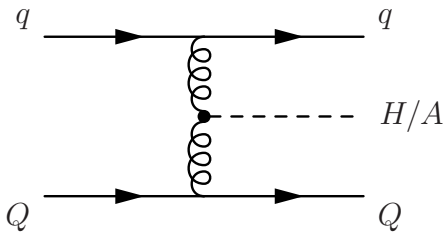


Figure 5.1: One diagram contributing to the process $qq \rightarrow qqH$. The dot represents the Higgs gluon coupling which is determined either through a top loop or an effective coupling.

The Feynman diagram contributing to this process is given by figure 5.1. The other diagrams are related to this one by crossing. As one can see, there is only a two gluon Higgs vertex, therefore not all of the effective D7 operators do contribute. To be precise, $\mathcal{L}_{D7,III}^H$ and $\mathcal{L}_{D7,III}^A$ are absent; they lead to vertices containing at least three gluons.

¹The probability is given by the parton distribution function (PDF) which can be derived from experimental data obtained at lower scales with the help of the DGLAP evolution equations [32, 33].

5.1.2 $qg \rightarrow qgH$

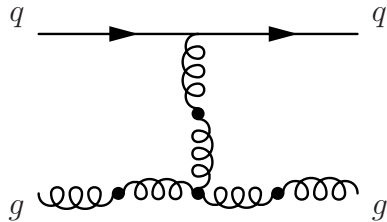


Figure 5.2: This diagram depicts the process $qg \rightarrow qgH/A$. The four dots display the interaction point where a Higgs can be radiated off. The coupling can be through a top loop or effective respectively.

In Fig. 5.2 are the different ways shown how the Higgs can be radiated off. All other diagrams contributing to this process can be obtained by crossing. Again, one has the two gluon-Higgs coupling, and in addition the three gluon-Higgs coupling has to be taken into account. That means that all effective Lagrangians do contribute to this process.

5.1.3 $gg \rightarrow ggH$

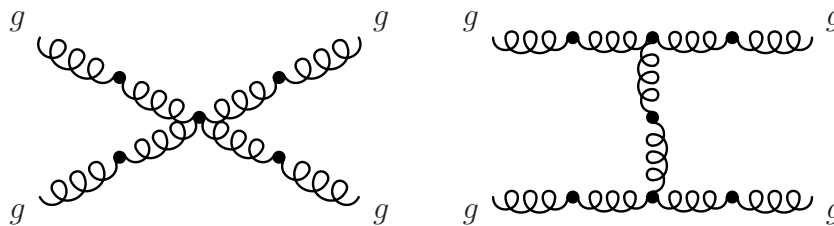


Figure 5.3: This two diagram show the possible processes for $gg \rightarrow ggH/A$. The dots display where a Higgs can be radiated off. The coupling can be through a top loop or effective.

The different topologies contributing to this process are depicted in figure 5.3. Here finally the two, three and also the four gluon Higgs coupling have to be taken into account.

5.2 Checks

After implementing the various D7 couplings, two kinds of checks were performed on the analytic amplitude: a gauge invariance and a Lorentz boost check.

5.2.1 Gauge invariance

Due to gauge invariance, an amplitude with one or more external gluons has to vanish if one replaces an outer polarization vector with the corresponding momentum vector. This follows from the fact, that the amplitude is invariant under the replacement $\epsilon_i^\mu \rightarrow \epsilon_i^\mu + c_i q_i^\mu$ for arbitrary c_i (see also section 4.3.1). For the process $qg \rightarrow qgH$ one

has two different polarization vectors that can be replaced to make the amplitude vanish, while for the $gg \rightarrow ggH$ process there are even four possibilities. Each part of the effective Lagrangians (5.1) and (5.2) was checked separately. For all possibilities of replacing a polarization vector, the amplitude vanishes numerically, as it is supposed to. Certainly this was done as well for a CP-even as for a CP-odd Higgs.

5.2.2 Lorentz boost

Since the amplitude is a Lorentz-scalar, it must be the same in each reference frame. One can therefore perform a Lorentz boost on all the outer momenta without changing the result. The total cross section was compared for the process $gg \rightarrow ggH$, once calculated in the center of mass frame and once in a boosted frame. The result was, for a CP-even and CP-odd Higgs, identical.

5.3 Total cross section for different Higgs masses

In this section the total cross sections for Hjj in pp collisions at $\sqrt{s} = 14\text{TeV}$ will be compared, once obtained by using the full loop calculation, the D5 effective theory and the D5+D7 effective theory. The factorization scale was taken to be the geometric average between the transverse momenta of the two jets: $\mu_f = \sqrt{p_{T1}p_{T2}}$. The renormalization scale for the strong coupling α_s was fixed at the Z_0 mass: $\mu_r = 91.188\text{GeV}$. (Varying the renormalization scale has large impact on the total cross section, however it should not alter the qualitative and quantitative results with respect to the shape and relative position of the different curves). The analysis was done for two kinds of cuts. The first consists of a minimal set of cuts which are needed to handle collinear singularities and are given by (5.3). The second are so called weak boson fusion cuts which reduce the QCD background for the Higgs production via weak boson fusion. These cuts are added to the ones in (5.3) and given by (5.4).

$$\begin{aligned} \text{minimal cuts : } p_{Tj} > 20\text{GeV}, & \quad |\eta_j| < 5, & \quad R_{jj} > 0.6 & \quad (5.3) \\ \text{additional WBF cuts : } |\eta_{j1} - \eta_{j2}| > 4, & \quad \eta_{j1} \cdot \eta_{j2} < 0, & \quad m_{jj} > 600\text{GeV} & \quad (5.4) \end{aligned}$$

The three subprocesses of the last section were considered separately.

$gg \rightarrow ggH$

In figure 5.4 one can see how the total cross section varies with the Higgs mass for the two sets of cuts. The effective theory improves in both cases when taking the correction given by \mathcal{L}_{D7}^H into account. Up to Higgs masses of 200GeV the total cross section obtained by using the effective theory plus corrections is almost identical as the one given by the full loop calculation. It would now be interesting to know the contributions of the different parts of the dimension 7 Lagrangian to this correction. First off all, examine $\mathcal{L}_{D7,IV}^H$. When considering only this part of the dimension 7 Lagrangian one finds that numerically the correction is zero. To verify this result, the amplitude was calculated with the help of MATHEMATICA using only vertices given by $\mathcal{L}_{D7,IV}^H$. The

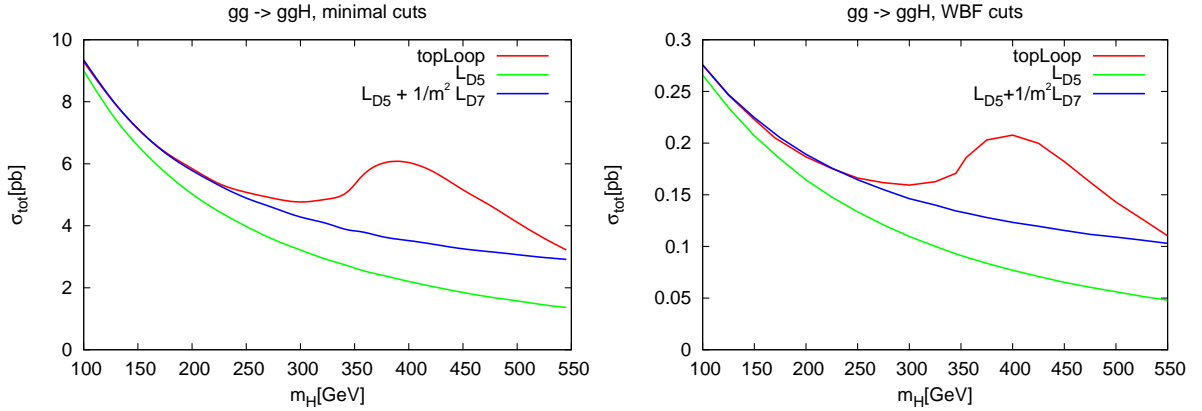


Figure 5.4: Total cross section for $gg \rightarrow ggH$ for a minimal set of cuts (left) and WBF cuts (right). The red curve shows the result obtained considering the full loop calculation. The green curve uses the effective Higgs gluon coupling described by \mathcal{L}_{D5} . The blue line takes the correction to \mathcal{L}_{D5} described by \mathcal{L}_{D7} into account.

result was, in agreement with VBFNLO, that the amplitude in this case indeed vanishes (analytically).

Next, consider the cross section obtained by taking only $\mathcal{L}_{D7_II}^H$ and $\mathcal{L}_{D7_III}^H$ into account. The total cross section is shown in figure 5.5. The purple crosses denote the result one obtains, taking both parts into account. It is hardly distinguishable from the D5 effective Lagrangian. Analytically one finds that for the process $gg \rightarrow ggH$ the amplitudes satisfy

$$-\frac{12}{11}A(\mathcal{L}_{D7_II}^H) = A(\mathcal{L}_{D7_III}^H) \quad (5.5)$$

where $A(\mathcal{L}_{D7_j})$ denotes the amplitudes derived by using Higgs-gluon vertices given by \mathcal{L}_{D7_j} . Hence the sum of both amplitudes is suppressed by one order of magnitude.

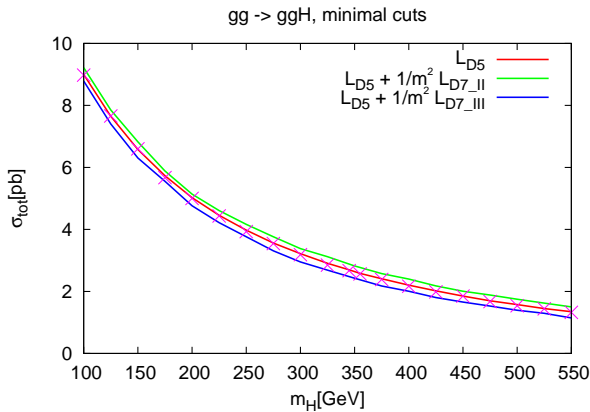


Figure 5.5: Red curve: effective theory \mathcal{L}_{D5} . The green and blue line show the corrections given by \mathcal{L}_{D7_II} and \mathcal{L}_{D7_III} respectively. The purple crosses finally depict the cross section obtained when taking both D7 corrections into account.

Altogether it follows that the correction to \mathcal{L}_{D5} must be given approximately by \mathcal{L}_{D7_I} ,

see figure 5.6. This is delightful, since this part of the dimension 7 Lagrangian can be expressed in terms of the dimension 5 Lagrangian plus formfactor:

$$\mathcal{L}_{\text{eff}}^H \approx \mathcal{L}_{D5}^H \left(1 + \frac{7}{120} \frac{m_H^2}{m_t^2} \right) \quad (5.6)$$

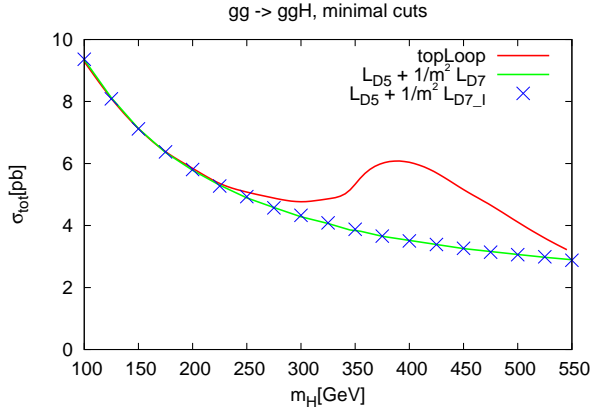


Figure 5.6: The red and green lines show the full loop calculation and the effective theory D5+D7. The blue \times are the cross section for $\mathcal{L}_{D5} + \frac{1}{m_t^2} \mathcal{L}_{D7_I}$.

qg \rightarrow qgH

The total cross section for this process is shown in figure 5.7. The D7 correction does not seem to give better results than the D5 effective theory alone. Some phase space region seems to spoil the top mass expansion. This will be investigated in the next section. Meanwhile, one should notice, that for WBF cuts the approximation becomes slightly better. Having a look at the four different parts of \mathcal{L}_{D7} one finds, that in this case the D7 correction is not only given by one part of the dimension 7 Lagrangian, but rather by the first three, while the contribution of $\mathcal{L}_{D7_{IV}}^H$ is negligible (the effect of $\mathcal{L}_{D7_{IV}}^H$ on the total cross section is less than 0.1%).

qQ \rightarrow qQH

The evaluation of the total cross section with the Higgs mass is given in figure 5.8 for both kinds of cuts. As in the qgH case the top mass expansion gets spoiled, and again the WBF cuts seem to cut out a part of the phase space region that spoils the approximation. The biggest part of the D7 Lagrangian cross section comes from $\mathcal{L}_{D7_{II}}$ and $\mathcal{L}_{D7_{III}}$, since again the contribution of $\mathcal{L}_{D7_{IV}}$ is negligible (it lowers the total cross section by approximately 1%). Remember that $\mathcal{L}_{D7_{III}}$ does not contribute here, since this Lagrangian does not lead to an Hgg vertex. Looking at the Hgg vertex given by $\mathcal{L}_{D7_{II}}$, which is $\propto (q_1^2 + q_2^2)$, forebodes that highly virtual gluons are responsible for the collapse of the effective theory.

CP-odd Higgs

The result obtained for a CP-odd Higgs boson is quite similar to the CP-even case as shown in figure 5.9 and 5.10. Again for the ggA subprocess the correction to

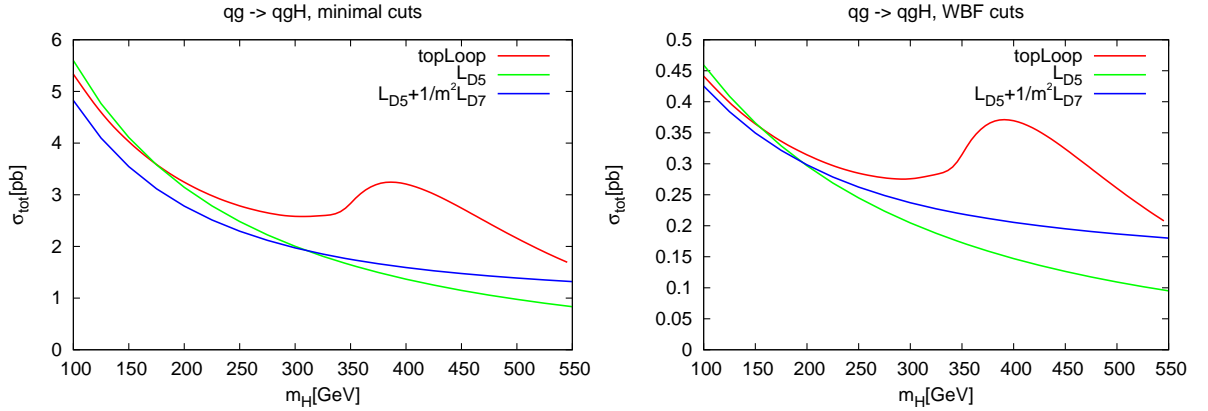


Figure 5.7: $qq \rightarrow qqH$ for minimal and WBF cuts. The red line gives the total cross section when considering the full loop calculation, while the green and blue line correspond to effective Higgs gluon coupling described by \mathcal{L}_{D5} and $\mathcal{L}_{D5} + \frac{1}{m_t^2} \mathcal{L}_{D7}$, respectively.

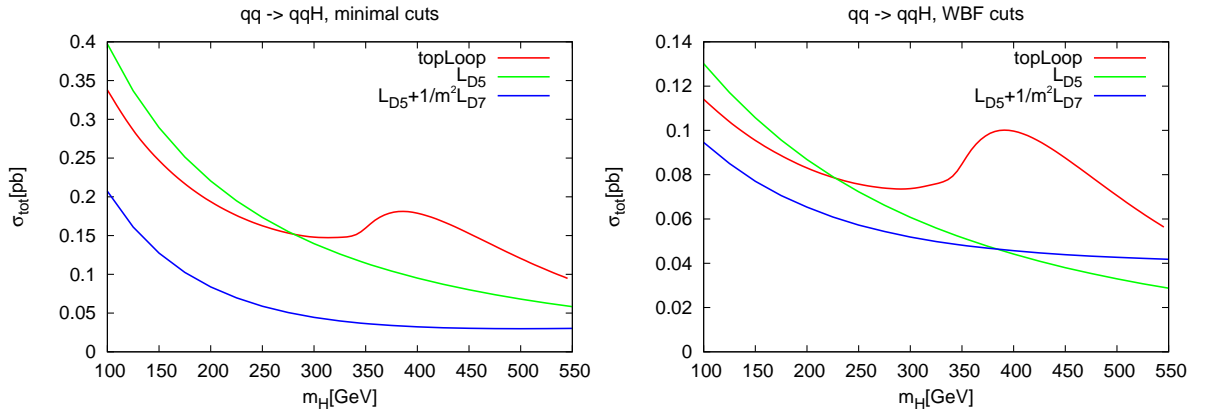


Figure 5.8: $qq \rightarrow qqH$ for minimal and WBF cuts. The red line shows σ_{tot} when considering the full loop calculation, while the green and blue curves show the total cross section for the effective D5 and D7 theory.

the D5 Lagrangian is given solely by \mathcal{L}_{D7-I}^A , while the sum of \mathcal{L}_{D7-II}^A and \mathcal{L}_{D7-III}^A vanishes analytically:

$$A(\mathcal{L}_{D7-II}^A) = -A(\mathcal{L}_{D7-III}^A) \quad (5.7)$$

where $A(\mathcal{L}_{D7-j}^A)$ denotes the amplitude for the $gg \rightarrow ggA$ process given by the particular Lagrangian. This means, that again one can express the D7 correction for this subprocess in terms of the dimension 5 effective Lagrangian plus formfactor:

$$\mathcal{L}_{\text{eff}}^A = \mathcal{L}_{D5}^A \left(1 + \frac{1}{12} \frac{m_A^2}{m_t^2} \right) \quad (5.8)$$

The other two subprocesses suffer again from phase space regions that spoil the heavy top mass expansion. One should mention, that applying WBF cuts leads to the same behavior as in the CP-even case; cutting out a part of the phase space region that spoils the approximation.

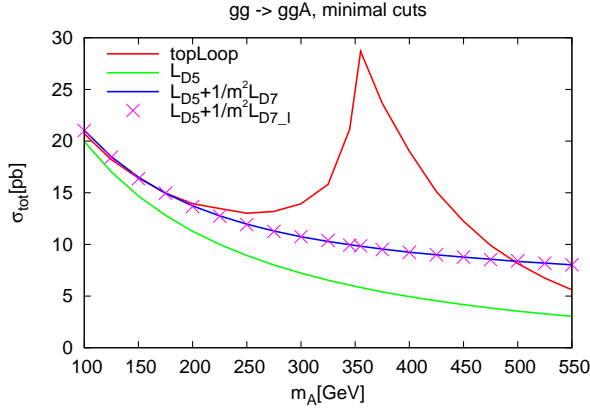


Figure 5.9: σ_{tot} for $gg \rightarrow ggA$ for a minimal set of cuts. The red curve shows the result obtained considering the full loop calculation. The green curve uses the effective Higgs gluon couplings described by \mathcal{L}_{D5} . The blue line takes the correction described by \mathcal{L}_{D7} into account, while the purple crosses consider only $\mathcal{L}_{D7,I}$.

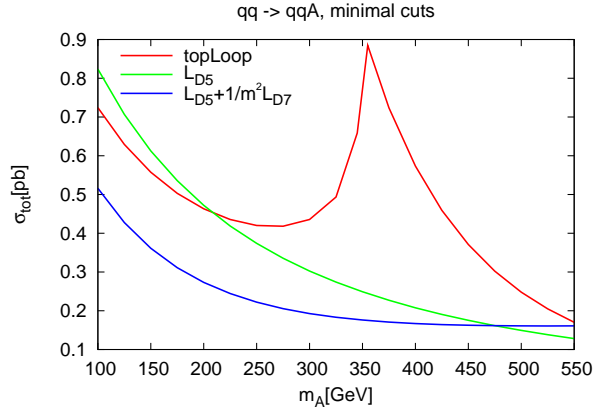
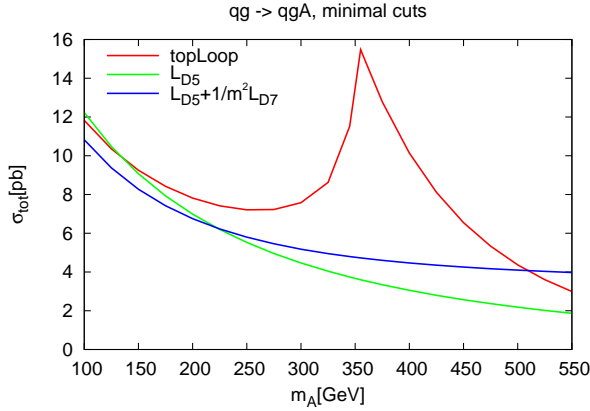


Figure 5.10: σ_{tot} for $qq \rightarrow qqA$ (left) and $qq \rightarrow qqA$ (right). The red, green and blue curve show the result for the full loop calculation, the D5 effective theory and the correction given by the D7 effective theory respectively.

5.4 Differential cross section: p_T distribution

In this section the phase space regions that spoil the large top mass approximation will be investigated. Additionally, the upcoming deviations are analyzed quantitatively and it is checked whether the error one obtains by considering the effective theories can be reduced by performing an appropriate cut on the phase space. There are some indications, that the effective theories get spoiled for kinematics involving highly virtual gluons with $|q_i|^2 \gtrsim m_t^2$:

- (i) We have seen at the beginning of chapter 4 that the ggH coupling with two on-shell gluons is perfectly described by the effective D5 theory.
- (ii) For the process $qq \rightarrow qqH$ only the ggH vertex is involved, which is mainly given by (see (B.10) and (B.11))

$$T_{D5}^{\mu_1 \mu_2} \left(1 + \frac{1}{120m_t^2} (7m_H^2 + 11(q_1^2 + q_2^2)) \right)$$

where q_1 and q_2 are the momenta of the intermediate gluons. One can deduce that for $|q_1^2 + q_2^2| \approx -m_t^2$ the $1/m_t^2$ suppressed term becomes the same magnitude as

the D5 approximation and for $\sqrt{|q_1^2 + q_2^2|} \gtrsim \sqrt{\frac{60}{11}}m_t \approx 408.7\text{GeV}$ one has to deal with negative weights. This can be visualized by considering only the t-channel exchange of the gluons and looking at the differential cross section $d\sigma/d\sqrt{q_1^2 + q_2^2}$, see figure 5.11.

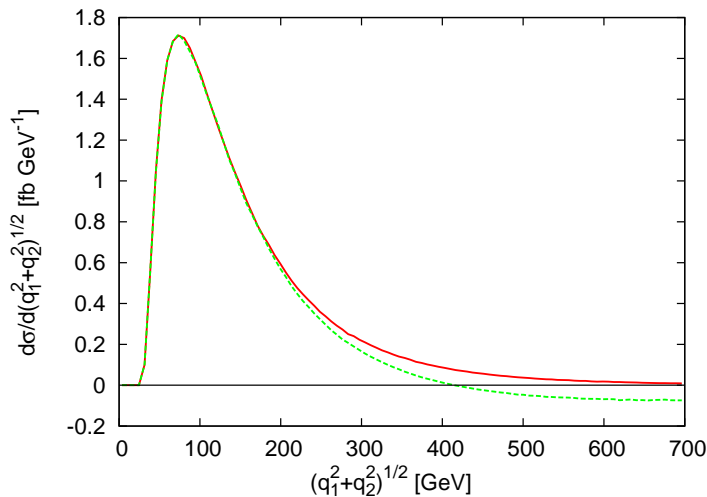


Figure 5.11: Differential cross section for the t-channel in $qq \rightarrow qqH$ for $m_H = 120\text{GeV}$. Red: top loop. Green: effective theory (D5+D7).

- (iii) The approximation becomes better the more gluons are involved in the process. Considering the parton distribution function for a 7TeV proton, the gluons peak at low x values whereas quarks are mainly distributed in higher x regions – and hence a large momentum transfer between the quark legs is likely [34].

In the same way as for the qqH subprocess one can also have a look at the differential distribution with respect to the momentum transfer between the quark legs in the qqH subprocess. One finds that for $|q^2| \ll -m_t^2$ the D5+D7 effective theory and the full loop calculation show no significant difference, only for values $|q^2| > m_t^2$ one encounters a deviation. Performing a cut on q^2 – the gluon momenta radiated from the quark leg, would give a great improvement to the effective theory.

For practical use it is desirable to have cuts that are easy applicable in an experiment. The momentum transfer q^2 could in general be reconstructed out of the two jets and the decay products of the Higgs, but one has to deal with large uncertainties; not to mention neutrinos among decay products. In contrast, the kinematics of the two hardest jets are accessible without difficulties. Kinematic variables that are related to this problem are the maximum p_T of the jets and also cuts that force the jets going into forward regions, like the WBF cuts (5.4).

The diagrams 5.12 - 5.17 show the $p_{T,\text{max}}$ spectrum of the differential cross section for the three subprocesses; as well for a minimal set of cuts as for WBF cuts. The corresponding differential K-factors for the D5 and D5+D7 effective theory with respect to the full loop calculation are given for two different Higgs masses: $m_H = 120\text{GeV}$ and $m_H = 200\text{GeV}$, which are around the preferred upper and lower bounds of a Standard Model Higgs given by the electroweak precision data. The differential K-factor is defined

as

$$\text{K-factor} \equiv \left(\frac{d\sigma}{dp_{T,\max}} \right)_{\text{topLoop}} / \left(\frac{d\sigma}{dp_{T,\max}} \right)_{\text{effective}} \quad (5.9)$$

To make a quantitative statement about how good or bad the approximations are, there is for each subprocess a table from which one can estimate the error obtained by taking a particular approximation. The tables are organized in the following way: σ_{tot} is the total cross section of the process considering the top loop. *D5-deviation* gives an upper and lower bound for the error one gets, when considering the D5 effective theory, while *D7-deviation* gives the error bounds for the D5+D7 effective theory. The lower bound is defined by the ratio:

$$\Delta\sigma_{\min} \equiv \left\| \frac{\sigma_{\text{toploop}} - \sigma_{\text{effective}}}{\sigma_{\text{toploop}}} \right\| \quad (5.10)$$

This is only a lower bound, since when calculating the total cross section, phase space regions that underestimate the full theory can compensate regions that overestimate the full theory, leading in the worst case to an apparent deviation of zero. To get an upper error bound one can use the following definition: Take for each phase space point the absolute value of the difference between the squared matrix elements of the full loop calculation and effective theory. Divide the number obtained after integrating over the phase space by σ_{toploop} :

$$\Delta\sigma_{\max} \equiv \int d\text{LIPS} \|M^2(\text{topLoop}) - M^2(\text{effective})\| / \sigma_{\text{toploop}} \quad (5.11)$$

Because of this definition of the error bounds, the latter bound gives the real discrepancy between effective and full calculation.

qq \rightarrow qqH

m_H	cuts	$\sigma_{\text{tot}} [\text{fb}]$	D5-deviation		D7-deviation	
			$(\Delta\sigma_{\min})$	$\Delta\sigma_{\max}$	$(\Delta\sigma_{\min})$	$\Delta\sigma_{\max} \%$
120GeV	minimal	295.31 ± 0.13	(17.7%)	24.6%	(42.3%)	54.9%
	WBF	105.64 ± 0.25	(13.2%)	15.4%	(17.7%)	19.8%
200GeV	minimal	193.82 ± 0.09	(13.8%)	28.0%	(56.2%)	73.1%
	WBF	83.09 ± 0.06	(4.8%)	17.9%	(22.2%)	23.2%
Applying an additional cut, $p_{T,\max} < 200\text{GeV}$, one obtains:						
120GeV	minimal	262.37 ± 0.23	(5.1%)	12.5%	(5.3%)	7.4%
	WBF	92.69 ± 0.14	(4.2%)	6.7%	(1.3%)	2.1%
200GeV	minimal	165.65 ± 0.15	(2.5%)	13.8%	(5.8%)	8.7%
	WBF	71.01 ± 0.11	(5.5%)	9.7%	(2.4%)	3.3%

Table 5.1: Total cross section and deviation of the effective theories for two different Higgs masses and the cuts (5.3) and (5.4) for $qq \rightarrow qqH$. σ_{tot} gives the total cross section using the full loop calculation. D5-deviation and D7-deviation give the deviation of the effective D5 and D5+D7 theories respectively, defined by (5.10) and (5.11).

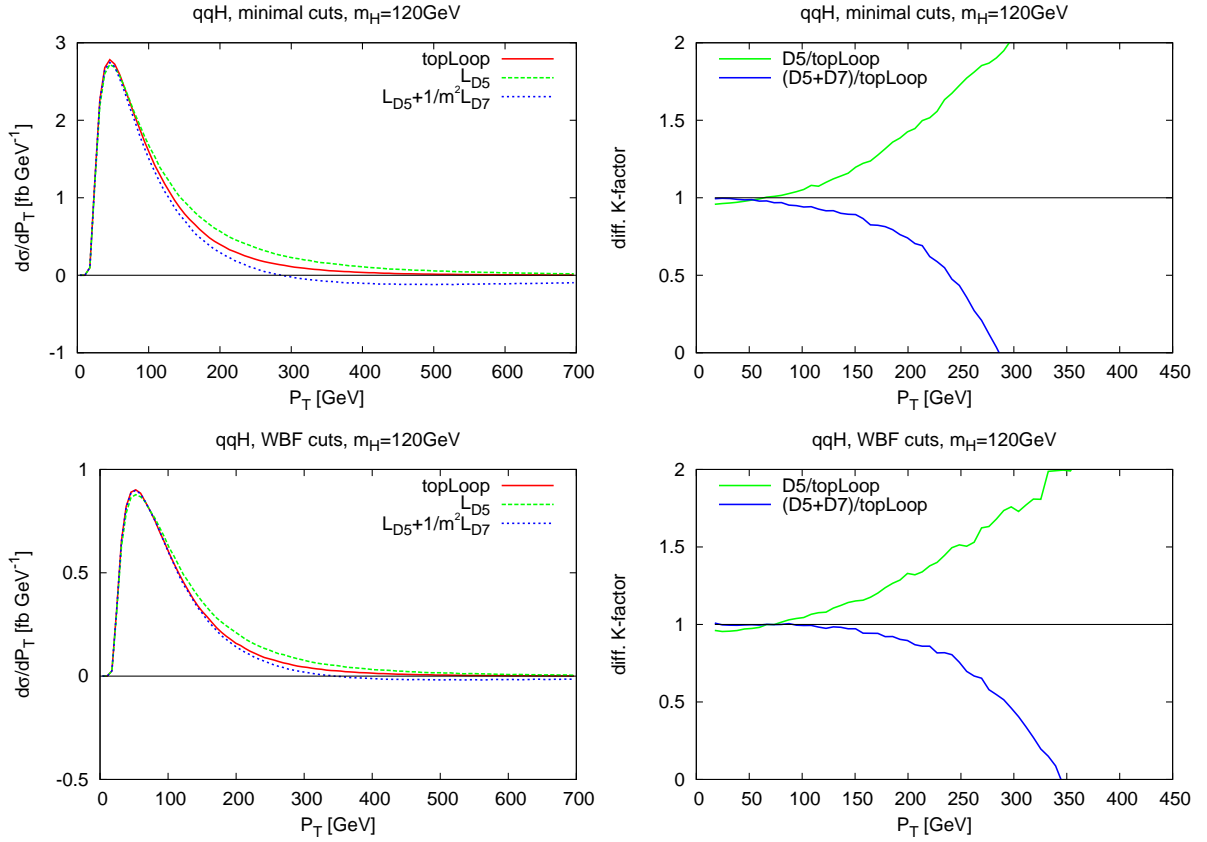


Figure 5.12: $qq \rightarrow qqH$ for minimal and WBF cuts (left) and differential K-factor as defined in (5.9) (right).

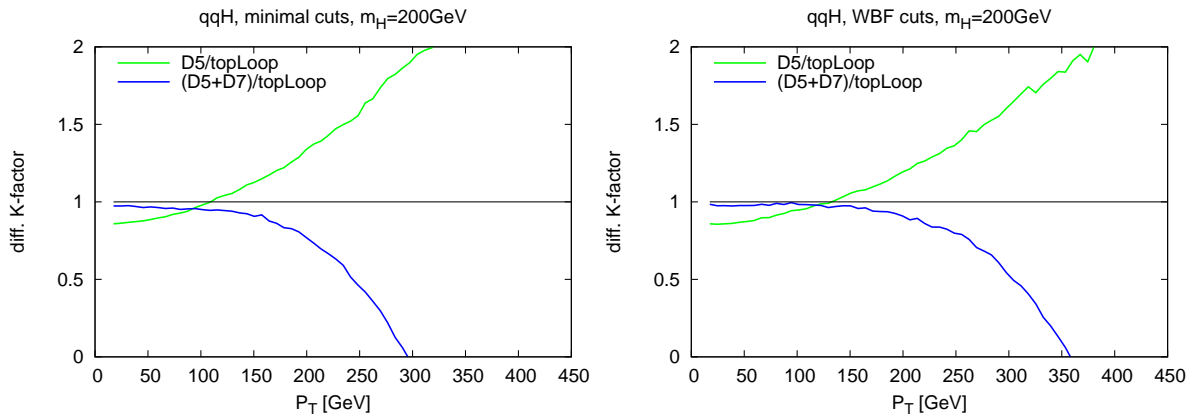


Figure 5.13: Differential K-factor for $qq \rightarrow qqH$ for $m_H = 200\text{GeV}$ as defined in (5.9). Left: minimal cuts. Right: WBF cuts.

Figure 5.12 shows the differential cross section over p_T of the hardest jet and the K-factor for the qqH subprocess for a Higgs mass of 120GeV. Since for a Higgs mass of 200GeV the differential p_T distribution has the same shape as for a 120GeV Higgs, only the differential K-factors are given in figure 5.13. The cross section peaks at low p_T

regions and fast approaches zero for $p_T > 300\text{GeV}$, at least for the full theory. The D5 effective theory unfortunately does not decline that fast, and for D7 the results for high p_T are unphysical (leading to negative weights). The differential K-factor denotes, that the effective theories brake down at phase space regions with $p_T \approx 150 - 200\text{GeV}$. On the other hand, for very low p_T one can see the effect of the mass correction, given by $\mathcal{L}_{D7,I}^H$. This contribution to the amplitude has the same phase as the D5 contribution \mathcal{L}_{D5}^H . This explains why the D5 approximation underestimates the full calculation for low p_T .

In table 5.1 one can read off the total cross section and deviations of the effective theories. It shows the real error one makes by considering the effective theory ($\Delta\sigma_{\max}$), calculated by (5.11) and aside the error one obtains by naive comparison of the total cross section is given in brackets ($\Delta\sigma_{\min}$). By comparing these numbers one can see, that one cannot trust in ($\Delta\sigma_{\min}$), which underestimates the real error by up to a factor five. Surprisingly, the effective D5 approximation is far away from being an excellent approximation, leading to large uncertainties of about 25 – 30% for minimal cuts, and 15% for WBF cuts. Applying an additional cut $p_{T,\max} < 200\text{GeV}$ reduces the error of the D5 effective theory already by a factor two. This can be further improved by the D7 correction, reducing the error down to 2 – 8%. One has to take into account, that the cut $p_{T,\max} < 200\text{GeV}$ reduces the total cross section by 10 – 15%. That means, that the total uncertainty, given by the sum of error and missing cross section, has almost the same magnitude as the original error given by using the D5 effective theory. However, if one wants to estimate the background for weak boson fusion processes, it would be possible to perform the $p_{T,\max}$ cut also for this process, being left with only the small error given above. In other words, to reduce the total error by considering the D7 correction, one should apply this cut to all observables.

qg → qgH

m_H	cuts	$\sigma_{\text{tot}}[\text{fb}]$	D5-deviation		D7-deviation	
			($\Delta\sigma_{\min}$)	$\Delta\sigma_{\max}$	($\Delta\sigma_{\min}$)	$\Delta\sigma_{\max}$
120GeV	minimal	4757.72 ± 6.67	(3.6%)	12.4%	(10.9%)	17.5%
	WBF	406.44 ± 0.34	(2.6%)	9.9%	(3.8%)	10.5%
200GeV	minimal	3263.16 ± 3.09	(3.3%)	18.5%	(14.4%)	23.6%
	WBF	314.45 ± 0.26	(5.8%)	15.6%	(5.2%)	13.2%
Applying an additional cut, $p_{T,\max} < 200\text{GeV}$, one obtains:						
120GeV	minimal	4296.56 ± 8.07	(1.3%)	7.3%	(2.4%)	3.9%
	WBF	365.05 ± 0.62	(1.6%)	6.0%	(0.1%)	3.6%
200GeV	minimal	2879.99 ± 4.27	(10.2%)	13.6%	(4.0%)	6.0%
	WBF	277.70 ± 0.47	(11.1%)	12.6%	(2.4%)	5.2%

Table 5.2: Total cross section and deviation of the effective theories for two different Higgs masses and the cuts (5.3) and (5.4) for $qg \rightarrow qgH$. σ_{tot} gives the total cross section using the full loop calculation. D5-deviation and D7-deviation give the deviation of the effective D5 and D5+D7 theories respectively, defined by (5.10) and (5.11).

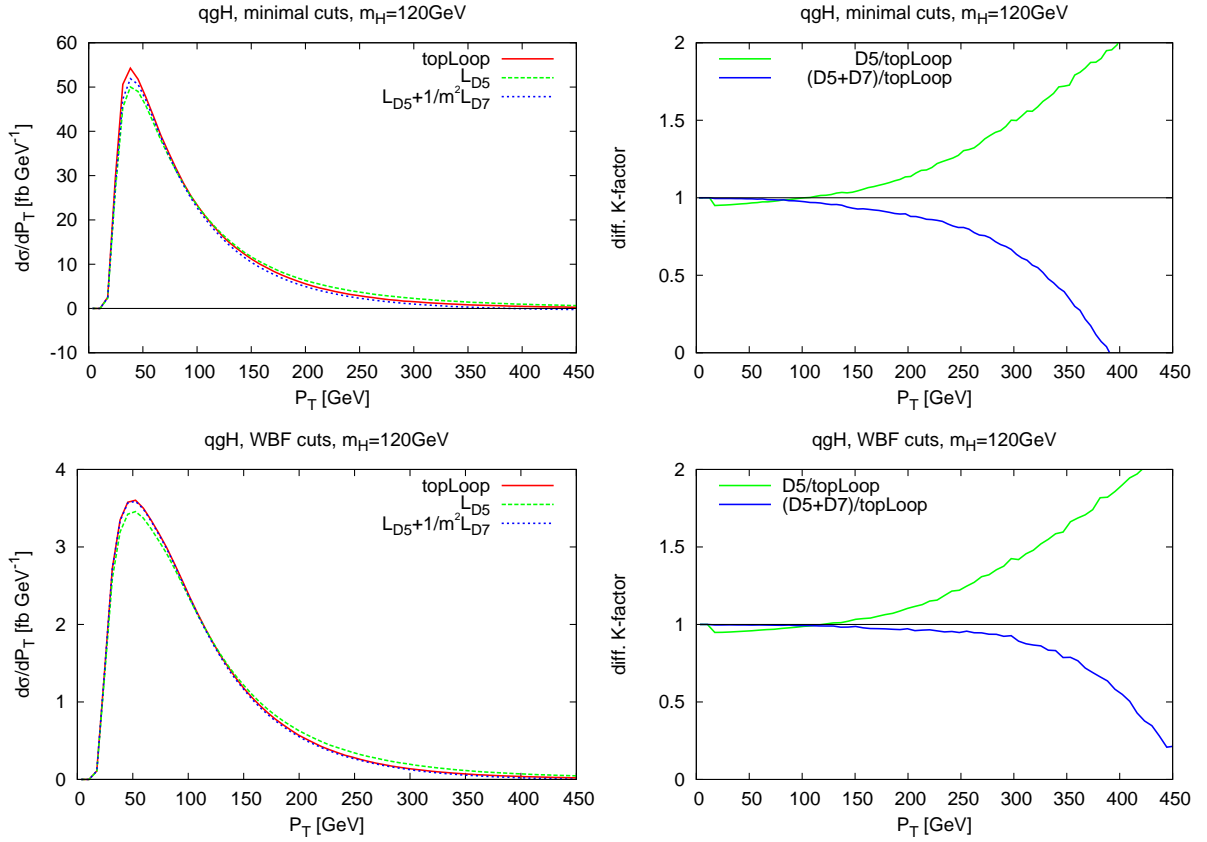


Figure 5.14: $qq \rightarrow qqH$ for minimal and WBF cuts and differential K-factor

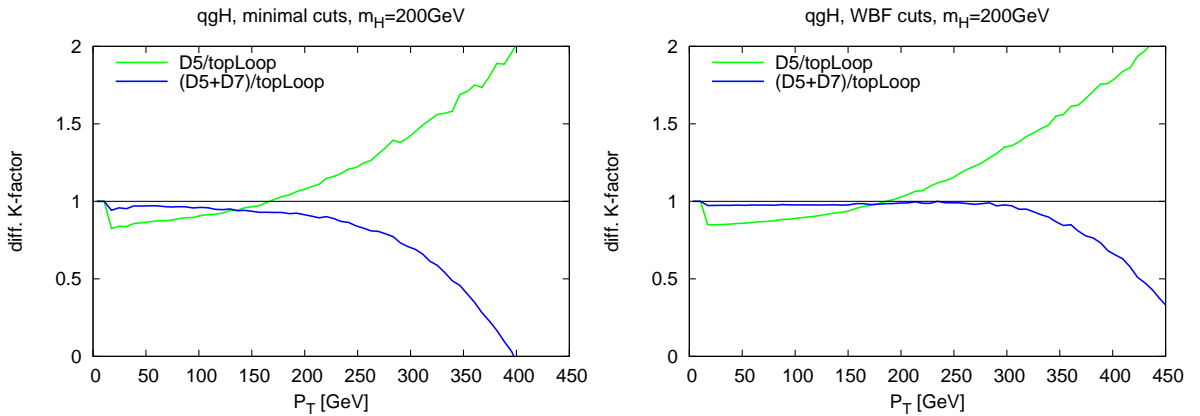


Figure 5.15: Differential K-factor for $qq \rightarrow qqH$ for $m_H = 200$ GeV. Left: minimal cuts. Right: WBF cuts

Figure 5.14 and 5.15 are, for reasons of comparison, arranged in the same way as for the qqH subprocess. Again one sees from the shape of the differential K-factor, that for large $p_{T,\max}$ the effective approximation breaks down. The discrepancy between the absolute values seem to be smaller than in the qqH case, the differential cross section $d\sigma/dp_T$ for the D7 effective theory is hardly distinguishable from the full calculation

(figure 5.14, left). In low p_T regions one can see the effect of the Higgs mass, given by $\mathcal{L}_{D7,I}^H$.

Having a look at the errors that arise when considering the effective theory, table 5.2, one finds as one would expect from figure 5.8, that they are smaller than in the qqH case. But still, using the D5 effective theory, gives a deviation from the full loop calculation up to 20%. The D7 correction without an additional cut on the phase space still gives no further improvement. It is interesting to notice, that the naive error underestimates the real one by at least a factor two. Applying the same cut as in the qqH case, $p_{T,\max} < 200\text{GeV}$, again reduces the error significantly. For the D5 + D7 effective theory it can thereby be reduced to 4 – 6%, while the D5 theory alone has errors of twice the magnitude. With this p_T cut the total cross section is reduced by about 10%. As mentioned above, hence it only makes sense to consider the D5+D7 approximation when the p_T cut is applied to all observables.

$gg \rightarrow ggH$

m_H	cuts	$\sigma_{\text{tot}}[\text{fb}]$	D5-deviation		D7-deviation	
			$(\Delta\sigma_{\min})$	$\Delta\sigma_{\max}$	$(\Delta\sigma_{\min})$	$\Delta\sigma_{\max}$
120GeV	minimal	8308.01 ± 7.79	(4.5%)	7.9%	(0.3%)	5.1%
	WBF	246.03 ± 0.17	(3.9%)	8.5%	(1.3%)	7.1%
200GeV	minimal	5840.85 ± 0.10	(13.6%)	16.6%	(0.1%)	7.9%
	WBF	186.03 ± 0.38	(11.7%)	15.7%	(1.6%)	8.0%
Applying an additional cut, $p_{T,\max} < 200\text{GeV}$, one obtains:						
120GeV	minimal	7703.46 ± 14.28	(5.9%)	6.6%	(0.1%)	2.5%
	WBF	227.92 ± 0.89	(5.4%)	7.1%	(0.1%)	4.6%
200GeV	minimal	5348.91 ± 10.57	(15.8%)	16.0%	(3.0%)	4.7%
	WBF	168.89 ± 0.68	(14.8%)	15.1%	(1.4%)	4.8%

Table 5.3: Total cross section and deviation of the effective theories for two different Higgs masses and the cuts (5.3) and (5.4) for $gg \rightarrow ggH$. σ_{tot} gives the total cross section using the full loop calculation. D5-deviation and D7-deviation give the deviation of the effective D5 and D5+D7 theories respectively, defined by (5.10) and (5.11).

The differential $p_{T,\max}$ distribution and the corresponding K-factor for the ggH subprocess are given in figure 5.16 for $m_H = 120\text{GeV}$ and the K-factors of a 200GeV Higgs in figure 5.17. In any of the four cases the $p_{T,\max}$ distribution shows almost the same behavior, as one can see by looking at the K-factors: Being in excellent agreement with the full loop calculation up to $\approx 200\text{GeV}$ and overestimating the full calculation for higher $p_{T,\max}$. The situation is quite different to the qqH and ggH case, where the D7 correction always underestimates the full theory for high $p_{T,\max}$, causing negative weights for sufficient large values of $p_{T,\max}$.

Having a look at the numbers in table 5.3, one finds that considering the D7 correction leads in any case to a better approximation than the D5 effective theory. Curiously, applying WBF cuts does not yield further improvement. A cut on $p_{T,\max}$ lowers again the total error made by considering the effective D7 calculation, whilst the total cross

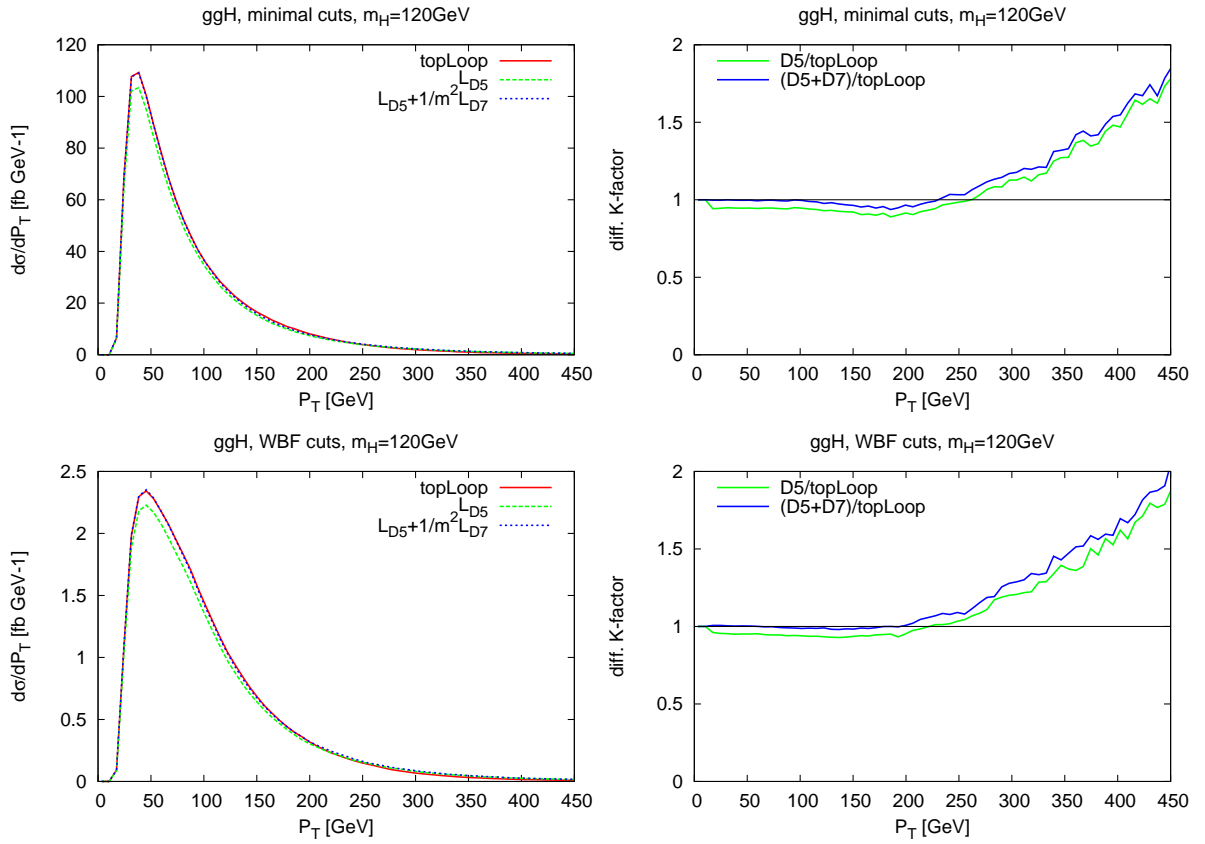


Figure 5.16: $gg \rightarrow ggH$ for minimal and WBF cuts and differential K-factor

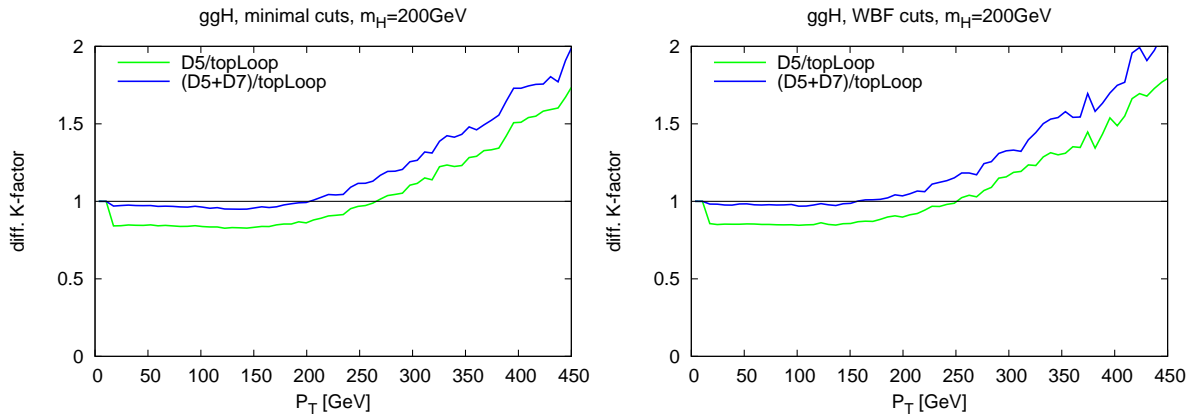


Figure 5.17: Differential K-factor for $gg \rightarrow ggH$ for $m_H = 200 \text{ GeV}$. Left: minimal cuts. Right: WBF cuts

section is reduced by $\approx 8\%$. The difference of the total deviation between the two effective theories reflects the fact, that the D7 correction is mainly given by the D5 calculation times a formfactor (5.6). For $m_H = 120 \text{ GeV}$ the D5 cross section increases by $\approx 2.7\%$ and for $m_H = 200 \text{ GeV}$ it is increased by $\approx 7.6\%$, giving approximately the differences between the error of the D5 and D7 calculation.

		$m_H = 120\text{GeV}$	$m_H = 200\text{GeV}$
D5 theory	minimal cuts	9.8%	11.4%
	WBF cuts	10.2%	15.9%
D5+D7, $p_{T,\text{max}} < 200$	minimal cuts	3.1%	5.2%
	WBF cuts	3.7%	4.8%

Table 5.4: Average error for effective theories considering all subprocesses for $pp \rightarrow Hjj$ via gluon fusion. The first two lines show the error by the D5 effective theory, while the last two lines take the D7 correction and a cut $p_{T,\text{max}} < 200$ into account.

5.5 Discussion

As we have seen in the last section, the calculation of cross sections for the process $pp \rightarrow Hjj$ may lead to unexpectedly high errors when calculating in the large top mass approximation. The main reason is the existence of highly virtual gluons which spoil the approximation. Appropriate cuts that suppress the appearance of these intermediate states could reduce the error by a factor two, but further improvement is desirable. As shown in the last section, it can be further reduced by considering the D7 correction to the effective theory and performing a cut on $p_{T,\text{max}}$. One may ask why a cut $p_{T,\text{max}} < 200\text{GeV}$ might be the best choice: First of all it is motivated by looking at the K-factors, figure 5.12 to 5.17, which in all three subprocesses is almost one, up to $p_T \approx 200\text{GeV}$. One has to keep in mind, that such a cut reduces the total cross section by approximately 10%. On the other hand, a less restrictive cut, e.g. $p_{T,\text{max}} < 350\text{GeV}$, would lower the cross section by only 2%, but one would still be left with uncertainties of about 10% – for the qqH subprocess even up to 20%.

The examined process is important due to two reasons: First, as mentioned in section 3.5, the coupling properties of a scalar Higgs can be measured by looking at the differential $\Delta\Phi_{jj}$ distribution of the cross section. Second, it is a background process to Higgs production via weak boson fusion. Applying the cut $p_{T,\text{max}} < 200\text{GeV}$ on the WBF process, one finds that one only loses 3.4% of the total cross section. This justifies such a cut for the background studies. The WBF signal is a promising channel for the discovery of a light or intermediate Higgs (120GeV – 200GeV); this process is actually known at NLO accuracy in α_s .² It is important to have also the QCD background at NLO accuracy since the LO calculation has large factorization- and renormalization scale dependencies. This NLO calculation was performed by [21] in the large top mass limit, and they have shown that a strong renormalization scale dependency remains, with the cross section varying by about 35% when the renormalization scale is changed by a factor 2. Nevertheless the NLO calculation also suffers from errors due to the $m_t \rightarrow \infty$ approximation. As we have seen in the last section, the cross section calculated using effective vertices also has to be treated as a function of p_T . The average errors for all three subprocesses for the LO calculation are summarized in table 5.4. Supposing that the NLO calculation uncertainties are of the same magnitude, one finds that the errors due to the effective theory are about half of the magnitude of the scale

²Recently the electroweak NLO corrections to this process were performed [35]

uncertainties. However, if one would perform a NLO calculation considering the D7 effective theory and applying an additional cut on p_T , the uncertainties due to the approximation might be reduced by a factor three. Additionally, the dimension 7 operators give rise to a six point function ($5gH$), a residual of the hexagon six point function appearing at NLO. As we will see in the next chapter, there seem to exist some MHV amplitudes for the D7 operators; hence implementing them into a program or extending MCFM (Monte Carlo for FeMtobarn processes [21]), where the next-to-leading order code is incorporated, might be easier than one would expect. Unfortunately the MCFM implementation of this NLO process has not been made public yet.

Chapter 6

MHV amplitudes for the dimension 7 operators

As seen in Chapter 3, MHV amplitudes are a powerful tool for calculating scattering amplitudes. It would therefore be nice to have corresponding compact expressions for the dimension 7 operators, (5.1) and (5.2). Trying to find MHV amplitudes for the individual parts of \mathcal{L}_{D7}^H and \mathcal{L}_{D7}^A most likely fails. A more promising ansatz is to proceed in the same way as suggested by [13], that is, splitting the effective Lagrangian into a selfdual and an antiselfdual part. Remember the definition of the (anti)selfdual field strength tensor:

$$G_{SD}^{\mu\nu} = \frac{1}{2}(G^{\mu\nu} + *G^{\mu\nu}), \quad G_{ASD}^{\mu\nu} = \frac{1}{2}(G^{\mu\nu} - *G^{\mu\nu}), \quad *G^{\mu\nu} \equiv \frac{i}{2}\epsilon^{\mu\nu\rho\sigma}G_{\rho\sigma} \quad (6.1)$$

The splitting may be possible for all parts of the dimension 7 Lagrangians but $\mathcal{L}_{D7,IV}^H$, since the involved operators do not have a corresponding dual. Nevertheless this is not that tragic, since this operator could be neglected for each of the pp to Hjj subprocesses; either because it vanishes analytically or its contribution is negligible.

The simplest case is the $\mathcal{L}_{D7,I}$ operator, since it is proportional to \mathcal{L}_{D5} . Considering H as the real part of a complex field and A as the imaginary part, $\phi = \frac{1}{2}(H + iA)$, one gets

$$\mathcal{L}_{D7,I}^{H,A} = \frac{C}{2} \left[H \text{Tr} G_{\mu\nu} G^{\mu\nu} + iA \text{Tr} G_{\mu\nu} *G^{\mu\nu} \right] \quad (6.2)$$

$$= C \left[\phi \text{Tr} G_{SD\mu\nu} G_{SD}^{\mu\nu} + \phi^\dagger \text{Tr} G_{ASD\mu\nu} G_{ASD}^{\mu\nu} \right] \quad (6.3)$$

with $C = 7\alpha_s m_A^2 / 720\pi v$ for the CP-even case and $C = -\alpha_s m_H^2 / 48\pi v$ for the CP-odd case. The Higgs amplitude can be recovered by the sum and difference of the ϕ and ϕ^\dagger amplitudes, respectively. The MHV amplitudes are the ones given in (3.18) and (3.22). For $\mathcal{L}_{D7,II}$ one can define the dual of $G_{\mu\nu\rho}^\mu$ in the same way as for the normal field strength tensor:

$$*G_{\mu\nu\rho}^\mu \equiv \frac{i}{2}\epsilon_{\nu\rho\sigma\tau} G_{\mu}^{\sigma\tau}$$

and the (anti)selfdual fields as in (6.1) just replacing $G_{\alpha\beta} \leftrightarrow G_{\mu\alpha\beta}^\mu$. Using the fact that

$$*G_{\mu\nu\rho}^\mu *G^{\nu\rho} = G_{\mu\nu\rho}^\mu G^{\nu\rho} \quad \text{and} \quad *G_{\mu\nu\rho}^\mu G^{\nu\rho} = G_{\mu\nu\rho}^\mu *G^{\nu\rho}$$

one finds

$$\mathcal{L}_{\text{D7,II}}^{\text{H,A}} = \frac{C}{2} \left[H \text{Tr} G_{\mu\nu\rho}^{\mu} G^{\nu\rho} + i A \text{Tr} G_{\mu\nu\rho}^{\mu} * G^{\nu\rho} \right] \quad (6.4)$$

$$= C \left[\phi \text{Tr} G_{\text{SD}\mu\nu\rho}^{\mu} G_{\text{SD}}^{\nu\rho} + \phi^{\dagger} \text{Tr} G_{\text{ASD}\mu\nu\rho}^{\mu} G_{\text{ASD}}^{\nu\rho} \right] \quad (6.5)$$

Here the constant C is given by $C = -11\alpha_s/360\pi v$ for the CP-even case and $C = \alpha_s/24\pi v$ for the CP-odd case.

The remaining part of the the effective Lagrangian is the one containing three field strength tensors. To split it into an selfdual and anti-selfdual part, one needs the following identities

$$\text{Tr} (G_{\nu}^{\mu} * G_{\rho}^{\nu} * G_{\mu}^{\rho}) = \text{Tr} (G_{\nu}^{\mu} G_{\rho}^{\nu} G_{\mu}^{\rho}) \quad \text{and} \quad \text{Tr} (*G_{\nu}^{\mu} * G_{\rho}^{\nu} * G_{\mu}^{\rho}) = \text{Tr} (G_{\nu}^{\mu} G_{\rho}^{\nu} * G_{\mu}^{\rho})$$

which can be shown with the help of ¹

$$\epsilon^{\mu\nu\rho\sigma} \epsilon_{\mu}{}^{\nu'\rho'\sigma'} = - \begin{vmatrix} g^{\nu\nu'} & g^{\nu\rho'} & g^{\nu\sigma'} \\ g^{\rho\nu'} & g^{\rho\rho'} & g^{\rho\sigma'} \\ g^{\sigma\nu'} & g^{\sigma\rho'} & g^{\sigma\sigma'} \end{vmatrix}$$

Using the equations above it is only a short calculation to show that

$$\mathcal{L}_{\text{D7,III}}^{\text{H,A}} = \frac{C}{2} \left[H \text{Tr} (G_{\nu}^{\mu} G_{\rho}^{\nu} G_{\mu}^{\rho}) + i A \text{Tr} (G_{\nu}^{\mu} G_{\rho}^{\nu} * G_{\mu}^{\rho}) \right] \quad (6.6)$$

$$= C \left[\phi \text{Tr} (G_{\text{SD}\nu}^{\mu} G_{\text{SD}\rho}^{\nu} G_{\text{SD}\mu}^{\rho}) + \phi^{\dagger} \text{Tr} (G_{\text{ASD}\nu}^{\mu} G_{\text{ASD}\rho}^{\nu} G_{\text{ASD}\mu}^{\rho}) \right] \quad (6.7)$$

with the constant $C = -i\alpha_s g/15\pi v$ for a CP-even and $C = i\alpha_s g/6\pi v$ for a CP-odd Higgs.

The easiest way to start is to look at the ϕggg scattering amplitude given by the selfdual part of $\mathcal{L}_{\text{D7,III}}^{\text{H,A}}$. Since it does not contain a ϕgg vertex, this amplitude is directly given by the ϕggg vertex contracted with external polarization vectors. The partial amplitude is explicitly given by:

$$\begin{aligned} A(\phi ggg) &= \frac{1}{2} \left((-i\epsilon^{q_3\varepsilon(q_1)\varepsilon(q_2)\varepsilon(q_3)} q_1 \cdot q_2 \pm \text{permutations of the } q_i) \right. \\ &\quad \left(-i\epsilon^{q_1 q_2 q_3 \varepsilon(q_1)} \varepsilon(q_2) \cdot \varepsilon(q_3) \pm \text{permutations of the } q_i) \right. \\ &\quad + i\epsilon^{q_2 q_3 \varepsilon(q_1)\varepsilon(q_3)} q_1 \cdot \varepsilon(q_2) + i\epsilon^{q_2 q_3 \varepsilon(q_1)\varepsilon(q_2)} q_1 \cdot \varepsilon(q_3) - i\epsilon^{q_1 q_3 \varepsilon(q_2)\varepsilon(q_3)} q_2 \cdot \varepsilon(q_1) \\ &\quad + i\epsilon^{q_1 q_3 \varepsilon(q_1)\varepsilon(q_2)} q_2 \cdot \varepsilon(q_3) - i\epsilon^{q_1 q_2 \varepsilon(q_2)\varepsilon(q_3)} q_3 \cdot \varepsilon(q_1) - i\epsilon^{q_1 q_2 \varepsilon(q_1)\varepsilon(q_3)} q_3 \cdot \varepsilon(q_2) \\ &\quad \left. + 3q_1 \cdot q_3 q_2 \cdot \varepsilon(q_1)\varepsilon(q_2) \cdot \varepsilon(q_3) \right) + 3q_1 \cdot \varepsilon(q_2) q_2 \cdot \varepsilon(q_3) q_3 \cdot \varepsilon(q_1) \end{aligned} \quad (6.8)$$

In Appendix D the basics of the spinor calculus are summarized which is needed to calculate helicity amplitudes. As described there, it is always possible to find polarization vectors that are orthogonal to each other, as long as all or all but one polarizations of the gluons are the same. Since this is always true for only three gluons, the second line in (6.8) vanishes for every helicity configuration. The first line also vanishes, since

¹taken from [4] A.1.10 p.743.

three polarization vectors are contracted with the epsilon tensor.²

If all gluons have helicity $h = -1$, one can see with the help of (D.1), that each of the remaining terms in (6.8) are proportional to $\langle 12 \rangle \langle 23 \rangle \langle 31 \rangle$, all with the same phase, leading to

$$A(\phi g^- g^- g^-) \propto \langle 12 \rangle \langle 23 \rangle \langle 31 \rangle$$

The case where all helicities are positive $h = +1$, each term is proportional to $[12][23][31]$, but the sum exactly cancels. For all other helicity configurations, each term in (6.8) vanishes separately.

As one might guess, the only non vanishing amplitude for the anti-selfdual part of the Lagrangian $\mathcal{L}_{D7,III}$ is the one with all helicities being positive:

$$A(\phi^\dagger g^+ g^+ g^+) \propto [12][23][31]$$

This leads to the following conjecture for the n -gluon partial amplitude of the selfdual part of $\mathcal{L}_{D7,III}$:

$$A(\phi, g_1, \dots, g_n) = 0, \quad \text{if } \#g^- \leq 2 \quad (6.9)$$

$$A(\phi, i^-, j^-, k^-) \propto \frac{\langle ij \rangle^2 \langle jk \rangle^2 \langle ki \rangle^2}{\langle 12 \rangle \dots \langle n-1, n \rangle \langle n1 \rangle} \quad (6.10)$$

That means, the amplitude vanishes if less than three gluons are negative, and the first non vanishing amplitudes – the MHV amplitudes – are the ones with exactly three negative helicity gluons. For the antiselfdual part just reverse helicities and exchange $\langle ij \rangle \leftrightarrow [ij]$. This conjecture was tested numerically for the four gluon amplitude. That is, the amplitude was calculated for a CP-even and a CP-odd Higgs and ϕ was constructed by taking the complex sum of both amplitudes $\phi = \frac{1}{2}(H+iA)$. The obtained amplitude was compared by the one, that is obtained via (6.10). The absolute values of the amplitudes are numerical in perfect agreement if one takes the proportionality constant equal 12 (the ratio is 1.0 up to 14 digits). Since conventions for calculating the MHV amplitudes were used, that differ from those used for calculating the Feynman diagrams, the relative phase to the dimension 5 amplitude still has to be fixed. This was done by calculating the amplitudes considering $\mathcal{L}_{D5} + \mathcal{L}_{D7,III}$. For a phase factor of (-1) again both calculations are in perfect agreement. Therefore, the four gluon partial amplitude for $\mathcal{L}_{D7,III}$ is given by³

$$A(\phi, i^-, j^-, k^-) = -12 \frac{\langle ij \rangle^2 \langle jk \rangle^2 \langle ki \rangle^2}{\langle 12 \rangle \langle 23 \rangle \langle 34 \rangle \langle 41 \rangle} \quad (6.11)$$

Since this amplitude is holomorphic in its' arguments, it should be possible to continue it off-shell and use it as an MHV-vertex. The four gluon amplitude for the all minus case was calculated, by using (6.11) as a MHV vertex and combining it with a pure QCD MHV-vertex. As expected, the absolute value of the amplitude was numerically

²see [13], Appendix B

³The color decomposition is given by (3.13)

in perfect agreement with the one calculated using Feynman graphs.

In the pure QCD case as well as the case where the ϕ field couples to the gluons via the dimension 5 operator, supersymmetric Ward identities relate MHV amplitudes containing only gluons to those containing one or two quark antiquark pairs [9, 15]. These identities can be derived, using the fact that the supercharge Q annihilates the vacuum. Following the line of arguments one can conclude, that the amplitudes containing a ϕ field (that couples to the SD part of \mathcal{L}_{D5}) and one $q\bar{q}$ pair should vanish if the total number of negative helicity particles is less than three (for ϕ^\dagger reverse helicities).

$$\begin{aligned} A_n(\phi, q^\mp, \bar{q}^\pm, g_3^+, \dots, g_n^+) &= 0 \\ A_n(\phi^\dagger, q^\pm, \bar{q}^\mp, g_3^-, \dots, g_n^-) &= 0 \end{aligned}$$

However, relating (6.10) to amplitudes containing a $q\bar{q}$ pair cannot be constructed in the same way, since for the proof it is essential that the MHV amplitudes are made out of exactly two negative (positive) helicity gluons. Nevertheless, it is worth to try to guess MHV amplitudes for the 4 parton case with one quark-antiquark pair and two gluons, since the amplitude is already available in VBFNLO. Being inspired by the pure QCD MHV amplitudes

$$A_n(g_i^-, g_j^-) = -\frac{\langle ij \rangle}{\langle ik \rangle} A_n(q_k^+, g_i^-, \bar{q}_j^-)$$

one can use trial and error by multiplying (6.11) with spinor products of the type $\langle ij \rangle / \langle jk \rangle$ where i and k represent the positive and negative helicity (anti)quark respectively, and j is one of the negative helicity gluons. It was worth the effort, since for one combination, the MHV amplitudes indeed coincide:

$$A(\phi, q_1^+, g_2^-, g_3^-, \bar{q}_4^-) = -12 \frac{\langle 12 \rangle \langle 24 \rangle \langle 23 \rangle^2 \langle 34 \rangle^2}{\langle 12 \rangle \langle 23 \rangle \langle 34 \rangle \langle 41 \rangle} = -12 \frac{\langle 24 \rangle \langle 23 \rangle \langle 34 \rangle}{\langle 41 \rangle} \quad (6.12)$$

The phase was checked to be correct by comparing the sum of the dimension 5 and dimension 7 result, as it was done in the pure gluonic case.

As a comment, deriving supersymmetric Ward identities for \mathcal{L}_{D7_III} for two quark-antiquark pairs should naively lead to the result, that the amplitude containing only one quark-antiquark pair should vanish. This is in agreement with the observation that this Lagrangian does not contribute to the $qq \rightarrow qqH$ amplitude.

The only missing part are now MHV amplitudes for \mathcal{L}_{D7_II} . We already know from the previous section, that the four gluon Higgs amplitude for \mathcal{L}_{D7_II} and \mathcal{L}_{D7_III} are proportional. A short calculation shows, that also the three gluon Higgs amplitudes are proportional. Further, the two gluon Higgs amplitude vanishes in both cases, as long as the gluons are on-shell. This raises the question if the amplitudes are the same for any number of external gluons. If so, the conjectures (6.9) and (6.10) would also be true for the selfdual part of \mathcal{L}_{D7_II} . So far, they for sure give the right expression for $n = 2, 3, 4$.

Chapter 7

Conclusions

The major challenge at the LHC will be the discovery or the exclusion of a Standard Model like Higgs boson. Therefore not only the existence of a new particle has to be guaranteed, but also its coupling properties and its spin have to be determined. In order to extract these from experimental data, one needs predictions with very small theoretical uncertainties – as well for the production process itself as for the background processes. A very promising discovery channel for a SM-like Higgs, is Higgs production via weak boson fusion. This process is actually known at NLO accuracy in α_s , while the QCD background process Higgs production via gluon fusion is only known at NLO if one takes the large top mass approximation into account. To perform this NLO calculation, the use of MHV amplitudes was made, since calculating scattering amplitudes therewith can be considerably faster than using the common method of Feynman diagrams.

The aim of this thesis was to determine the impact of helicity amplitudes, especially MHV amplitudes, for Higgs plus two jets via gluon fusion in the large top mass limit. In order to use the effective theory as an alternative to the full loop calculation (e.g. in a NLO calculation), it was examined to what extent it is valid, and in addition a correction described by dimension 7 operators was considered.

In Chapter 3 the strategy for calculating scattering amplitudes for Higgs plus n -partons with MHV techniques was reviewed. The main idea is to split the Lagrangian into a selfdual and an antiselfdual part. The so-derived MHV amplitudes were implemented into the parton level Monte Carlo program VBFNLO for the process $pp \rightarrow Hjj$. The time spent for calculating these amplitudes was compared to the time needed to calculate the amplitudes with Feynman diagrams. We saw that for the most time consuming subprocess $gg \rightarrow ggH$, the calculation using MHV amplitudes is almost a factor 3 faster than calculating with Feynman diagrams, while for the other two subprocesses the calculation with MHV amplitudes is comparable. Further the contribution of different helicity configurations to the total cross section as well as to the differential cross section $d\sigma/d\Phi_{jj}$ was studied. It was shown that the amplitudes which are MHV provide the bulk of the total cross section. In addition, exactly these amplitudes are responsible for the azimuthal angle modulation of the differential cross section.

Chapter 4 focuses on the large top mass limit. In this limit, one can expand the amplitude describing the Higgs-gluon coupling via a top loop into a power series in $1/m_{\text{top}}$.

The first coefficient proportional to $\mathcal{O}(1/m_t)^0$ can be described by the well known dimension 5 effective theory. It was recovered for a CP-even and for a CP-odd Higgs. The second coefficient, which is proportional to $\mathcal{O}(1/m_t)^2$, can be described by an effective dimension 7 theory. The derivation of the dimension 7 Lagrangian was explained in detail. We saw that this Lagrangian is ambiguous, and one has to take a particular choice which is motivated by the kinematics of the process.

In Chapter 5 the various operators describing the dimension 7 effective theory were implemented into VBFNLO for the process $pp \rightarrow Hjj$ via gluon fusion. The effective dimension 5 (D5) and dimension 7 (D7) theories were compared with respect to the full calculation containing the top loop. We found out, that the D5 theory leads to unexpectedly high errors, of about 10% – 15%. Processes leading to high P_T jets in the final state spoil the effective theories. The errors can be reduced by considering the D7 theory and performing additional cuts on the phase space. Since the above mentioned NLO calculation for this process also uses the D5 theory, it suffers from errors of presumably the same magnitude. Including the D7 Lagrangians could help to reduce these errors.

In Chapter 6 the effective D7 Lagrangians for a CP-even and a CP-odd Higgs were split into a selfdual and antiselfdual part in order to derive MHV amplitudes – in the same way as it was done for the D5 theory. One part of the D7 Lagrangian is proportional to the D5 Lagrangian; the corresponding MHV amplitudes are therefore trivial. For the two other parts of the Lagrangian, a conjecture for the n -gluon ϕ amplitude was given and shown to agree numerically with the known result for $n = 4$. Finally, for one of these two parts, a MHV amplitude for the $qqggH$ amplitude was found.

Appendix A

Feynman Rules and conventions

The following Feynman rules were used for the calculations:

$$\begin{array}{c} a, \mu \\ \text{---} \text{---} \text{---} \\ \diagup \quad \diagdown \\ \text{---} \quad \text{---} \end{array} = ig\gamma^{\mu t^a} \quad (\text{A.1})$$

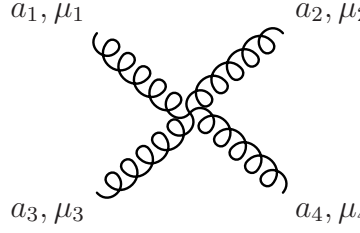
$$\text{---} \text{---} \text{---} = \frac{i(\not{p} + m)}{p^2 - m^2 + i\epsilon} \quad (\text{A.2})$$

$$\begin{array}{c} \diagup \\ \diagdown \\ \text{---} \end{array} = -i\frac{m_f}{v} \quad (\text{CP-even Higgs}) \quad (\text{A.3})$$

$$\begin{array}{c} \diagup \\ \diagdown \\ \text{---} \end{array} = -\gamma^5 \frac{m_f}{v} \quad (\text{CP-odd Higgs}) \quad (\text{A.4})$$

$$a_1, \mu_1 \text{---} \text{---} \text{---} \text{---} a_2, \mu_2 = \frac{-ig^{\mu_1\mu_2} \delta^{a_1 a_2}}{p^2} \quad (\text{A.5})$$

$$\begin{array}{c} a_1, \mu_1 \\ \text{---} \text{---} \text{---} \\ \diagup \quad \diagdown \\ \text{---} \quad \text{---} \\ a_2, \mu_2 \quad a_3, \mu_3 \end{array} = g f^{a_1 a_2 a_3} [g^{\mu_1 \mu_2} (q_1 - q_2)^{\mu_3} + g^{\mu_2 \mu_3} (q_2 - q_3)^{\mu_1} + g^{\mu_3 \mu_1} (q_3 - q_1)^{\mu_2}] \quad (\text{A.6})$$



$$\begin{aligned}
&= -ig^2 \left[f^{a_1 a_2 b} f^{a_3 a_4 b} (g^{\mu_1 \mu_3} g^{\mu_2 \mu_4} - g^{\mu_1 \mu_4} g^{\mu_2 \mu_3}) \right. \\
&\quad + f^{a_1 a_3 b} f^{a_2 a_4 b} (g^{\mu_1 \mu_2} g^{\mu_3 \mu_4} - g^{\mu_1 \mu_4} g^{\mu_2 \mu_3}) \quad (\text{A.7}) \\
&\quad \left. + f^{a_1 a_4 b} f^{a_2 a_3 b} (g^{\mu_1 \mu_2} g^{\mu_3 \mu_4} - g^{\mu_1 \mu_3} g^{\mu_2 \mu_4}) \right]
\end{aligned}$$

Notice that the Feynman rules used in VBFNLO use the conventions of Barger, Phillips [31], which differ in the gluon-fermion vertex by an additional (-1) . So one has to be careful and has to consider an additional minus sign for the phase when an odd number of gluon-fermion vertices appear.

Conventions

As long as not indicated explicitly the following conventions are taken:

Metric:

$$g^{\mu\nu} = \text{diag}(1, -1, -1, -1) \quad (\text{A.8})$$

Gamma matrices:

$$\gamma^\mu = \begin{pmatrix} 0 & \sigma^\mu \\ \bar{\sigma}^\mu & 0 \end{pmatrix} \quad \text{with} \quad \begin{aligned} \sigma^\mu &= (\mathbb{1}, \vec{\sigma}) \\ \bar{\sigma}^\mu &= (\mathbb{1}, -\vec{\sigma}) \end{aligned} \quad (\text{A.9})$$

$$\gamma^5 \equiv -i\gamma^0\gamma^1\gamma^2\gamma^3 \quad (\text{A.10})$$

$$\text{Tr}(\gamma^\mu\gamma^\nu\gamma^\rho\gamma^\sigma\gamma^5) = -4i\epsilon^{\mu\nu\rho\sigma} \quad (\text{A.11})$$

where $\vec{\sigma}$ are the Pauli matrices.

SU(3) color matrices:

$$\text{Tr}(T^a T^b) = \frac{1}{2}\delta^{ab} \quad (\text{A.12})$$

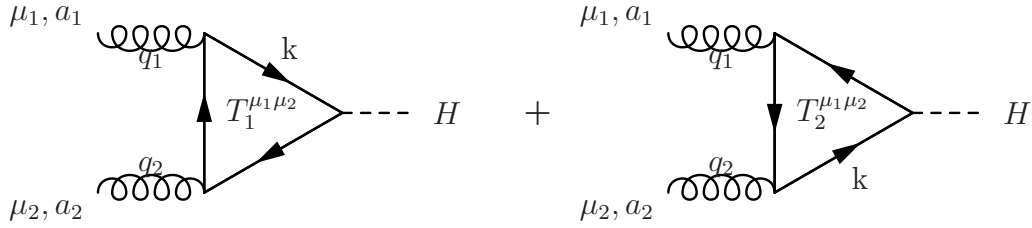
$$[T^a, T^b] = if^{abc}T^c \quad (\text{A.13})$$

Appendix B

Calculation of effective vertices

All calculations were performed with the help of MATHEMATICA.

B.1 Effective Hgg vertex



The analytic expression reads (with $q_{12} = q_1 + q_2$)

$$\begin{aligned}
 T_1^{\mu_1 \mu_2} &= (-1) \int \frac{d^d k}{(2\pi)^d} \text{Tr} \left\{ \frac{i}{\not{k} - m_t} (ig\gamma^{\mu_1} t^{a_1}) \frac{i}{\not{k} + \not{q}_1 - m_t} (ig\gamma^{\mu_2} t^{a_2}) \frac{i}{\not{k} + \not{q}_{12} - m_t} \left(\frac{-im_t}{v} \right) \right\} \\
 &= (-\delta^{a_1 a_2}) \frac{1}{2} \frac{m_t g^2}{v} \int \frac{d^d k}{(2\pi)^d} \frac{\text{Tr} \left\{ (\not{k} + m_t) \gamma^{\mu_1} (\not{k} + \not{q}_1 + m_t) \gamma^{\mu_2} (\not{k} + \not{q}_{12} + m_t) \right\}}{[k^2 - m_t^2] [(k + q_1)^2 - m_t^2] [(k + q_{12})^2 - m_t^2]} \quad (\text{B.1})
 \end{aligned}$$

Dimensional regularization was used to handle the singularities appearing in intermediate steps. The expression was evaluated in the following way:

- Shift the integration variable: $k + q_1 \rightarrow k$
- Introduce Feynman parameters according to

$$\frac{1}{ABC} = \int_0^1 dx \int_0^1 dy \int_0^1 dz \frac{2\delta(x + y + z - 1)}{(xA + yB + zC)^3} \quad (\text{B.2})$$

- Define

$$l = k - yq_1 + zq_2 \quad (\text{B.3})$$

$$\Delta = m_t^2 + (zq_2 - yq_1)^2 - yq_1^2 - zq_2^2 \quad (\text{B.4})$$

and express everything in terms of l and Δ , e.g. shift the integration variable.

$$\Rightarrow T_1^{\mu\nu} = \text{const} \cdot \int_0^1 dy \int_0^{1-y} dz \int \frac{d^d l}{(2\pi)^d} \frac{2\text{Tr}\{l, q_1, q_2\}}{[l^2 - \Delta]^3} \quad (\text{B.5})$$

- The integral is now symmetric in l , hence one can drop all terms in the numerator containing an odd number of l 's. Further, symmetry allows one to replace $l^{\mu_1} l^{\mu_2} \rightarrow \frac{1}{d} l^2 g^{\mu_1 \mu_2}$
- The numerator contains a rational part $\propto l^0$ and a divergent part $\propto l^2$, which has to be regularized. Performing the integral over the divergent part (with $\epsilon = (4 - d)/2$) one gets:¹

$$\int \frac{d^d l}{(2\pi)^d} \frac{g^{\mu_1 \mu_2} l^2 (\frac{4}{d} - 1)}{[l^2 - \Delta]^3} = \frac{ig^{\mu_1 \mu_2}}{2} \frac{1}{(4\pi)^{2-\epsilon}} \epsilon \Gamma(\epsilon) \left(\frac{1}{\Delta}\right)^\epsilon$$

$$\stackrel{\epsilon \rightarrow 0}{=} \frac{ig^{\mu_1 \mu_2}}{32\pi^2} \quad (\text{B.6})$$

For the rational part one only has to calculate the finite integral leading to

$$\int \frac{d^4 k}{(2\pi)^4} \frac{N_{\text{rat}}}{[l^2 - \Delta]^3} = \frac{-i}{32\pi^2} \frac{N_{\text{rat}}}{\Delta} \quad (\text{B.7})$$

where N_{rat} is a function independent of l .

- Expand $1/\Delta$ into a geometric series:

$$\frac{1}{\Delta} \equiv \frac{1}{m_t^2 + R} = \frac{1}{m_t^2} \frac{1}{1 + \frac{R}{m_t^2}} = \frac{1}{m_t^2} \left(1 - \frac{R}{m_t^2} + \left(\frac{R}{m_t^2}\right)^2 - \dots \right) \quad (\text{B.8})$$

R is a polynomial of the gluon momenta q_1, q_2 and the Feynman parameters y and z

- Integrate out the Feynman parameters y and z .
- Exploit Furry's theorem [26] to get the result for the three point function $T^{\mu_1 \mu_2}$:
 $T_1^{\mu_1 \mu_2} = T_2^{\mu_1 \mu_2} = \frac{1}{2} T^{\mu_1 \mu_2}$.

Expressing the result as

$$T^{\mu_1 \mu_2} = T_{D5}^{\mu_1 \mu_2} + T_{D7}^{\mu_1 \mu_2} \cdot \left(\frac{1}{m_t^2}\right) + T_{D9}^{\mu_1 \mu_2} \cdot \left(\frac{1}{m_t^2}\right)^2 + \dots \quad (\text{B.9})$$

one finally finds

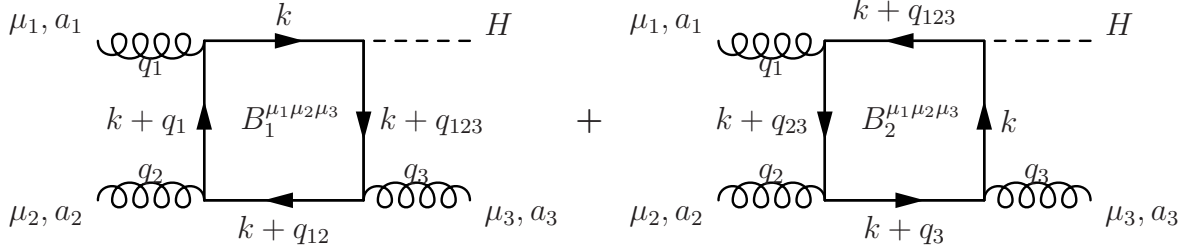
$$T_{D5}^{\mu_1 \mu_2} = -\frac{i\alpha_s}{3\pi v} \delta^{a_1 a_2} (g^{\mu_1 \mu_2} q_1 \cdot q_2 - q_1^{\mu_2} q_2^{\mu_1}) \quad (\text{B.10})$$

$$T_{D7}^{\mu_1 \mu_2} = \frac{i\alpha_s}{180\pi v} \delta^{a_1 a_2} [(g^{\mu_1 \mu_2} q_1 \cdot q_2 - q_1^{\mu_2} q_2^{\mu_1})(-7q_1 \cdot q_2 - 9q_1^2 - 9q_2^2)$$

$$+ g^{\mu_1 \mu_2} q_1^2 q_2^2 - q_1^2 q_2^{\mu_1} q_2^{\mu_2} - q_2^2 q_1^{\mu_1} q_1^{\mu_2} + (q_1 \cdot q_2) q_1^{\mu_1} q_2^{\mu_2}] \quad (\text{B.11})$$

¹The integrals can be found in various integral tables, e.g. in the appendix of [26].

B.2 Effective $Hggg$ vertex



The analytic expression of a generic four point integral is

$$B_1^{\mu_1\mu_2\mu_3} = (-1) \int \frac{d^4k}{(2\pi)^4} \text{Tr} \left\{ \frac{i}{\not{k} - m} (ig\gamma^{\mu_1} t^{a_1}) \frac{i}{\not{k} + \not{q}_1 - m} (ig\gamma^{\mu_2} t^{a_2}) \right. \quad (\text{B.12}) \\ \left. \times \frac{i}{\not{k} + \not{q}_{12} - m} (ig\gamma^{\mu_3} t^{a_3}) \frac{i}{\not{k} + \not{q}_{123} - m} \left(\frac{-im}{v} \right) \right\}$$

The full four point function is given by the sum over all six permutations of the gluons. This integral is finite, so no regulator is needed. The calculation is similar to the calculation of the three point function.

- Shift the integration variable: $k \rightarrow k - q_1$
- Use Feynman-Parameters according to:

$$\frac{1}{ABCD} = \int_0^1 dx_1 dx_2 dx_3 dx_4 \delta(x_1 + x_2 + x_3 + x_4 - 1) \frac{3!}{[x_1 A + x_2 B + x_3 C + x_4 D]^4} \quad (\text{B.13})$$

- Define

$$l^\mu = k^\mu - x_2 q_1^\mu + x_3 q_2^\mu + x_4 q_3^\mu + x_4 q_4^\mu \quad (\text{B.14})$$

$$\Delta = m^2 + x_2^2 q_1^2 - x_2 q_1^2 - 2x_2 x_3 q_1 \cdot q_2 - 2x_2 x_4 q_1 \cdot q_2 - 2x_2 x_4 q_1 \cdot q_3 + x_3^2 q_2^2 \quad (\text{B.15}) \\ + x_4^2 q_2^2 - x_3 q_2^2 + 2x_3 x_4 q_2^2 - x_4 q_2^2 + 2x_4^2 q_2 \cdot q_3 + 2x_3 x_4 q_2 \cdot q_3 - 2x_4 q_2 \cdot q_3$$

so that the denominator becomes $DN(q_1, q_2, q_3, q_4, l) = (l^2 - \Delta)^4$

- Discard all odd numbers of l due to symmetric integration.
- The momentum integral looks somewhat like (with A_1 and A_2 independent of l)

$$\int \frac{d^4l}{(2\pi)^4} \frac{\text{Tr}(\dots)}{DN(\dots)} = \int \frac{d^4k}{(2\pi)^4} \left\{ A_1 \frac{l^\mu l^\nu |l|^2}{DN} + A_2 \frac{1}{DN} \right\} \quad (\text{B.16})$$

Performing the integral using

$$\int \frac{d^4l}{(2\pi)^4} \frac{1}{(l^2 - \Delta)^4} = i \frac{1}{16\pi^2} \frac{1}{6} \frac{1}{\Delta^2} \quad (\text{B.17})$$

$$\int \frac{d^4l}{(2\pi)^4} \frac{l^2 |l^\mu l^\nu}{(l^2 - \Delta)^4} = -i \frac{1}{16\pi^2} \frac{4 |g^{\mu\nu}}{12} \frac{1}{\Delta} \quad (\text{B.18})$$

one gets

$$B_1^{\mu_1\mu_2\mu_3} = i \frac{g^3 m}{(4\pi)^2 v} \text{Tr}(t^{a_1} t^{a_2} t^{a_3}) \int_0^1 dx_1 dx_2 dx_3 dx_4 \delta(\sum x_i - 1) \left(A_3 \frac{1}{\Delta} + A_4 \frac{1}{\Delta^2} \right)$$

where A_3, A_4 are functions of the external momenta and Feynman parameters.

- Expand the denominators into a power series in $1/m_t^2$

$$\frac{1}{\Delta} = \frac{1}{m^2 + R} = \frac{1}{m^2} \left(\frac{1}{1 + \frac{R}{m^2}} \right) = \frac{1}{m^2} \left(1 - \frac{R}{m^2} + \frac{R^2}{m^4} - \dots \right) \quad (\text{B.19})$$

$$\frac{1}{\Delta^2} = \frac{1}{(m^2 + R)^2} = \frac{1}{m^4} \left(1 - 2\frac{R}{m^2} + 3\frac{R^2}{m^4} + \dots \right) \quad (\text{B.20})$$

- Perform the integral over the Feynman parameters, being left with

$$B_1^{\mu_1\mu_2\mu_3}(q_1, q_2, q_3) = \text{Tr}(t^{a_1} t^{a_2} t^{a_3}) \bar{B}_1^{\mu_1\mu_2\mu_3} \quad (\text{B.21})$$

From Furry's theorem one gets

$$\bar{B}_1^{\mu_1\mu_2\mu_3}(q_1, q_2, q_3) = -\bar{B}_2^{\mu_1\mu_2\mu_3}(q_1, q_2, q_3) = \bar{B}^{\mu_1\mu_2\mu_3}(q_1, q_2, q_3) \quad (\text{B.22})$$

The color structure of the sum of the two diagrams above is

$$\begin{aligned} & \text{Tr}(t^{a_1} t^{a_2} t^{a_3}) \bar{B}_1^{\mu_1\mu_2\mu_3}(q_1, q_2, q_3) + \text{Tr}(t^{a_3} t^{a_2} t^{a_1}) \bar{B}_2^{\mu_1\mu_2\mu_3}(q_1, q_2, q_3) \\ &= [\text{Tr}(t^{a_1} t^{a_2} t^{a_3}) - \text{Tr}(t^{a_3} t^{a_2} t^{a_1})] \bar{B}^{\mu_1\mu_2\mu_3}(q_1, q_2, q_3) = \frac{i}{2} f^{a_1 a_2 a_3} \bar{B}^{\mu_1\mu_2\mu_3}(q_1, q_2, q_3) \end{aligned}$$

using the identity

$$\text{Tr}(t^{a_1} t^{a_2} t^{a_3}) = \frac{1}{4} (d^{a_1 a_2 a_3} + i f^{a_1 a_2 a_3}) \quad (\text{B.23})$$

- The full amplitude can be recovered by summing over the six permutations of the gluons. It is proportional to a single color factor $f^{a_1 a_2 a_3}$

$$\begin{aligned} B^{\mu_1\mu_2\mu_3}(q_1, q_2, q_3) &= \frac{i}{2} f^{a_1 a_2 a_3} \left(\bar{B}^{\mu_1\mu_2\mu_3}(q_1, q_2, q_3) + \bar{B}^{\mu_2\mu_3\mu_1}(q_2, q_3, q_1) \right. \\ &\quad \left. + \bar{B}^{\mu_3\mu_1\mu_2}(q_3, q_1, q_2) \right) \end{aligned} \quad (\text{B.24})$$

Again, expressing the result as

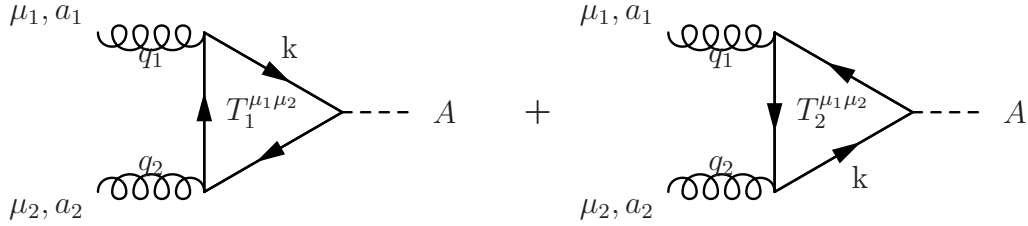
$$B^{\mu_1\mu_2\mu_3} = B_{D_5}^{\mu_1\mu_2\mu_3} + B_{D_7}^{\mu_1\mu_2\mu_3} \cdot \left(\frac{1}{m_t^2} \right) + B_{D_9}^{\mu_1\mu_2\mu_3} \cdot \left(\frac{1}{m_t^2} \right)^2 + \dots \quad (\text{B.25})$$

one finds

$$B_{D_5}^{\mu_1\mu_2\mu_3} = \frac{g\alpha_s}{3\pi v} f^{a_1 a_2 a_3} \left((q_2^{\mu_1} - q_3^{\mu_1}) g^{\mu_2\mu_3} + (q_3^{\mu_2} - q_1^{\mu_2}) g^{\mu_1\mu_3} + (q_1^{\mu_3} - q_2^{\mu_3}) g^{\mu_1\mu_2} \right) \quad (\text{B.26})$$

$$\begin{aligned}
B_{D7}^{\mu_1\mu_2\mu_3} = & \frac{g\alpha_s}{180\pi v} (-q_1^{\mu_1} q_2^{\mu_2} q_1^{\mu_3} - 2q_1^{\mu_1} q_3^{\mu_2} q_1^{\mu_3} + 2q_1^{\mu_1} q_1^{\mu_2} q_2^{\mu_3} + q_1^{\mu_1} q_2^{\mu_2} q_2^{\mu_3} + q_1^{\mu_1} q_1^{\mu_2} q_3^{\mu_3}) \quad (\text{B.27}) \\
& - q_1^{\mu_1} q_3^{\mu_2} q_3^{\mu_3} - 9g^{\mu_1\mu_3} q_1^{\mu_2} q_1^2 + g^{\mu_1\mu_3} q_2^{\mu_2} q_1^2 + 11g^{\mu_1\mu_3} q_3^{\mu_2} q_1^2 + 9g^{\mu_1\mu_2} q_1^{\mu_3} q_1^2 \\
& - 11g^{\mu_1\mu_2} q_2^{\mu_3} q_1^2 - g^{\mu_1\mu_2} q_3^{\mu_3} q_1^2 - q_1^{\mu_1} g^{\mu_2\mu_3} q_1 \cdot q_2 - 7g^{\mu_1\mu_3} q_1^{\mu_2} q_1 \cdot q_2 \\
& + g^{\mu_1\mu_3} q_2^{\mu_2} q_1 \cdot q_2 - 18g^{\mu_1\mu_3} q_3^{\mu_2} q_1 \cdot q_2 - 4g^{\mu_1\mu_2} q_1^{\mu_3} q_1 \cdot q_2 + 4g^{\mu_1\mu_2} q_2^{\mu_3} q_1 \cdot q_2 \\
& + q_1^{\mu_1} g^{\mu_2\mu_3} q_1 \cdot q_3 + 4g^{\mu_1\mu_3} q_1^{\mu_2} q_1 \cdot q_3 - 4g^{\mu_1\mu_3} q_3^{\mu_2} q_1 \cdot q_3 + 7g^{\mu_1\mu_2} q_1^{\mu_3} q_1 \cdot q_3 \\
& + 18g^{\mu_1\mu_2} q_2^{\mu_3} q_1 \cdot q_3 - g^{\mu_1\mu_2} q_3^{\mu_3} q_1 \cdot q_3 - q_1^{\mu_1} g^{\mu_2\mu_3} q_2^2 - 10g^{\mu_1\mu_3} q_1^{\mu_2} q_2^2 \\
& + 10g^{\mu_1\mu_3} q_3^{\mu_2} q_2^2 + 11g^{\mu_1\mu_2} q_1^{\mu_3} q_2^2 - 9g^{\mu_1\mu_2} q_2^{\mu_3} q_2^2 + g^{\mu_1\mu_2} q_3^{\mu_3} q_2^2 + 18g^{\mu_1\mu_3} q_1^{\mu_2} q_2 \cdot q_3 \\
& - g^{\mu_1\mu_3} q_2^{\mu_2} q_2 \cdot q_3 + 7g^{\mu_1\mu_3} q_3^{\mu_2} q_2 \cdot q_3 - 18g^{\mu_1\mu_2} q_1^{\mu_3} q_2 \cdot q_3 - 7g^{\mu_1\mu_2} q_2^{\mu_3} q_2 \cdot q_3 \\
& + g^{\mu_1\mu_2} q_3^{\mu_3} q_2 \cdot q_3 + q_1^{\mu_1} g^{\mu_2\mu_3} q_3^2 - 11g^{\mu_1\mu_3} q_1^{\mu_2} q_3^2 - g^{\mu_1\mu_3} q_2^{\mu_2} q_3^2 + 9g^{\mu_1\mu_3} q_3^{\mu_2} q_3^2 \\
& + 10g^{\mu_1\mu_2} q_1^{\mu_3} q_3^2 - 10g^{\mu_1\mu_2} q_2^{\mu_3} q_3^2 + q_3^{\mu_1} (11q_3^{\mu_2} (q_1^{\mu_3} - q_2^{\mu_3}) + 2q_2^{\mu_2} q_2^{\mu_3} + q_2^{\mu_2} q_3^{\mu_3} \\
& + q_1^{\mu_2} (-11q_1^{\mu_3} - 36q_2^{\mu_3} + 2q_3^{\mu_3})) - 10g^{\mu_2\mu_3} q_1^2 + 18g^{\mu_2\mu_3} q_1 \cdot q_2 - 7g^{\mu_2\mu_3} q_1 \cdot q_3 \\
& - 11g^{\mu_2\mu_3} q_2^2 + 4g^{\mu_2\mu_3} q_2 \cdot q_3 - 9g^{\mu_2\mu_3} q_3^2 + q_2^{\mu_1} (36q_3^{\mu_2} q_1^{\mu_3} + 11q_1^{\mu_2} (q_1^{\mu_3} - q_2^{\mu_3})) \\
& + 11q_3^{\mu_2} q_2^{\mu_3} - 2q_3^{\mu_2} q_3^{\mu_3} - q_2^{\mu_2} (2q_1^{\mu_3} + q_3^{\mu_3}) + 10g^{\mu_2\mu_3} q_1^2 + 7g^{\mu_2\mu_3} q_1 \cdot q_2 \\
& - 18g^{\mu_2\mu_3} q_1 \cdot q_3 + 9g^{\mu_2\mu_3} q_2^2 - 4g^{\mu_2\mu_3} q_2 \cdot q_3 + 11g^{\mu_2\mu_3} q_3^2)
\end{aligned}$$

B.3 Effective Agg vertex



The analytic expression for the three point function containing a CP-odd Higgs A is:

$$\begin{aligned}
T_1^{\mu_1\mu_2} = & (-1) \int \frac{d^4k}{(2\pi)^4} \text{Tr} \left\{ \frac{i}{\not{k} - m_t} (ig\gamma^{\mu_1} t^{a_1}) \frac{i}{\not{k} + \not{q}_1 - m_t} (ig\gamma^{\mu_2} t^{a_2}) \frac{i}{\not{k} + \not{q}_{12} - m_t} \right. \\
& \left. \times \left(-\frac{\gamma^5 m_t}{v} \right) \right\} \quad (\text{B.28})
\end{aligned}$$

In the CP-odd case there is no regulator needed for the three point function. Due to the additional γ^5 in the trace there is only one tensor structure proportional to $\epsilon^{\mu\nu\alpha\beta} q_{1\alpha} q_{2\beta}$ and there are no singularities. The way the calculation was performed is alike the CP-even case:

- Shift the integration variable $k \rightarrow k - p$
- Introduce Feynman parameters as given in (B.2)
- Define

$$l^\mu = k^\mu - x_2 q_1^\mu + x_3 q_2^\mu \quad (\text{B.29})$$

$$\Delta = x_2^2 q_1^2 - x_2 x_3 q_1 \cdot q_2 + x_3^2 q_2^2 - x_3 q_2^2 + m^2 \quad (\text{B.30})$$

so that the denominator becomes $(l^2 - \Delta)^3$. After performing the trace one is left with

$$T_1^{\mu_1\mu_2} = -\delta^{ab} \frac{4m_t^2 g^2}{2v} \int_0^1 dx_2 \int_0^{1-x_2} dx_3 \int \frac{d^4k}{(2\pi)^4} \frac{2\epsilon^{\mu_1\mu_2\alpha\beta} q_{1\alpha} q_{2\beta}}{(l^2 - \Delta)^3} \quad (\text{B.31})$$

- Perform the integration over the loop momenta using

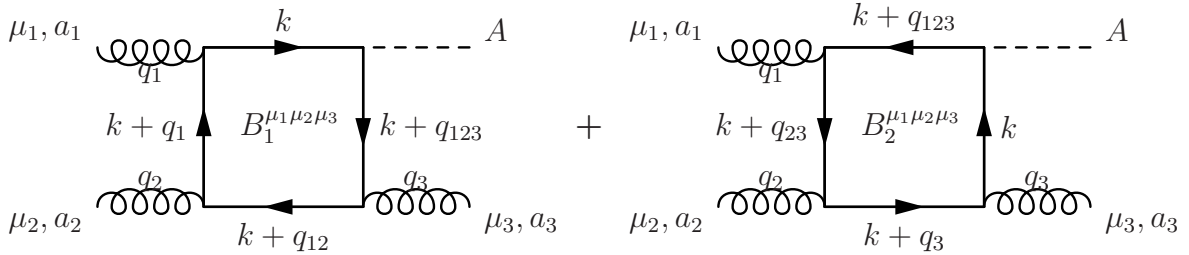
$$\int \frac{d^4k}{(2\pi)^4} \frac{1}{(l^2 - \Delta)^3} = \frac{-i}{(4\pi)^2} \frac{\Gamma(1)}{\Gamma(3)} \frac{1}{\Delta} = \frac{-i}{2(4\pi)^2} \frac{1}{\Delta} \quad (\text{B.32})$$

- The remaining steps are equal to the CP-even case: expand $1/\Delta$ as in (B.8), integrate out the Feynman parameters and exploit Furry's theorem to get $T^{\mu_1\mu_2}$.

The final result is

$$T^{\mu_1\mu_2} = \underbrace{\frac{i\alpha_s \delta^{ab}}{2\pi v} \epsilon^{\mu_1\mu_2\alpha\beta} q_{1\alpha} q_{2\beta}}_{T_{D5}^{\mu_1\mu_2}} + \underbrace{\frac{i\alpha_s \delta^{ab}}{12\pi v} \epsilon^{\mu_1\mu_2\alpha\beta} q_{1\alpha} q_{2\beta} (q_1^2 + q_1 \cdot q_2 + q_2^2)}_{T_{D7}^{\mu_1\mu_2}} \left(\frac{1}{m_t^2} \right) \quad (\text{B.33})$$

B.4 Effective *Aggg* vertex



The analytic expression is given by

$$B_1^{\mu_1\mu_2\mu_3} = (-1) \int \frac{d^4k}{(2\pi)^4} \text{Tr} \left\{ \frac{i}{\not{k} - m} (ig\gamma^{\mu_1} t^{a_1}) \frac{i}{\not{k} + \not{q}_1 - m} (ig\gamma^{\mu_2} t^{a_2}) \right. \\ \left. \times \frac{i}{\not{k} + \not{q}_{12} - m} (ig\gamma^{\mu_3} t^{a_3}) \frac{i}{\not{k} + \not{q}_{123} - m} \left(-\frac{\gamma^5 m}{v} \right) \right\} \quad (\text{B.34})$$

Again, the calculation is quite similar to the CP-even case:

- Shift $k \rightarrow k - q_1$ and introduce Feynman parameters according to B.13
- Define

$$l^\mu = k^\mu - x_2 q_1^\mu + x_3 q_2^\mu + x_4 (q_2^\mu + q_3^\mu) \quad (\text{B.35})$$

$$\Delta = m^2 + (x_2 - 1)x_2 q_1^2 - 2x_2 x_3 q_1 \cdot q_2 - 2x_2 x_4 q_1 \cdot q_2 - 2x_2 x_4 q_1 \cdot q_3 \\ - x_3 q_2^2 + x_3^2 q_2^2 - x_4 q_2^2 + 2x_3 x_4 q_2^2 + x_4^2 q_2^2 - 2x_4 q_2 \cdot q_3 + 2x_3 x_4 q_2 \cdot q_3 \\ + 2x_4^2 q_2 \cdot q_3 - x_4 q_3^2 + x_4^2 q_3^2 \quad (\text{B.36})$$

Express everything in terms of l and Δ so that the denominator is proportional to $(l^2 - \Delta)^4$.

- Evaluate the trace and discard all odd numbers of l^μ in the nominator. The nominator can be splitted into two parts, one propoortonal to l^2 and one containing no l 's.
- Perform the integration over the loop momenta using (B.17) and (B.18) and expand $1/\Delta^n$ into a taylor series.
- Sum over the six permutations of the outer gluons and exploit Furry's theorem to express everything by one single color factor as in (B.24).

The result expressed as

$$B^{\mu_1\mu_2\mu_3} = B_{D_5}^{\mu_1\mu_2\mu_3} + B_{D_7}^{\mu_1\mu_2\mu_3} \cdot \left(\frac{1}{m_t^2}\right) + B_{D_9}^{\mu_1\mu_2\mu_3} \cdot \left(\frac{1}{m_t^2}\right)^2 + \dots \quad (\text{B.37})$$

is given by

$$B_{D_5}^{\mu_1\mu_2\mu_3} = \frac{\alpha_s g}{2\pi v} f^{a_1 a_2 a_3} \epsilon^{\mu_1 \mu_2 \mu_3 \sigma} (q_1 + q_2 + q_3)_\sigma \quad (\text{B.38})$$

$$\begin{aligned} B_{D_7}^{\mu_1\mu_2\mu_3} = & \frac{\alpha_s g}{24\pi v} (-\epsilon^{\mu_3 q_1 q_2 q_3} g^{\mu_1 \mu_2} - \epsilon^{\mu_2 q_1 q_2 q_3} g^{\mu_1 \mu_3} + \epsilon^{\mu_2 \mu_3 q_1 q_3} q_2^{\mu_1} + \epsilon^{\mu_2 \nu^3 q_2 q_3} q_2^{\mu_1} \\ & + \epsilon^{\mu_2 \mu_3 q_1 q_2} q_3^{\mu_1} - \epsilon^{\mu_2 \mu_3 q_2 q_3} q_3^{\mu_1} - \epsilon^{\mu_1 q_1 q_2 q_3} g^{\mu_2 \mu_3} - \epsilon^{\mu_1 \mu_3 q_1 q_3} q_1^{\mu_2} - \epsilon^{\mu_1 \mu_3 q_2 q_3} q_1^{\mu_2} \\ & + \epsilon^{\mu_1 \mu_3 q_1 q_2} q_3^{\mu_2} + \epsilon^{\mu_1 \mu_3 q_1 q_3} q_3^{\mu_2} + \epsilon^{\mu_1 \mu_2 q_1 q_2} q_1^{\mu_3} - \epsilon^{\mu_1 \mu_2 q_2 q_3} q_1^{\mu_3} - \epsilon^{\mu_1 \mu_2 q_1 q_2} q_2^{\mu_3} \\ & - \epsilon^{\mu_1 \mu_2 q_1 q_3} q_2^{\mu_3} + \epsilon^{\mu_1 \mu_2 \mu_3 q_1} q_1^2 + \epsilon^{\mu_1 \mu_2 \mu_3 q_2} q_1^2 + \epsilon^{\mu_1 \mu_2 \mu_3 q_3} q_1^2 + \epsilon^{\mu_1 \mu_2 \mu_3 q_1} q_1 \cdot q_2 \\ & + \epsilon^{\mu_1 \mu_2 \mu_3 q_2} q_1 \cdot q_2 + \epsilon^{\mu_1 \mu_2 \mu_3 q_3} q_1 \cdot q_2 + \epsilon^{\mu_1 \mu_2 \mu_3 q_1} q_1 \cdot q_3 + \epsilon^{\mu_1 \mu_2 \mu_3 q_2} q_1 \cdot q_3 \\ & + \epsilon^{\mu_1 \mu_2 \mu_3 q_3} q_1 \cdot q_3 + \epsilon^{\mu_1 \mu_2 \mu_3 q_1} q_2^2 + \epsilon^{\mu_1 \mu_2 \mu_3 q_2} q_2^2 + \epsilon^{\mu_1 \mu_2 \mu_3 q_3} q_2^2 + \epsilon^{\mu_1 \mu_2 \mu_3 q_1} q_2 \cdot q_3 \\ & + \epsilon^{\mu_1 \mu_2 \mu_3 q_2} q_2 \cdot q_3 + \epsilon^{\mu_1 \mu_2 \mu_3 q_3} q_2 \cdot q_3 + \epsilon^{\mu_1 \mu_2 \mu_3 q_1} q_3^2 + \epsilon^{\mu_1 \mu_2 \mu_3 q_2} q_3^2 + \epsilon^{\mu_1 \mu_2 \mu_3 q_3} q_3^2) \end{aligned} \quad (\text{B.39})$$

where $\epsilon^{\mu_1 \mu_2 \mu_3 q_1} = \epsilon^{\mu_1 \mu_2 \mu_3 \alpha} q_{1\alpha}$ etc.

Appendix C

Identities between effective Lagrangians

To show the following identities, it is useful to express the field strength tensors with help of the covariant derivative in the adjoint representation (4.15-4.17). Using partial integration and the fact, that the boundary terms vanish one has:

$$\begin{aligned}
HG^{a\nu\rho}G^a{}_{\mu\nu\rho} &= HG^{a\nu\rho}D^{ab\mu}G^b{}_{\mu\nu\rho} \\
&= HG^{a\nu\rho}(\partial^\mu\delta^{ab}G^b{}_{\mu\nu\rho} - gA^{c\mu}f^{abc}G^b{}_{\mu\nu\rho}) \\
&\stackrel{\text{P.I.}}{=} -(\partial^\mu H)G^{a\nu\rho}G^a{}_{\mu\nu\rho} - H(\partial^\mu G^{a\nu\rho})G^a{}_{\mu\nu\rho} - gHG^{a\nu\rho}A^{c\mu}f^{abc}G^b{}_{\mu\nu\rho} \\
&= -(\partial^\mu H)G^{a\nu\rho}G^a{}_{\mu\nu\rho} - HG^b{}_{\mu\nu\rho}(\partial^\mu\delta^{ba} - gA^{c\mu}f^{bac})G^a{}_{\mu\nu\rho} \\
&= -(\partial^\mu H)G^{a\nu\rho}G^a{}_{\mu\nu\rho} - HG^b{}_{\mu\nu\rho}D^{ba\mu}G^{a\nu\rho} \\
&= -(\partial^\mu H)G^{a\nu\rho}(\partial_\mu\delta^{ab} - gA_\mu^c f^{abc})G^b{}_{\nu\rho} - HG^b{}_{\mu\nu\rho}G^{b\mu\nu\rho} \\
&= -(\partial^\mu H)G^{a\nu\rho}\partial_\mu G^a{}_{\nu\rho} + g(\partial^\mu H)A_\mu^c f^{abc}G^{a\nu\rho}G^b{}_{\nu\rho} - HG^a{}_{\mu\nu\rho}G^{a\mu\nu\rho}
\end{aligned}$$

The second term in the last line vanishes since $G^{a\nu\rho}G^b{}_{\nu\rho}$ is symmetric under exchange of a and b , while f^{abc} is antisymmetric.

Further, partial integration of the first term displays that

$$\begin{aligned}
-(\partial^\mu H)G^{a\nu\rho}\partial_\mu G^a{}_{\nu\rho} &= (\partial_\mu\partial^\mu H)G^{a\nu\rho}G^a{}_{\nu\rho} + (\partial^\mu H)(\partial_\mu G^{a\nu\rho})G^a{}_{\nu\rho} \\
\Rightarrow -(\partial^\mu H)G^{a\nu\rho}\partial_\mu G^a{}_{\nu\rho} &= \frac{1}{2}(\partial_\mu\partial^\mu H)G^{a\nu\rho}G^a{}_{\nu\rho}
\end{aligned}$$

Inserting this into the equation above, one finally gets

$$HG^{a\nu\rho}G^a{}_{\mu\nu\rho} = \frac{1}{2}(\partial_\mu\partial^\mu H)G^{a\nu\rho}G^a{}_{\nu\rho} - HG^a{}_{\mu\nu\rho}G^{a\mu\nu\rho} \quad (\text{C.1})$$

An almost identical calculation holds for the case, where an additional epsilon tensor is contracted, as it appears in the effective Lagrangian for an CP-odd Higgs.

$$\begin{aligned}
A\epsilon^{\nu\rho\alpha\beta}G^a{}_{\alpha\beta}G^a{}_{\mu\nu\rho} &= \text{same calculation as in the CP-even case} \\
&= \epsilon^{\nu\rho\alpha\beta}(-(\partial^\mu A)G^a{}_{\alpha\beta}\partial_\mu G^a{}_{\nu\rho} + g(\partial^\mu A)A_\mu^c f^{abc}G^a{}_{\alpha\beta}G^b{}_{\nu\rho} - AG^a{}_{\mu\nu\rho}G^{a\mu}{}_{\alpha\beta})
\end{aligned}$$

The second term vanishes due to the symmetry in a and b of $\epsilon^{\nu\rho\alpha\beta}G_{\alpha\beta}^a G_{\nu\rho}^b = \epsilon^{\nu\rho\alpha\beta}G_{\alpha\beta}^b G_{\nu\rho}^a$ and f^{abc} is antisymmetric under exchange of a, b . Partial integrating the first term gives

$$\begin{aligned} -\epsilon^{\nu\rho\alpha\beta}(\partial^\mu A)G_{\alpha\beta}^a \partial_\mu G_{\nu\rho}^a &= \epsilon^{\nu\rho\alpha\beta}((\partial_\mu \partial^\mu A)G_{\alpha\beta}^a G_{\nu\rho}^a + (\partial^\mu A)(\partial_\mu G_{\alpha\beta}^a)G_{\nu\rho}^a) \\ &= \epsilon^{\nu\rho\alpha\beta}((\partial_\mu \partial^\mu A)G_{\alpha\beta}^a G_{\nu\rho}^a + (\partial^\mu A)(\partial_\mu G_{\nu\rho}^a)G_{\alpha\beta}^a) \\ \Rightarrow -\epsilon^{\nu\rho\alpha\beta}(\partial^\mu A)G_{\alpha\beta}^a \partial_\mu G_{\nu\rho}^a &= \frac{1}{2}(\partial_\mu \partial^\mu A)\epsilon^{\nu\rho\alpha\beta}G_{\alpha\beta}^a G_{\nu\rho}^a \end{aligned}$$

where in the second line it was used that $\epsilon^{\mu\nu\alpha\beta} = \epsilon^{\alpha\beta\mu\nu}$ and indices were relabelled. Putting everything together one finds:

$$A\epsilon^{\nu\rho\alpha\beta}G_{\alpha\beta}^a G_{\mu\nu\rho}^a = \frac{1}{2}(\partial_\mu \partial^\mu A)\epsilon^{\nu\rho\alpha\beta}G_{\alpha\beta}^a G_{\nu\rho}^a - A\epsilon^{\nu\rho\alpha\beta}G_{\mu\nu\rho}^a G_{\alpha\beta}^a \quad (\text{C.2})$$

There is one more identity to be shown, which was used for the calculations. It is the one connecting $\epsilon^{\mu\nu\alpha\beta}G_{\mu\nu\rho}^a G_{\alpha\beta}^a$ with $\epsilon^{\mu\nu\alpha\beta}G_{\rho\mu\nu}^a G_{\alpha\beta}^a$. To derive the expression recall that $G_{\mu\nu\rho}^a$ is proportional to the commutator $[D_\mu, [D_\nu, D_\rho]]$. Exploit the Jacobi-Identity

$$[D_\mu, [D_\nu, D_\rho]] + [D_\nu, [D_\rho, D_\mu]] + [D_\rho, [D_\mu, D_\nu]] = 0$$

to get

$$G_{\mu\nu\rho}^a + G_{\nu\rho\mu}^a + G_{\rho\mu\nu}^a = 0$$

Making use of the antisymmetry in the last two indices of $G_{\mu\nu\rho}^a$ and the fact, that all indices are dummy, either contractet with $g^{\rho\sigma}$ or $\epsilon^{\mu\nu\alpha\beta}$, so that one can always relabel the indices, e.g. $\mu \leftrightarrow \alpha \wedge \nu \leftrightarrow \beta$, leads to

$$\begin{aligned} g^{\rho\sigma}\epsilon^{\mu\nu\alpha\beta}G_{\mu\nu\rho}^a G_{\alpha\beta\sigma}^a &= g^{\rho\sigma}\epsilon^{\mu\nu\alpha\beta}(-G_{\nu\rho\mu}^a - G_{\rho\mu\nu}^a)(-G_{\beta\sigma\alpha}^a - G_{\sigma\alpha\beta}^a) \\ &= g^{\rho\sigma}\epsilon^{\mu\nu\alpha\beta}(G_{\nu\rho\mu}^a G_{\beta\sigma\alpha}^a + G_{\nu\rho\mu}^a G_{\sigma\alpha\beta}^a + G_{\rho\mu\nu}^a G_{\beta\sigma\alpha}^a + G_{\rho\mu\nu}^a G_{\sigma\alpha\beta}^a) \\ &= g^{\rho\sigma}\epsilon^{\mu\nu\alpha\beta}(G_{\mu\rho\nu}^a G_{\alpha\sigma\beta}^a - G_{\mu\rho\nu}^a G_{\sigma\alpha\beta}^a - G_{\rho\mu\nu}^a G_{\alpha\sigma\beta}^a + G_{\rho\mu\nu}^a G_{\sigma\alpha\beta}^a) \\ &= g^{\rho\sigma}\epsilon^{\mu\nu\alpha\beta}(G_{\mu\nu\rho}^a G_{\alpha\beta\sigma}^a - 2G_{\mu\rho\nu}^a G_{\sigma\alpha\beta}^a + G_{\rho\mu\nu}^a G_{\sigma\alpha\beta}^a) \\ &= g^{\rho\sigma}\epsilon^{\mu\nu\alpha\beta}(G_{\mu\nu\rho}^a G_{\alpha\beta\sigma}^a + 2G_{\mu\rho\nu}^a G_{\alpha\beta\sigma}^a + 2G_{\mu\rho\nu}^a G_{\beta\sigma\alpha}^a + G_{\rho\mu\nu}^a G_{\sigma\alpha\beta}^a) \\ &= g^{\rho\sigma}\epsilon^{\mu\nu\alpha\beta}(G_{\mu\nu\rho}^a G_{\alpha\beta\sigma}^a - 2G_{\mu\nu\rho}^a G_{\alpha\beta\sigma}^a - 2G_{\mu\nu\rho}^a G_{\alpha\beta\sigma}^a + G_{\rho\mu\nu}^a G_{\sigma\alpha\beta}^a) \\ &= g^{\rho\sigma}\epsilon^{\mu\nu\alpha\beta}(-3G_{\mu\nu\rho}^a G_{\alpha\beta\sigma}^a + G_{\rho\mu\nu}^a G_{\sigma\alpha\beta}^a) \end{aligned}$$

and hence

$$\Rightarrow \epsilon^{\mu\nu\alpha\beta}G_{\mu\nu\rho}^a G_{\alpha\beta}^a = \frac{1}{4}\epsilon^{\mu\nu\alpha\beta}G_{\rho\mu\nu}^a G_{\alpha\beta}^a \quad (\text{C.3})$$

Appendix D

Spinor calculus

Calculating scattering amplitudes in QCD using the Weyl-Van der Waerden spinor calculus leads for specific helicity amplitudes to extraordinary short expressions. The upcoming problem is, that calculating them is not always that straight forward. The case of pure QCD for an arbitrary number of gluons was solved by Berends and Giele using recursive techniques [8]. In this thesis one often is interested of calculating amplitudes with a scalar coupling to the (anti)selfdual part of the gluonic field strength tensor, whereby contractions of epsilon tensors with outer momenta and polarization vectors appear. This leads to new subtleties. In the following a strategy for calculating them will be given, using a representation proposed in [9].

The solution of the massless Dirac equation (with definite helicity) is:

$$\begin{aligned} u_{\pm}(k) &= \frac{1}{2}(1 \pm \gamma_5)u(k) & \overline{u_{\pm}(k)} &= \overline{u(k)}(1 \mp \gamma_5) \\ v_{\mp}(k) &= \frac{1}{2}(1 \pm \gamma_5)u(k) & \overline{v_{\mp}(k)} &= \overline{v(k)}(1 \mp \gamma_5) \end{aligned}$$

Define:

$$\begin{aligned} |i^{\pm}\rangle &\equiv |k_i^{\pm}\rangle \equiv u_{\pm}(k_i) = v_{\mp}(k_i) \\ \langle i^{\pm}| &\equiv \langle k_i^{\pm}| \equiv \overline{u_{\pm}(k_i)} = \overline{v_{\mp}(k_i)} \end{aligned}$$

and spinor products:

$$\begin{aligned} \langle ij \rangle &\equiv \langle i^- | j^+ \rangle = \overline{u_-(k_i)} u_+(k_j) \\ [ij] &\equiv \langle i^+ | j^- \rangle = \overline{u_+(k_i)} u_-(k_j) \end{aligned}$$

Useful identities are:

- Gordon identity: $\langle i^{\pm} | \gamma^{\mu} | i^{\pm} \rangle = 2k_i^{\mu}$
- Projection operator: $|i^{\pm}\rangle \langle i^{\pm}| = \frac{1}{2} (1 \pm \gamma_5) \not{k}_i$
- Antisymmetry: $\langle ij \rangle = -\langle ji \rangle$, $[ij] = -[ji]$, $\langle ii \rangle = [ii] = 0$
- Fierz rearrangement: $\langle i^+ | \gamma^{\mu} | j^+ \rangle \langle k^+ | \gamma_{\mu} | l^+ \rangle = 2[ik] \langle lj \rangle$

- Charge conjugation of current: $\langle i^+ | \gamma^\mu | j^+ \rangle = \langle j^- | \gamma^\mu | i^- \rangle$
- Schouten identity: $\langle ij \rangle \langle kl \rangle = \langle ik \rangle \langle jl \rangle + \langle il \rangle \langle kj \rangle$

The polarization vector for a massless gauge boson with momentum k of definite helicity $h = \pm 1$ can be expressed as:

$$\epsilon_\mu^\pm(k, q) = \pm \frac{\langle q^\pm | \gamma_\mu | k^\mp \rangle}{\sqrt{2} \langle q^\mp | k^\pm \rangle}$$

where q is an arbitrary reference momenta which must not be proportional to k . It has the right property of a polarization vector, viz. it is transverse to k , complex conjugation reverses its' helicity and it has the standard normalization. A right choice of the reference momenta q_i can simplify the calculation substantially due to the following properties (with $\epsilon_i^\pm(q) \equiv \epsilon^\pm(k_i, q_i = q)$):

$$\begin{aligned} \epsilon_i^\pm(q) \cdot q &= 0 \\ \epsilon_i^+(q) \cdot \epsilon_j^+(q) &= \epsilon_i^-(q) \cdot \epsilon_j^-(q) = 0 \\ \epsilon_i^+(k_j) \cdot \epsilon_j^-(q) &= \epsilon_i^+(q) \cdot \epsilon_j^-(k_i) = 0 \\ \not{\epsilon}_i^+(k_j) |j^+\rangle &= \not{\epsilon}_i^-(k_j) |j^-\rangle = 0 \\ \langle j^+ | \not{\epsilon}_i^-(k_j) &= \langle j^- | \not{\epsilon}_i^+(k_j) = 0 \end{aligned}$$

Now, if all helicities of the n external gluons are the same, take all the reference momenta to be identical, $q_i \equiv q$. If all but one helicities are identical, choose the reference momenta of the differing gluon to be $q_1 = k_n$ and for the remaining $n - 1$ gluons $q_2 = q_3 = \dots = q_n = k_1$. With the relations above it follows that for this specific helicity configurations one has

$$\epsilon_i \cdot \epsilon_j = 0$$

From a technical point of view, this is the reason for the vanishing of so many helicity configurations and the existence of MHV amplitudes.

Contractions with an epsilon tensor can be expressed in terms of spinor products in the following way ($\epsilon^{\mu_1 \mu_2 \mu_3 \mu_4} k_{1\mu_1} k_{2\mu_2} k_{3\mu_3} k_{4\mu_4} \equiv \epsilon(k_1, k_2, k_3, k_4)$):

$$\begin{aligned} -4i\epsilon(k_1, k_2, k_3, k_4) &= \text{Tr}(\gamma_5 \not{k}_1 \not{k}_2 \not{k}_3 \not{k}_4) \\ &= \text{Tr}\left(\frac{1}{2}(1 + \gamma_5) \not{k}_1 \not{k}_2 \not{k}_3 \not{k}_4\right) - \text{Tr}\left(\frac{1}{2}(1 - \gamma_5) \not{k}_1 \not{k}_2 \not{k}_3 \not{k}_4\right) \\ &= \text{Tr}(|k_1^+\rangle \langle k_1^+ | k_2^-\rangle \langle k_2^- | k_3^+\rangle \langle k_3^+ | k_4^-\rangle \langle k_4^- |) \\ &\quad - \text{Tr}(|k_1^-\rangle \langle k_1^- | k_2^+\rangle \langle k_2^+ | k_3^-\rangle \langle k_3^- | k_4^+\rangle \langle k_4^+ |) \\ &= [12] \langle 23 \rangle [34] [41] - \langle 12 \rangle [23] \langle 34 \rangle [41] \end{aligned}$$

where in the last line the cyclic invariance of the trace was used. When calculating the $\phi g g g$ scattering given by the selfdual part of $\mathcal{L}_{\text{D7-III}}$, one often has to deal with ϵ tensors

contracting two or more polarization vectors. They can also be expressed in terms of spinor products by fierzing the upcoming expressions:

$$\begin{aligned}
4i\epsilon(\epsilon^+(k_1), \epsilon^+(k_2), k_3, k_4) &= \text{Tr}(\gamma_5 \not{\epsilon}^+(k_1) \not{k}_3 \not{\epsilon}^+(k_2) \not{k}_4) \\
&= \text{Tr}\left(\frac{1}{2}(1 + \gamma_5) \not{\epsilon}^+(k_1) \not{k}_3 \not{\epsilon}^+(k_2) \not{k}_4\right) \\
&\quad - \text{Tr}\left(\frac{1}{2}(1 - \gamma_5) \not{\epsilon}^+(k_1) \not{k}_3 \not{\epsilon}^+(k_2) \not{k}_4\right) \\
&= \text{Tr}\left(\gamma^\mu \frac{\langle \xi^- | \gamma_\mu | k_1^- \rangle}{\sqrt{2} \langle \xi^- | k_1^+ \rangle} |k_3^- \rangle \langle k_3^- | \gamma^\nu \frac{\langle \xi^- | \gamma_\nu | k_2^- \rangle}{\sqrt{2} \langle \xi^- | k_2^+ \rangle} |k_4^- \rangle \langle k_4^- | \right) \\
&\quad - \text{Tr}\left(\gamma^\mu \frac{\langle \xi^- | \gamma_\mu | k_1^- \rangle}{\sqrt{2} \langle \xi^- | k_1^+ \rangle} |k_3^+ \rangle \langle k_3^+ | \gamma^\nu \frac{\langle \xi^- | \gamma_\nu | k_2^- \rangle}{\sqrt{2} \langle \xi^- | k_2^+ \rangle} |k_4^+ \rangle \langle k_4^+ | \right) \\
&= \frac{\langle k_4^- | \gamma^\mu | k_3^- \rangle \langle \xi^- | \gamma_\mu | k_1^- \rangle \langle k_3^- | \gamma^\nu | k_4^- \rangle \langle \xi^- | \gamma_\nu | k_2^- \rangle}{2 \langle \xi^- | k_1^+ \rangle \langle \xi^- | k_2^+ \rangle} \\
&\quad - \frac{\langle k_4^+ | \gamma^\mu | k_3^+ \rangle \langle \xi^- | \gamma_\mu | k_1^- \rangle \langle k_3^+ | \gamma^\nu | k_4^+ \rangle \langle \xi^- | \gamma_\nu | k_2^- \rangle}{2 \langle \xi^- | k_1^+ \rangle \langle \xi^- | k_2^+ \rangle} \\
&= \frac{[31] \langle \xi 4 \rangle [42] \langle \xi 3 \rangle - [41] \langle \xi 3 \rangle [32] \langle \xi 4 \rangle}{2 \langle \xi 1 \rangle \langle \xi 2 \rangle} \tag{D.1}
\end{aligned}$$

If more than two polarization vectors are contracted to the epsilon tensor, one can demonstrate, as claimed in [13], that this expression vanishes.

Bibliography

- [1] D. J. Gross and F. Wilczek, ‘ULTRAVIOLET BEHAVIOR OF NON-ABELIAN GAUGE THEORIES,’ Phys. Rev. Lett. **30** (1973) 1343.
- [2] H. D. Politzer, ‘Asymptotic Freedom: An Approach To Strong Interactions,’ Phys. Rept. **14** (1974) 129.
- [3] K. G. Wilson, ‘CONFINEMENT OF QUARKS,’ Phys. Rev. D **10** (1974) 2445.
- [4] M. Böhm, A. Denner and H. Joos, ‘Gauge theories of the strong and electroweak interaction,’ *Stuttgart, Germany: Teubner (2001) 784 p*
- [5] L. D. Faddeev and V. N. Popov, ‘Feynman diagrams for the Yang-Mills field,’ Phys. Lett. B **25** (1967) 29.
- [6] A. Djouadi, ‘The anatomy of electro-weak symmetry breaking. I: The Higgs boson in the standard model,’ arXiv:hep-ph/0503172.
- [7] S. J. Parke and T. R. Taylor, ‘An Amplitude for n Gluon Scattering,’ Phys. Rev. Lett. **56** (1986) 2459.
- [8] F. A. Berends and W. T. Giele, ‘Recursive Calculations for Processes with n Gluons,’ Nucl. Phys. B **306** (1988) 759.
- [9] L. J. Dixon, ‘Calculating scattering amplitudes efficiently,’ arXiv:hep-ph/9601359.
- [10] M. L. Mangano and S. J. Parke, ‘Multiparton amplitudes in gauge theories,’ Phys. Rept. **200** (1991) 301 [arXiv:hep-th/0509223].
- [11] E. Witten, ‘Perturbative gauge theory as a string theory in twistor space,’ Commun. Math. Phys. **252** (2004) 189 [arXiv:hep-th/0312171].
- [12] F. Cachazo, P. Svrcek and E. Witten, ‘MHV vertices and tree amplitudes in gauge theory,’ JHEP **0409** (2004) 006 [arXiv:hep-th/0403047].
- [13] L. J. Dixon, E. W. N. Glover and V. V. Khoze, ‘MHV rules for Higgs plus multi-gluon amplitudes,’ JHEP **0412** (2004) 015 [arXiv:hep-th/0411092].
- [14] G. Georgiou and V. V. Khoze, ‘Tree amplitudes in gauge theory as scalar MHV diagrams,’ JHEP **0405** (2004) 070 [arXiv:hep-th/0404072].

-
- [15] S. D. Badger, E. W. N. Glover and V. V. Khoze, “MHV rules for Higgs plus multi-parton amplitudes,” *JHEP* **0503** (2005) 023 [arXiv:hep-th/0412275].
- [16] V. Del Duca, W. Kilgore, C. Oleari, C. Schmidt and D. Zeppenfeld, “Gluon-fusion contributions to $H + 2$ jet production,” *Nucl. Phys. B* **616** (2001) 367 [arXiv:hep-ph/0108030].
- [17] K. Hagiwara and D. Zeppenfeld, “Amplitudes for Multiparton Processes Involving a Current at $e^+ e^-$, $e^+ p$, and Hadron Colliders,” *Nucl. Phys. B* **313** (1989) 560.
- [18] G. Klamke and D. Zeppenfeld, “Higgs plus two jet production via gluon fusion as a signal at the CERN LHC,” *JHEP* **0704** (2007) 052 [arXiv:hep-ph/0703202].
- [19] R. V. Harlander and W. B. Kilgore, “Next-to-next-to-leading order Higgs production at hadron colliders,” *Phys. Rev. Lett.* **88** (2002) 201801 [arXiv:hep-ph/0201206].
- [20] C. Anastasiou, “Nnlo QCD Corrections For The Differential Higgs Boson Production Cross-Section In Gluon Fusion,” *AIP Conf. Proc.* **806** (2006) 75.
- [21] J. M. Campbell, R. K. Ellis and G. Zanderighi, “Next-to-leading order Higgs + 2 jet production via gluon fusion,” *JHEP* **0610** (2006) 028 [arXiv:hep-ph/0608194].
- [22] A. Djouadi, “The anatomy of electro-weak symmetry breaking. II: The Higgs bosons in the minimal supersymmetric model,” arXiv:hep-ph/0503173.
- [23] R. A. Diaz, “Phenomenological analysis of the two Higgs doublet model. ((W)),” arXiv:hep-ph/0212237.
- [24] J. F. Gunion, H. E. Haber, G. L. Kane and S. Dawson, “THE HIGGS HUNTER’S GUIDE,”
- [25] H. M. Georgi, S. L. Glashow, M. E. Machacek and D. V. Nanopoulos, “Higgs Bosons From Two Gluon Annihilation In Proton Proton Collisions,” *Phys. Rev. Lett.* **40** (1978) 692.
- [26] M. E. Peskin and D. V. Schroeder, “An Introduction To Quantum Field Theory,” *Reading, USA: Addison-Wesley (1995) 842 p*
- [27] Wolfram Research, Inc., *Mathematica*, Version 5.2, Champaign, IL (2005).
- [28] J. Kublbeck, H. Eck and R. Mertig, “Computeralgebraic generation and calculation of Feynman graphs using FeynArts and FeynCalc,” *Nucl. Phys. Proc. Suppl.* **29A** (1992) 204.
- [29] J. C. Ward, “An Identity in Quantum Electrodynamics,” *Phys. Rev.* **78** (1950) 182.
- [30] Y. Takahashi, “On the generalized Ward identity,” *Nuovo Cim.* **6** (1957) 371.

-
- [31] V. D. Barger and R. J. N. Phillips, “COLLIDER PHYSICS,” *REDWOOD CITY, USA: ADDISON-WESLEY (1987) 592 P. (FRONTIERS IN PHYSICS, 71)*
- [32] G. Altarelli and G. Parisi, “Asymptotic Freedom In Parton Language,” *Nucl. Phys. B* **126** (1977) 298.
- [33] H. L. Lai *et al.* [CTEQ Collaboration], “Global QCD analysis of parton structure of the nucleon: CTEQ5 parton distributions,” *Eur. Phys. J. C* **12** (2000) 375 [arXiv:hep-ph/9903282].
- [34] S. Kretzer, H. L. Lai, F. I. Olness and W. K. Tung, “CTEQ6 parton distributions with heavy quark mass effects,” *Phys. Rev. D* **69** (2004) 114005 [arXiv:hep-ph/0307022].
- [35] M. Ciccolini, A. Denner and S. Dittmaier, “Strong and electroweak corrections to the production of Higgs+2jets via weak interactions at the LHC,” arXiv:0707.0381 [hep-ph].

Zusammenfassung

Das Standardmodell der Teilchenphysik (SM) beschreibt alle bekannten fundamentalen Teilchen und deren Wechselwirkung als Quantenfeldtheorie einer exakten lokalen $SU(3)$ Eichgruppe und einer spontan gebrochenen lokalen $SU(2)_L \times U(1)_Y$ Eichgruppe. Die Vorhersagen des SM wurden in den unzähligen hochpräzisionsexperimenten, welche teilweise unter grössten Anstrengungen durchgeführt wurden, immer wieder bestätigt. Jedoch gibt es, trotz diesem Erfolg, noch immer einen unbekannt Parameter welchen es zu bestimmen gilt: die Masse des sogenannten Higgs Teilchens. Um die Existenz dieses Teilchens bestätigen bzw. ausschliessen zu können – und damit auch den Mechanismus der elektroschwachen Symmetriebrechung, ist einer der Hauptgründe die zum Bau des Large Hadron Colliders (LHC) geführt haben. Der LHC ist ein Proton-Proton Beschleuniger mit einer Schwerpunktsenergie von 14TeV und einer unglaublich hohen Luminosität, welches jedes zuvor dagewesene Experiment in den Schatten stellt.

Die ungebrochene $SU(3)$ Symmetrie des SM ist die Theorie der starken Wechselwirkung – die sogenannte Quanten Chromodynamik, oder kurz QCD. Die nicht-Abelsche Natur der QCD erlaubt es den trägern der starken Wechselwirkung, den sogenannten Gluonen, direkt miteinander wechselzuwirken. Dies und die Tatsache, dass die starke Wechselwirkung bei grossen Abständen sehr gross wird, machen Vorhersagen basierend auf störungstheoretischen Rechnungen schwer handhabbar. Da Protonen aus stark wechselwirkender Materie aufgebaut sind (Protonen bestehen aus Quarks und Gluonen), werden Streuprozesse am LHC von QCD induzierten Prozessen dominiert. In der Vergangenheit wurden daher grosse Anstrengungen unternommen, Vorhersagen für QCD Ereignisse möglich zu machen. In den letzten Jahren ist diesbezüglich ein neuer, vielversprechender Ansatz aufgekommen, welcher bis dato unbekannte (mathematische) Eigenschaften von so genannten maximal helizitätsverletzenden (MHV) Amplituden ausnutzt. Diese Methode wurde zuerst nur für Amplituden formuliert, welche die Streuung von n Gluonen beschreiben, jedoch wurde sie erweitert auf Amplituden mit ein oder zwei Quark-, Antiquark Paaren, massiven Vektorbosonen oder skalaren Teilchen, wie z.B. das Higgs Boson.

Einer der vielversprechendsten Entdeckungskanäle für ein Standard Model Higgs Boson am LHC, ist die Higgserzeugung durch die annihilation schwacher Eichbosonen (auch WBF Prozesse genannt). Dieser Prozess ist momentan zu next-to leading order (NLO) Genauigkeit in der starken Kopplungskonstanten α_s bekannt. Die charakteristische Signatur dieses Prozesses sind die zwei resultierenden Jets in Vorwärtsrichtung. Der mit diesem verwandte Prozess, Higgsproduktion plus zwei Jets induziert durch Gluonfusion, erzeugt einen irreduziblen Hintergrund und muss daher mit hoher Genauigkeit

vorhergesagt werden. Bis jetzt ist dieser Hintergrund jedoch nur auf leading order (LO) bekannt. Die Rechnung enthält eine Quark-Schleife, welche die Higgs-Gluon Kopplung ermöglicht. Eine NLO Rechnung für diesen Prozess ist zwar prinzipiell erhältlich, jedoch nur unter der Annahme, dass die Masse des Top-Quarks wesentlich grösser ist als alle anderen vorkommenden Grössen ($m_{\text{top}} \rightarrow \infty$). In diesem Grenzwert koppelt das Higgs direkt an die Gluonen. Ein wesentlicher Bestandteil der NLO Rechnung sind die oben erwähnten MHV-Amplituden, durch welche die Rechendauer des Programms stark verkürzt wird.

In dieser Diplomarbeit wird der Prozess $pp \rightarrow Hjj$ durch Gluonfusion untersucht. Ziel ist es, herauszufinden inwiefern MHV Amplituden von phänomenologischem Interesse sind. Da sich MHV Amplituden mit einem Higgs Boson nur in der Näherung $m_{\text{top}} \rightarrow \infty$ formulieren lassen, wird die Gültigkeit dieser Näherung untersucht. Weiter werden erstmalig die mit $1/m_{\text{top}}^2$ unterdrückten Terme genauer betrachtet und nachgeprüft, ob man durch Berücksichtigung dieser, die durch die Näherung auftretenden Unsicherheiten, reduzieren kann. Die Diplomarbeit ist wie folgt aufgebaut:

In Kapitel 2 werden die Grundzüge von Eichtheorien, speziell die der QCD wiederholt. Es wird gezeigt, wie sich die QCD aus der QED durch Verallgemeinerung von einer Abelschen auf eine nicht-Abelsche Eichgruppe ableiten lässt. Werden Übergangsamplituden auf Baumgraph-Niveau berechnet, so lassen sich die Amplituden einer nicht-Abelschen Eichgruppe in so genannte partielle Amplituden zerlegen (im Fall der QCD spricht man von farbgeordneten Amplituden). Diese Zerlegung wird durch betrachten der zugrundeliegenden Algebra motiviert. Schliesslich wird am Ende des Kapitels noch kurz auf den Higgs Sektor eingegangen, welcher für die Erzeugung der Massen und der Symmetriebrechung des elektroschwachen Sektors zuständig ist. Es wird explizit gezeigt, wie durch die Fermionkopplung an das skalare Higgsfeld Massenterme generiert werden können ohne Eichinvarianz zu verletzen.

Für die oben erwähnten partiellen Amplituden existieren, für bestimmte Helizitätskonfigurationen der externen Teilchen, erstaunlich kompakte Ausdrücke, welche MHV-Amplituden genannt werden. In Kapitel 3 wird gezeigt, wie diese MHV-Amplituden genutzt werden können, um Amplituden einer beliebigen Helizitätskonfiguration zu konstruieren. Dies wird zuerst für reine QCD Prozesse beschrieben, und dann auf Prozesse mit zusätzlich einem Higgs als externes Teilchen verallgemeinert. Diese MHV-Amplituden wurden in das parton level Monte Carlo Program VBFNLO für den Prozess $pp \rightarrow Hjj$ implementiert und das Tempo für Berechnungen mit diesen Amplituden wurde mit dem für Berechnungen mit herkömmlichen Feynman Diagrammen verglichen. Für die Subprozesse mit einem oder zwei Quarks im Endzustand ergibt sich mit MHV-Amplituden kein nennenswerter Zeitvorteil, für den Subprozess mit zwei Gluonen im Endzustand, welches auch der mit Feynman Amplituden am aufwendigsten zu Berechnende ist, ist man jedoch mit MHV Techniken um einen Faktor drei schneller. Im folgenden Abschnitt werden dann die Beiträge verschiedener Helizitätskonfigurationen zu dem differentiellen Wirkungsquerschnitt $d\sigma/d\Delta\Phi_{jj}$ betrachtet. Diese Verteilung zeigt ein oszillierendes Verhalten, dessen genaue Form davon abhängt, ob das Higgs Boson CP-geraden oder CP-ungeraden Charakter (bzw. eine Mischung aus beiden) besitzt. Den grössten Anteil am Wirkungsquerschnitt haben die zugehörigen MHV-Amplituden. Auch sind es genau diese Amplituden, die eine Oszillation zeigen. Durch das Betra-

chten einer komplexen Summe aus CP-geradem und CP-ungeradem Higgs wird diese Eigenschaft ersichtlich.

Die MHV-Amplituden mit einem Higgs sind nur im Grenzfall $m_{\text{top}} \rightarrow \infty$ erhältlich. In diesem Fall kann die Higgs-Gluon Kopplung durch eine effektive Lagrangedichte beschrieben werden, die Operatoren der Dimension 5 (D5) enthält. In Kapitel 4 diese effektive Theorie genauer betrachtet. Neben der bekannten D5 Theorie wird der mit $1/m_{\text{top}}^2$ unterdrückte Korrekturterm bestimmt, welcher durch eine effektive Lagrangedichte aus Operatoren der Dimension 7 (D7) beschrieben werden kann. Die Form des D7 Lagrangians ist, anders als die des D5 Lagrangians, nicht eindeutig. Vielmehr muss man sich auf ein unabhängiges Set von D7 Operatoren festlegen. Bei genauerer Betrachtung der auftretenden Kinematik, erweist sich jedoch eine bestimmte Kombination von Operatoren als sinnvoll. Die mit $1/m_{\text{top}}^2$ unterdrückten Korrekturterme werden sowohl für ein CP-gerades als auch ein CP-ungerades Higgs-Boson hergeleitet.

In Kapitel 5 wird die Auswirkung der D7 Operatoren auf die drei Subprozesse qqH , qgH und ggH untersucht. Dazu wurden die durch die D7 Operatoren gegebenen Amplituden in VBFNLO implementiert. Man findet, dass für Impulsüberträge $q^2 \gg m_{\text{top}}^2$ die Näherung zusammenbricht. Jedoch können die dafür relevanten Phasenraumregionen durch einen cut auf den maximalen Transversalimpuls des härtesten Jets beseitigt werden. Ein cut $p_{T,\text{max}} < 200\text{GeV}$ erscheint als angebracht. Dabei sollte man beachten, dass dieser cut den totalen Wirkungsquerschnitt um ca. 10% reduziert. Dies sollte jedoch nicht weiter stören solange man diesen Prozess als Hintergrundprozess zu Vektorbosonfusionsprozessen (WBF) betrachtet, da hierfür ein cut $p_{T,\text{max}} < 200\text{GeV}$ den totalen Wirkungsquerschnitt nur um ca. 3.4% verringert. Eine genaue Untersuchung zeigt, dass die durch die effektive Theorie auftretenden Unsicherheiten von 10% – 16%, je nach Higgsmasse und angewandeter cuts, durch Berücksichtigung der D7 Korrektur und dem cut $p_{T,\text{max}} < 200\text{GeV}$ deutlich reduziert werden können. Da die NLO Rechnung im Limes $m_{\text{top}} \rightarrow \infty$ berechnet wurde, ist anzunehmen, dass die Rechnung von zusätzlichen Unsicherheiten der gleichen Grössenordnung behaftet ist. Würde man in einer NLO Rechnung die D7 Operatoren berücksichtigen, könnten diese jedoch reduziert werden.

Die NLO Rechnung nutzt die Kompaktheit der MHV-Amplituden aus, um die für die reellen Korrekturen benötigten zwei nach vier Prozesse möglichst effizient zu berechnen. Es wäre daher von grossem Vorteil, wenn man auch MHV-Amplituden für die D7 Operatoren zur Verfügung hätte. In Kapitel 6 werden MHV-Amplituden für die D7 Operatoren behandelt. Es wird ein analytischer Ausdruck für die n -Gluon-Higgs Streuung gegeben, welcher gut motiviert ist, aber nicht bewiesen wird. Jedoch wird gezeigt, dass die vier Gluon-Higgs Amplitude, gegeben durch die MHV-Amplituden, numerisch mit dem bekannten Ergebnis, welches man aus Feynman Diagrammen erhält, übereinstimmt.

Kapitel 7 enthält eine abschliessende Diskussion der vorhergehenden Ergebnisse.

Verwendete Konventionen und sämtliche Rechnungen sind im Anhang zusammengefasst.

Danksagung

In erster Linie möchte ich mich bei Herrn Zeppenfeld für die Möglichkeit bedanken, meine Diplomarbeit auf einem so aktuellen wie auch interessanten Themengebiet anfertigen zu können. Bedanken möchte ich mich auch für die gute Betreuung und dafür, dass man jederzeit willkommen war wenn es Fragen gab.

Bei Herrn Kühn bedanke ich mich für die Bereitschaft, das Korreferat zu übernehmen.

Besonders möchte ich mich bei allen Institutsmitgliedern für die angenehme Atmosphäre bedanken und dafür, dass sie immer für Fragen und Diskussion offen waren. Insbesondere bedanke ich mich bei Gunnar Klämke und Michael Kubocz, von deren Kenntnissen in *ggflo* ich stark profitieren konnte.

Ein besonderer Dank geht an meine Mitdiplomanden und Zimmerkollegen, Christoph Englert, Christoph Hackstein und Matthias Werner für die zahlreichen Diskussionen und die Unterstützung untereinander.

Ein grosses Dankeschön an die Korrekturleser Christoph Englert und Michael Kubocz.

Zu guter letzt bedanke ich mich bei meiner Familie, die mich während meines ganzen Studiums ohne wenn und aber unterstützt hat.